Grant Agreement N°: 101004145

Topic: SPACE-29-TEC-2020

DYNASAT

Dynamic spectrum sharing and bandwidth-efficient techniques for high-throughput MIMO Satellite systems

D3.4: Bandwidth Efficient Techniques evaluation

Revision: v.3.0

Work package	WP3
Task	Task 3.3
Due date	23/12/2021
Submission date	30/11/2022
Deliverable lead	UNIBO
Version	3.0

Abstract

This deliverable is an interim version of the outcomes of Task 3.3 “Bandwidth efficient techniques for satellite network performance evaluation.” In particular, based on the review of the technical literature and the related discussions on the potential techniques provided in D3.1, this document reports a detailed description of the simulator structure, Key Performance Indicators, and preliminary numerical assessment for the short-term MU-MIMO and Multi-Connectivity techniques identified and designed in D3.2.

Keywords: Non-Terrestrial Networks, Beamforming, MU-MIMO, spectrum sharing, NTN services, 3GPP

Document Revision History

Version	Date	Description of change	List of contributor(s)
V0.1	5/09/2021	Document creation	UNIBO
V0.2	23/11/2021	First version	UNIBO, MAGISTER
V0.3	25/11/2021	Multi-connectivity part clarified	MAGISTER
V0.4	7/12/2021	Link-level simulator description	UNIPR
V0.5	12/12/2021	MU-MIMO numerical results	UNIBO
V0.6	15/12/2021	MC preliminary results	MAGISTER
V1.0	17/12/2021	First version submitted to SAB	UNIBO
V1.1	23/12/2021	Submission to EC	UNIBO
V2.0	1/04/2022	Updated version after the Y1 technical review: clarification added below Table 2 on the parameters for VSAT terminals in Ka-band	UNIBO
V3.0	15/11/2022	Updated based on the intermediate technical review: clarification on the past changes	UNIBO

Disclaimer

Project co-funded by the European Commission under SPACE-29-TEC-2020		
Nature of the deliverable:	R	
Dissemination Level		
PU	Public, fully open, e.g. web	√
CI	Classified, information as referred to in Commission Decision 2001/844/EC	
CO	Confidential to DYNASAT project and Commission Services	

* *R: Document, report (excluding the periodic and final reports)*
DEM: Demonstrator, pilot, prototype, plan designs
DEC: Websites, patents filing, press & media actions, videos, etc.
OTHER: Software, technical diagram, etc

EXECUTIVE SUMMARY

Task 3.3 is aimed at assessing the performance of the techniques selected from D3.1 and designed in the companion document D3.2 in the DYNASAT mega-constellation. This interim version of the task outcomes provides a detailed description of the simulator, the Key Performance Indicators, and preliminary numerical results for the following techniques:

- Multi-User Multiple Input Multiple Output (MU-MIMO) techniques
    - Both single and multiple satellites scenarios are available. The latter refers to the possibility of covering hot-spot areas with a peak in the throughput request from the on-ground users by exploiting a hybrid frequency reuse scheme in which a portion of the coverage is served with N colours and the hot-spot sub-regions with full frequency reuse and beamforming techniques. The following techniques have been implemented, as thoroughly described in D3.2:
        - Minimum Mean Square Error (MMSE)
        - Multi-Beam (MB)
        - Spatially Sampled MMSE (SS-MMSE)
    - The on-ground users can be fixed or moving according to the user terminal scenarios described in 3GPP TS 22.261 and TR 38.821. The system parameters are aligned with the specifications provided in TR 38.821 and TR 38.811, with the only exception being the antenna array model on-board the satellites, defined in ITU-R Recommendation M.2101 and in the DYNASAT Technical Note on “Satellite Antenna Model.”
- Multi-Connectivity techniques
    - Both inter-beam single satellite NTN-NTN MC and inter-satellite NTN-NTN MC candidate scenarios with LEO satellites and stationary (non-mobile) UEs available.
    - Priority for NTN-NTN MC (no TN-NTN) asynchronous multi-connectivity.
    - MC is assumed to use different frequency bands.

TABLE OF CONTENTS

LIST OF FIGURES

LIST OF TABLES

ABBREVIATIONS

3GPP	Third Generation Partnership Project
BER	Bit error rate
BLER	Block error rate
CDF	Cumulative Distribution Function
CL	Clutter Loss
CPC	Centralised Precoding Computation
CPE	Common phase error
CRC	Cyclic redundancy check
CSI	Channel State Information
DCI	Downlink control information
DLSCH	Downlink shared channel
DMRS	Demodulation reference signal
DPC	Distributed Precoding Computation
ECEF	Earth-Centered Earth-Fixed
eMBB	enhanced Mobile Broadband
FFR	Full Frequency Reuse
FoV	Field of View
gNB-CU	gNB Centralised Unit
gNB-DU	gNB Distributed Unit
HARQ	Hybrid automatic repeat request
IMUX	Input Multiplexer
INR	Interference-to-Noise Ratio
ISL	Inter Satellite Link
ITU-R	International Telecommunication Union – Radiocommunication sector
LB-MMSE	Location Based MMSE
LDPC	Low density parity check
LEO	Low Earth Orbit
LOS	Line-of-Sight
KPI	Key Performance Indicator
MB	Multi-Beam
MC	Multi-Connectivity
MIMO	Multiple Input Mulitple Output
MMSE	Minimum Mean Square Error
MU-MIMO	Multi User MIMO
MN	Master Node
MPC	Maximum Power Constraint
NCC	Network Control Center

NLOS	Non-Line-Of-Sight
NR	New Radio
NTN	Non-Terrestrial Network
OFDM	Orthogonal frequency division multiplexing
OMUX	Output Multiplexer
PAC	Per Antenna Constraint
PCID	Physical Cell ID
PDSCH	Physical downlink shared channel
PHY	Phyiscal layer
pLOS	pure LOS
PoC	Proof of Concept
PRACH	Physical random access channel
PTRS	Phase tracking reference signal
PUSCH	Physical uplink shared channel
RRM	Radio Resource Management
RTT	Round Trip Time
SINR	Signal-to-Interference-plus-Noise Ratio
SIR	Signal-to-Interference Ratio
SLS	System Level Simulator
SN	Secondary Node
SNR	Signal-to-Noise Ratio
sMPC	satellite MPC
SPC	Sum Power Constraint
SSB	Signal synchronization block
SS-MMSE	Spatially Sampled MMSE
SSP	Sub Satellite Point
SSPA	Solid state power amplifier
sSPC	satellite SPC
TN	Terrestrial Network
TR	Technical Report
TS	Technical Specification
UDP	User Datagram Protocol
UE	User Equipment
ULSCH	Uplink shared channel
VSAT	Very Small Aperture Terminal

1 INTRODUCTION

In this Section, we report the MU-MIMO and Multi-Connectivity techniques selected for preliminary numerical results in D3.1 and D4.1, respectively. For the sake of completeness, these are briefly summarised in the following sections, before moving to the simulator descriptions and outcomes.

1.1 MU-MIMO techniques

Based on the preliminary design of MU-MIMO techniques detailed in D3.2, the following algorithms, summarised in Table 1, are considered for the preliminary assessment:

- Minimum Mean Square Error (MMSE): this is a long-term technique, but it is already considered for the short-term numerical assessment since it provides a benchmark performance for the other techniques. This technique, which requires the knowledge of the Channel State Information (CSI) vector of each user at the transmitter, can be implemented in both the beam and feed spaces, with single and multiple satellites, and with all of the proposed normalisations;
- Multi-Beam (MB): this short-term technique is based on the excitation coefficients providing the beamforming matrix for the desired beam lattice, with the precoding vector of a given user terminal equal to the beamforming vector of its closest beam center. MB precoding is implemented in the feed space only, since in the beam space it is equivalent to a non-precoded system, and it can be exploited with single or multiple satellites. Finally, given the built-in normalisation for the beamforming weights, this approach does not require different normalisation solutions, since all of them lead to the same result;
- Spatially Sampled MMSE (SS-MMSE): this short-term technique has been introduced in D3.4 by observing that, for a given beam index reported by the user as in MB precoding, in addition to the steering vector, the Network Control Center (NCC) can also estimate the slant range by exploiting the known local topography and constellation orbital parameters. This information is used to build an approximated MMSE matrix for the given beam center direction, without taking into account other stochastic terms or impairments, *e.g.*, large scale losses or scintillation. This technique can be used in both the beam and feed spaces, with single and multiple satellites, and with all of the proposed normalisations.

Table 1 - Summary of the MU-MIMO techniques retained from D3.2.

MU-MIMO technique	Precoding matrix	Channel coefficients @TX	Information @TX
MMSE	$\left(\tilde{\mathbf{H}}^H\tilde{\mathbf{H}} + \mathrm{diag}(\boldsymbol{\alpha})\mathbf{I}_{N_F}\right)^{-1}\tilde{\mathbf{H}}^H$	$\tilde{h}_{i,n} = g_{i,n}^{(tx)} g_{i,n}^{(rx)} \frac{\lambda}{4\pi d_{i,n}} \sqrt{\frac{L_{i,n}}{\kappa B T_i}} e^{-j\frac{2\pi}{\lambda}d_{i,n}}$ channel @user terminals	CSI
MB	$\mathbf{w}_{:,k} = \mathbf{b}_{:,j}, j = \arg\min_{i=1,\dots,N_B} \lVert\mathbf{c}_i - \mathbf{p}_k\rVert^2$	$b_{n,\ell} = \frac{1}{\sqrt{N_F}} e^{-jk_0\mathbf{r}_n\cdot\mathbf{c}_\ell}$ steering vectors @beam centers	Beam ID
SS-MMSE	$j = \arg\min_{i=1,\dots,N_B} \lVert\mathbf{c}_i - \mathbf{p}_k\rVert^2$ $\left(\tilde{\mathbf{H}}_c^H\tilde{\mathbf{H}}_c + \mathrm{diag}(\boldsymbol{\alpha})\mathbf{I}_{N_F}\right)^{-1}\tilde{\mathbf{H}}_c^H$	$\tilde{h}_{j,n} = g_{j,n}^{(tx)} g_{j,n}^{(rx)} \frac{\lambda}{4\pi d_{j,n}} \sqrt{\frac{1}{\kappa B T_j}} e^{-j\frac{2\pi}{\lambda}d_{j,n}}$ channel @beam centers	Beam ID

The main characteristics and assumptions for each technique will be reviewed while describing the simulator structure step-by-step in Section 2.1.

1.2 Multi-connectivity techniques

The multi-connectivity is selected to be demonstrated in WP5 of the project. Techniques and modelling related to multi-connectivity will be defined later in the project in D5.2. Here is described initial ideas to model multi-connectivity in the demonstrations.

Algorithmic considerations for multi-connectivity from D3.2

- Whether to enable MC for a UE and under which conditions.
- How to split the traffic between the MN and SN.

Three potential MC scenarios have been identified in D5.1

1. Single satellite neighbouring multi-beam MC
2. Multi-satellite overlapping coverage FRF1 MC
3. Multi-satellite overlapping coverage FRF3 MC

Additionally, a simple MC scenario is described in the Section 3.1.4. The preliminary MC simulation results are produced within this scenario and can be found from Section 3.1.3. In the initial implementation for the preliminary results MC can be set only on/off for all UEs at simulation initialization phase. When MC on mode is selected, then traffic is halved between MN and SN.

2 MU-MIMO TECHNIQUES: SIMULATOR DESCRIPTION AND PRELIMINARY NUMERICAL ASSESSMENT

In this Section, we report the description of the software simulator structure, assumptions, and Key Performance Indicators (KPIs) for the benchmark algorithm (MMSE) and the short-term techniques (MB and SS-MMSE). Then, the numerical assessment is provided for both a stand-alone satellite and a swarm of satellites of the DYNASAT constellation.

2.1 Simulator structure and assumptions

The high-level block diagram of the software simulator for MU-MIMO is shown in Figure 1. The following macro-blocks can be identified:

- **system configuration**: the input parameters are used to identify any ancillary information (*e.g.*, the carrier frequency based on the operating band) and derived parameters (*e.g.*, the receiver antenna model based on the receiver type) required in the simulator;
- **scenario generation**: based on the desired system configuration, a stand-alone or multiple satellite scenario is generated. This includes: i) the identification of the beam radius; ii) the generation of the on-ground beam lattice for the considered beam radius: iii) the computation of the beamforming matrix for the desired beam lattice; and iv) the computation of the pre-determined beamforming codebook for MB and SS-MMSE;
- **system deployment**: the Monte Carlo simulation is run. At each iteration: i) the users are uniformly distributed in the coverage area; ii) they estimate their reference beam (MB, SS-MMSE) or CSI (MMSE); iii) the users and the satellite are moved to their new locations after a delay that includes the precoding and scheduling processing at the ground segment; iv) the precoded signals are sent from the satellites and received at the user terminals, defining the Signal-to-Interference-plus-Noise Ratio (SINR);
- **Key Performance Indicators**: the average system performance and the related Cumulative Distribution Function (CDF) curves are obtained, as detailed below.

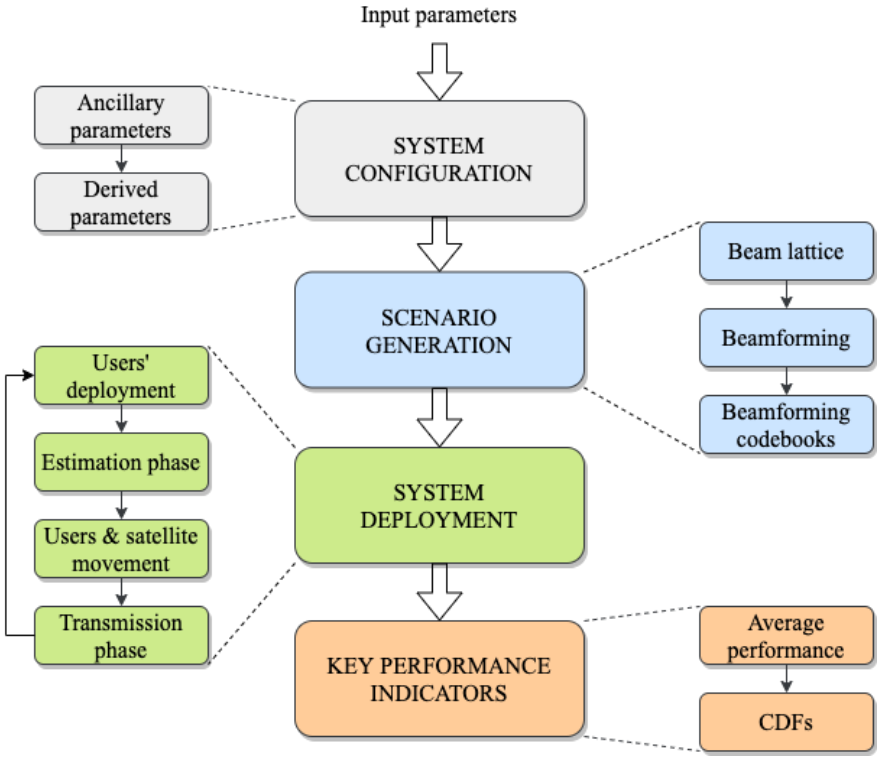

Figure 1 - MU-MIMO simulator structure.

2.1.1 System configuration

In this macro-block, the input parameters are provided to the simulator so as to obtain a set of ancillary and derived parameters that will be needed in the following blocks. Below, we describe these parameters, also reporting the main assumptions and/or references for their values. As for the latter, it shall be noticed that the logic in the simulator construction was to be as much as possible aligned to the 3GPP Non-Terrestrial Network (NTN) Study Items, while being aligned with the DYNASAT objectives and design principles.

Table 2 - Input parameters and allowed ranges.

Parameter	Range
System band	S, Ka
Beamforming space	feed, beam
Receiver type	VSAT, handheld
Receiver scenario	fixed, pedestrian, public safety, vehicular, aircraft
Propagation scenario	pLOS, LOS, NLOS
Total on-board power density	> 0 W/MHz
Number of tiers	≥ 1 tier
User density	> 0 users/km^2

The input parameters, reported in Table 2 with the allowed ranges, define the scenario[1]:

- system band: as per 3GPP TR 38.821, [1], both S and Ka band systems can be simulated. Depending on the selected band, different values of the carrier frequency, f_c, and user bandwidth, B_{UE}, are possible, as reported in Table 3. It shall be noticed that, while the simulator gives the possibility to simulate Ka-band systems for any evaluation that might be needed in the future, the focus of the project is on S-band systems;
- beamforming space: as extensively discussed in D3.2, beamforming is implemented in both the feed and the beam space, with the former that is expected to provide better results in terms of the average system capacity;
- receiver type and scenario: both Very Small Aperture Terminal (VSAT) and handheld terminals are considered, as defined in TR 38.821. Moreover, both terminal types can be considered as fixed or moving with different speeds, denoted as v_{UT}, as defined in 3GPP TS 22.261, [2], and reported in Table 4. While all combinations are possible, there are some of them that will not be considered in the numerical assessment since not reasonable (*e.g.*, VSAT terminals with pedestrian speed) or currently not foreseen by 3GPP (*e.g.*, VSAT for public safety). In addition, it is worth to mention that in TR 38.821 a refinement of these cases was introduced, in which the public safety receiver can be either a handheld terminal travelling at 100 km/h or a VSAT travelling at 250 km/h, which motivates the presence of two public safety scenarios in Table 4. Please note that, while the project focuses on handheld terminals, VSAT terminals are considered so as to have a performance benchmark to understand the impact of directive radiation patterns with large gain on the MU-MIMO performance.
- propagation scenario: this parameter defines the propagation environment based on TR 38.821 and TR 38.811. In particular, the following options are available: i) pure Line-Of-Sight (pLOS) scenario, in which only the free space loss and the phase rotation due to the slant range are considered, in addition to noise and interference; ii) a LOS scenario, in

[1] It shall be noticed that, while these parameters are those identifying the simulation scenario, other parameters that are considered as ancillary can be modified, if needed.

which log-normal fading (shadowing), atmospheric losses, and scintillation are included; and iii) a Non-LOS (NLOS) scenario in which the users also experience a Clutter Loss (CL). For the LOS and NLOS scenarios, we refer to TR 38.811, [3], in which three propagation environments are defined: urban, sub-urban, and dense urban; the computation and logic behind these losses are summarised in the next sections, when discussing the channel coefficients;

- total on-board power density: this is the total power density available per satellite, $P_{t,dens}$, in Watts per MHz. The values for this parameter are obtained from 3GPP TR 38.821;
- number of tiers: this parameter, n_{tier}, provides the number of tiers around the central beam located at the Sub Satellite Point (SSP) in the stand-alone scenario or the number of tiers covered by the satellites swarm in the multiple satellite scenario;
- user density: this value, δ_{UT}, defines the number of users per square km that are uniformly distributed in the coverage area at each Monte Carlo iteration.

Table 3 - System carrier frequency and user bandwidth, [1].

Band	Carrier frequency f_c [GHz]	User bandwidth B_{UE} [MHz]
S-band	2	30
Ka-band	20	400

Table 4 - Receiver characteristics per scenario, [2].

Receiver scenario	Receiver speed v_{UE} [km/h]	Receiver type
Fixed	0	VSAT, handheld
Pedestrian[2]	3	handheld
Public safety A	100	handheld
Public safety B	250	VSAT
Vehicular	250	VSAT
Aircraft	1000	VSAT

The ancillary parameters that are defined based on the system configuration are reported in Table 5 and described below:

- beam edge gain: this parameter defines the radiation pattern value at beam edge with respect to the beam center and it is fixed to $\Delta G_{edge} = -3$ dB, if not otherwise specified;
- satellite altitude: altitude of the satellite above the ground level, h_{sat};
- SSP coordinates: latitude and longitude coordinates of the satellites' SSPs;
- satellite antenna array: parameters required for the definition of the on-board antenna array for each satellite. As per D2.1, this includes:
  - the number of radiating elements on the horizontal and vertical array axis, n_H and n_V, respectively;
  - the horizontal and vertical spacing of the elements, $d_H = 0.55\lambda$ and $d_V = 0.55\lambda$, respectively, with λ being the signal wavelength;
  - the radiating element gain, $G_{el}[\text{dBi}] = 5.3$ dBi;

[2] The pedestrian terminal speed is not defined by 3GPP and defined assuming an average running/fast walking person.

- the 3 dB bandwidth of the single element on the array horizontal and vertical axis, $\tilde{\vartheta}_{3dB} = 90°$ and $\tilde{\varphi}_{3dB} = 90°$, respectively;
- the front-to-back ratio on the array horizontal and vertical axis, $A_m = 30$ dB and $SLA_m = 30$ dB, respectively;

- UE antenna parameters: depending on the receiver type, the antenna configuration detailed in TR 38.821 and reported in Table 6 are considered. It shall be noticed that in TR 38.821 it is stated that a 3 dB polarisation loss shall be included for handheld terminals; however, since the two array elements at the receiver provide an antenna gain of 3 dBi, we are considering an overall antenna gain equal to 0 dBi for these receivers.

Table 5 – Ancillary and derived parameters and allowed ranges.

Parameter	Range/description
Beam edge gain	< 0 dB
Satellite altitude	600 km or 610 km based on the DYNASAT constellation parameters
SSP coordinates	global latitude and longitude coordinates
Satellite antenna array	parameters defining the planar antenna array on-board each satellite
UT antenna parameters	parameters defining the UT receiver antenna as per TR 38.821

Table 6 - Receiving antenna parameters, [3].

Parameter	VSAT	handheld
Antenna type	Directional, with 60 cm diameter (model provided in TR 38.811)	omnidirectional with 2 radiating elements
Polarisation	circular	linear
RX antenna gain $G_{max}^{(rx)}$[dBi]	39.7 dBi	0 dBi per element
Antenna temperature T_a[K]	150 K	290 K
Noise figure N_f[dB]	1.2 dB	7 dB

Based on the above configuration and parameters, the following additional data can be obtained:

- satellite field of view (FoV): angular field of view of the satellite

$$\rho = \sin^{-1}\left(\frac{R_E}{R_E + h_{sat}}\right) \text{ [deg]} \quad (1)$$

where $R_E = 6371$ km is the Earth radius assuming a spherical Earth model;

- total on-board power: total power available on-board each satellite for the transmission, computed as

$$P_t[\text{dB}] = P_{t,dens}[\text{dB}] + 10\log_{10} B_{UE} \quad (2)$$

With respect to the total power, it is worth mentioning that the handheld terminals experience a 3 dB polarisation loss due to the linear polarisation; however, since there are 2 radiating elements, this loss is compensated as per TR 38.821. Thus, equation (2) applies to both VSAT and handheld terminals.

- noise power: total noise power at the receiver, defined as follows:

$$P_N[\text{dB}] = N_f[\text{dB}] + 10\log_{10}\left(T_0[K] + (T_a[K] - T_0[K])^{-0.1N_f[dB]}\right) \quad (3)$$

where $T_0 = 290$ K is the reference ambient temperature;

- satellite antenna gain: maximum antenna gain from the on-board array, defined as

$$G_{max}^{(tx)} = G_{el} + 10\log_{10} n_H n_V \approx 35.4 \text{ dBi} \quad (4)$$

2.1.2 Scenario generation

In this block of the simulator, the multi-beam scenario is created for a stand-alone satellite or a swarm of N_S satellites depending on the number of SSP coordinates values, which then allows to compute the beamforming matrix and the pre-computed precoding matrices for the MB and SS-MMSE algorithms.

To this aim, the first step is the identification of the beam radius based on the following procedure:

- a single beam below the SSP is generated in (u, v) coordinates. Let us denote by $\mathbf{p}$ the $M \times 2$ array of (u, v) coordinates for the considered directions, *i.e.*, $\mathbf{p}_i = [u_i, v_i]$ with (u_i, v_i) being the coordinates of the i-th direction. Based on the antenna model in D2.1 and the MU-MIMO design in D3.2, the radiation pattern in the i-th direction, when beamforming is not yet implemented, is obtained as:

$$g^{(tx)}(u_i, v_i) = g_E(u_i, v_i) \sum_{n=1}^{n_H n_V} g_n(u_i, v_i) = g_E(u_i, v_i) \sum_{n=1}^{n_H n_V} e^{jk_0 \mathbf{r}_n \cdot \mathbf{p}_i} \quad (5)$$

  with $\mathbf{r}_n$ being the position of the n-th antenna array element on its plane. The $n_H n_V$-dimensional unit-norm beamforming vector in the direction of the SSP, $(0,0)$, is given by:

$$\mathbf{b} = \frac{1}{\sqrt{n_H n_V}} \sum_{n=1}^{n_H n_V} e^{jk_0 \mathbf{r}_n \cdot \mathbf{c}_i} \quad (6)$$

  Thus, the radiation pattern in the i-th direction when beamforming is implemented to obtain a beam directed towards the SSP can be written as:

$$g_{bf}^{(tx)}(u_i, v_i) = g_E(u_i, v_i) \sum_{n=1}^{n_H n_V} g_n(u_i, v_i) b_n^*(u_i, v_i) = \mathbf{g}_{feed}(u_i, v_i)\mathbf{b}^H \quad (7)$$

  where $\mathbf{g}_{feed}(u_i, v_i)$, with $g_{feed,n}(u_i, v_i) = g_E(u_i, v_i) g_n(u_i, v_i)$, is the $n_H n_V$-dimensional row vector of array radiation patterns in the i-th direction and H denotes the Hermitian operator;

- the beamwidth, ϑ_{edge}[3], is obtained by first finding the coordinates of the directions at which the above radiation pattern is ΔG_{edge} dB below the value at the beam boresight direction:

$$\left\{(u, v): 20\log_{10}\left|g_{bf}^{(tx)}(u, v)\right| - G_{max}^{(tx)} \leq -\Delta G_{edge}\right\} \quad (8)$$

  then, since many coordinates will satisfy this condition (basically all directions outside the desired beam footprint), the angle is obtained as the angle between the beam center direction (SSP) and the direction at which we obtain the value of $20\log_{10}\left|g_{bf}^{(tx)}(u, v)\right| - G_{max}^{(tx)}$ that is the closest to $-\Delta G_{edge}$ dB.

Once ϑ_{edge} is known, the beam lattice is built with the procedure reported in TR 38.821. In particular, the Adjacent Beam Spacing (ABS) in (u, v) coordinates is defined as:

[3] Differently from the literature and 3GPP specifications, in which this angle is denoted as ϑ_{3dB} because beams are typically identified at -3 dB from the beam center, we use this nomenclature to highlight that we might also use different values at beam edge, ΔG_{edge}.

$$ABS = \sqrt{3}\sin\vartheta_{edge} \tag{9}$$

This value defines the beam radius on the (u, v) plane that can be used to generate the desired hexagonal beam lattice with n_{tier} tiers. As an example, let us assume to operate in S-band, thus implying that $f_c = 2$ GHz and $\lambda = 0.1499$ m, and the antenna model in D2.1 and D3.2, with $n_H = n_V = 32$. The procedure defined by equations (5) to (8) leads to $\vartheta_{edge} = 1.4325°$ and, thus, $ABS = 0.0433$.

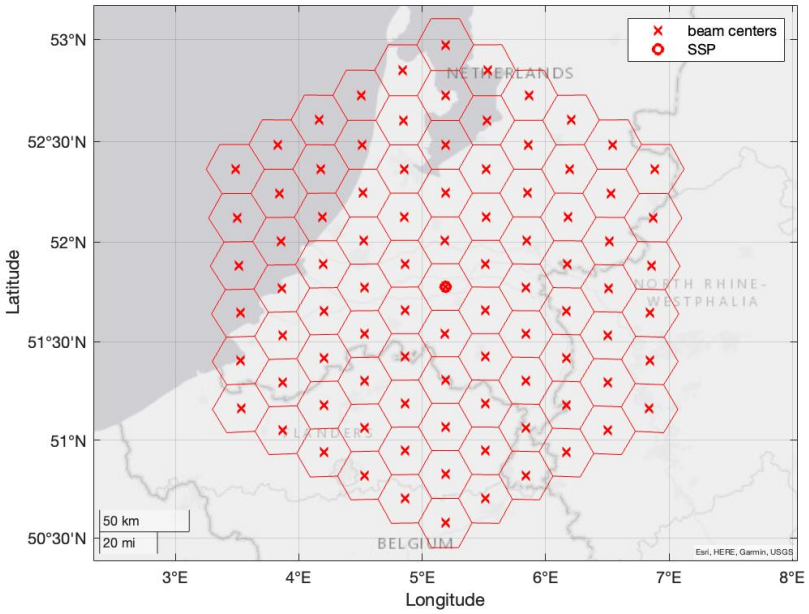

Figure 2 - Example of a beam lattice in S-band with $n_{tier} = 5$ and a stand-alone satellite.

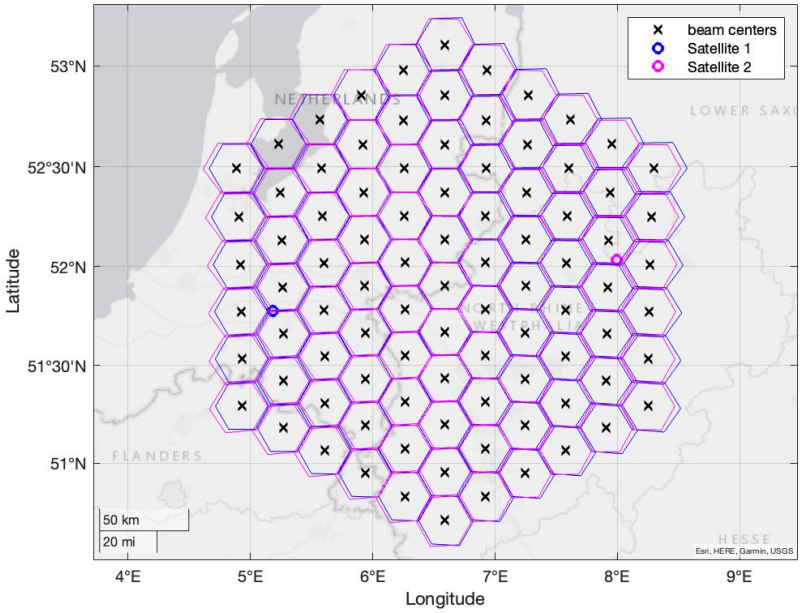

Figure 3 - Example of a beam lattice in S-band with $n_{tier} = 5$ and two satellites.

In Figure 2, we show the beam lattice obtained with this procedure for a satellite with SSP located at $5.1863°E$ and $51.7757°N$, in which $n_{tier} = 5$ tiers around the SSP were generated. In Figure 3,

we show the beam lattice that is jointly covered by two satellites of the DYNASAT constellation at $(5.1863°E, 51.7757°N)$ and $(7.9965°E, 52.0327°N)$ (further details on this scenario are reported in the next sections). Notably, the beam elongations in opposite directions that can be observed with multiple satellites are due to the different locations from which the beams are generated. This scenario corresponds to a **hot-spot case**, in which a specific area is experiencing a large throughput request from the users, which can only be met by means of aggressive frequency reuse schemes with beamforming and precoding. Please note that, for the sake of simplicity, we are considering that all beams are in the hot-spot region; however, in the next phase of the study, we will consider a larger coverage area with a 3 or 4 colours frequency reuse scheme in which one or more smaller regions with adjacent beams requesting larger connectivity are present. This situation is shown in Figure 4 for a stand-alone satellite, to highlight that these traffic conditions will be addressed with one or more satellites. The hot-spot areas will be covered by the satellites by means of full frequency reuse (shown in blue in the figures below), exploiting MU-MIMO techniques, while the remaining colours will be used to cover the other beams in which no traffic request peak is present.

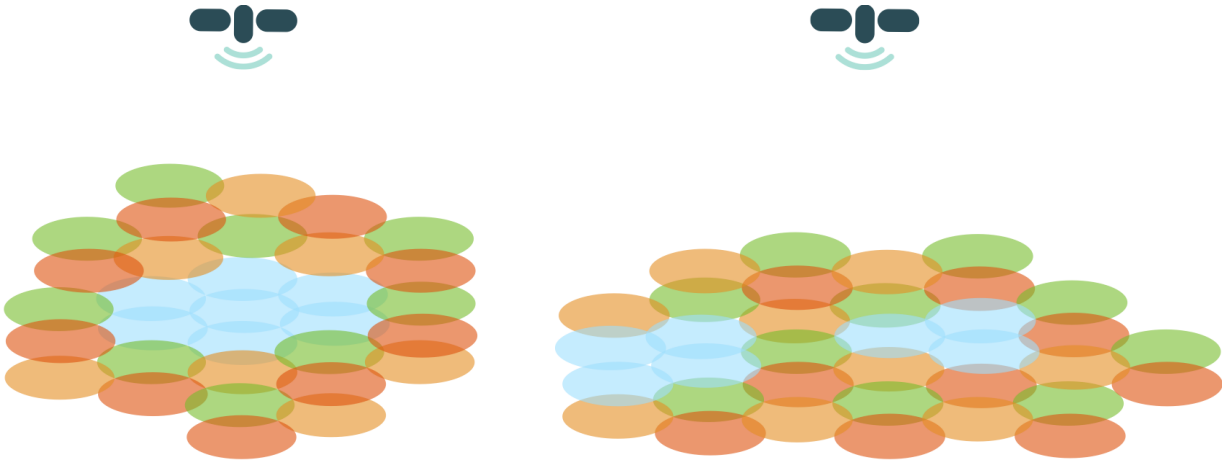

(a) 1 hot-spot area *(b) 2 hot-spot areas*

Figure 4 - Example of hot-spot scenarios with a stand-alone satellite.

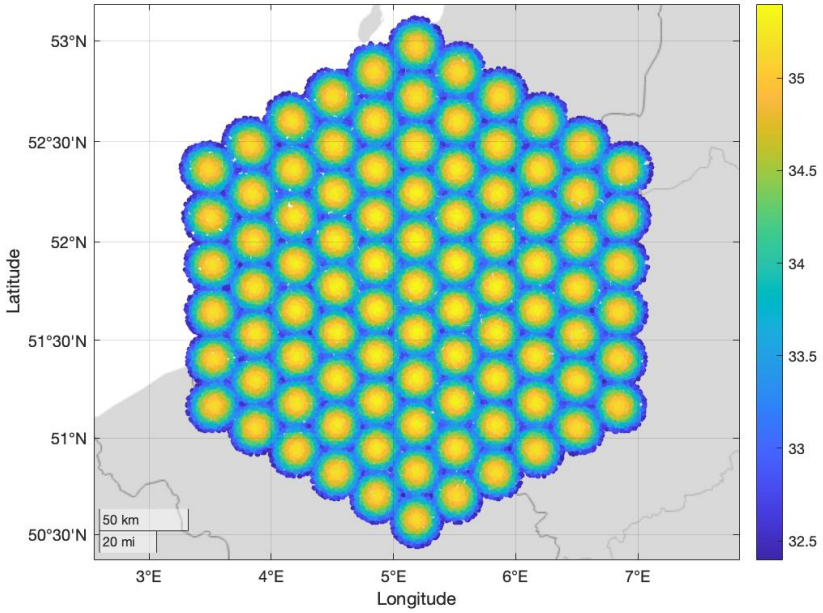

Figure 5 - Example of the antenna gain in [dBi] *in S-band with* $n_{tier} = 5$ *and a stand-alone satellite.*

Once the coordinates of the desired beam centers are available, the beamforming matrix can be obtained as reported in equation (6) for the case of a single beam. In particular, in the multiple satellites scenario, a beamforming matrix is computed for each satellite. By denoting as $\mathbf{c}_j^{(s)}$ the (u,v) coordinates of the j-th beam center, with $j = 1, \dots, N_B$, from the s-th satellite, the corresponding $N_F \times N_B$ beamforming matrix, with $N_F = n_H n_V$, is given by:

$$\mathbf{B}^{(s)} = \left[\mathbf{b}_1^{(s)}, \dots, \mathbf{b}_{N_B}^{(s)}\right], \text{with } b_{j,n}^{(s)} = \frac{1}{\sqrt{n_H n_V}} \sum_{n=1}^{n_H n_V} e^{jk_0 \mathbf{r}_n^{(s)} \cdot \mathbf{c}_j^{(s)}} \tag{10}$$

with $\mathbf{r}_n^{(s)}$ being the position vector of the n-th radiating element on-board the s-th satellite. Figure 5 and Figure 6 show the resulting antenna gain values for uniformly distributed users in the beam lattice with the stand-alone and two satellites scenarios, respectively; in the latter case, the antenna gain is shown for one satellite only. These gains were obtained with the antenna model introduced in D2.1 and D3.2.

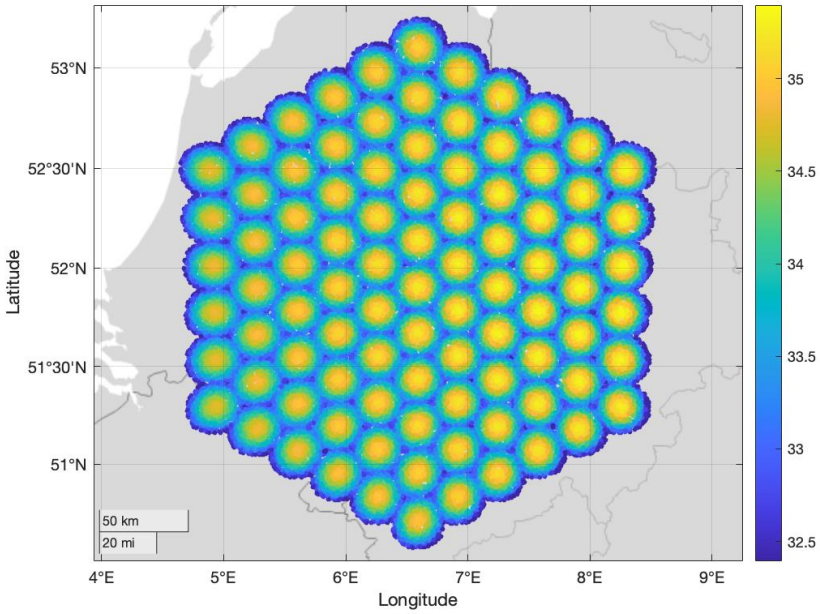

Figure 6 - Example of one antenna gain in [dBi] *in S-band with* $n_{tier} = 5$ *and two satellites.*

2.1.2.1 MB and SS-MMSE codebooks for stand-alone satellites

The last operation performed in this step is the computation of the pre-determined beamforming codebooks for the MB and SS-MMSE techniques. While the details for these algorithms are provided in deliverable D3.2, hereafter we only report the most relevant aspects.

With MB precoding, the precoding matrix is given by the steering vectors in the directions of the beam centers previously defined from each satellite:

$$\mathbf{W}_{MB}^{(s)} = \left[\mathbf{w}_{:,1}^{(s)}, \dots \mathbf{w}_{:,\ell}^{(s)}, \dots, \mathbf{w}_{:,N_B}^{(s)}\right], \text{with } \mathbf{w}_{:,k}^{(s)} = \mathbf{b}_{:,j}^{(s)}, \mathbf{b}_{:,j}^{(s)}, j = \arg \min_{i=1,\dots,N_B} \left\| \mathbf{c}_i^{(s)} - \mathbf{p}_k \right\|^2 \tag{11}$$

As extensively discussed in D3.2, this algorithm does not need different normalisation approaches, given the normalisation of the beamforming coefficients in (6). Thus, the following normalised precoding matrix is considered:

$$\breve{\mathbf{W}}_{MB}^{(s)} = \sqrt{\frac{P_t}{\mathrm{tr}\left(\mathbf{W}_{MB}^{(s)} \left(\mathbf{W}_{MB}^{(s)}\right)^H\right)}} \mathbf{W}_{MB}^{(s)} \tag{12}$$

with P_t computed as shown in equation (2). In Figure 7, we show the EIRP allocated to each beam (*i.e.*, the beam space precoding case) with the three normalisations.

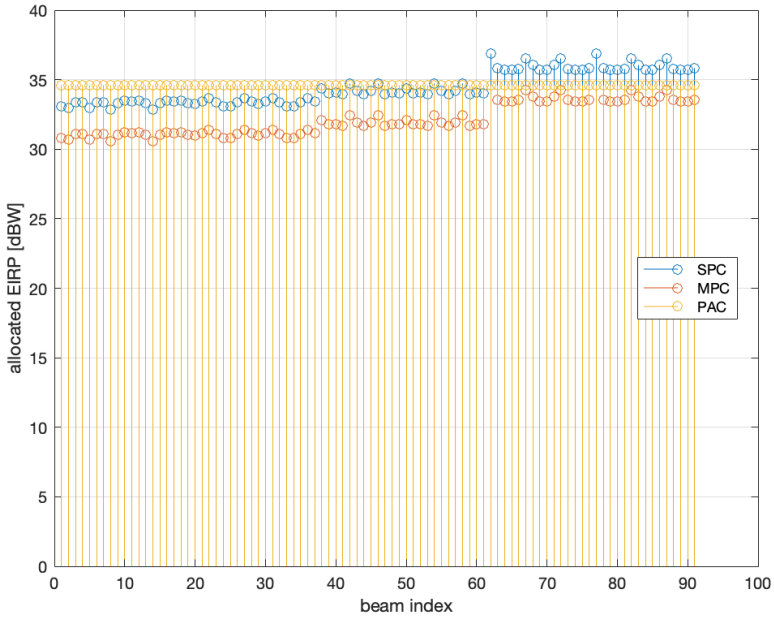

Figure 7 - EIRP allocations with beam space SS-MMSE precoding per beam with a stand-alone satellite.

It can be noticed that SPC and MPC do not allocate the same EIRP level to all beams, since the proportions are defined by the MMSE algorithm. Moreover, the proportions of EIRP allocated by these two normalisations are the same, with MPC being scaled down by a constant factor on all beams. This is in line with the above equations and with the fact that neither SPC nor MPC modify the orthogonality in the MMSE precoding matrix. With PAC, all beams are allocated the same amount of power: in this example, we have $N_B = 91$ beams and $P_{t,dens} = 4$ dBW/MHz, leading to an on-board available $EIRP = 54.17$ dBW, *i.e.*, 34.58 dBW per beam.

2.1.2.2 MB and SS-MMSE codebooks for multiple satellites

With SS-MMSE precoding, the MMSE algorithm is used by pre-computing the channel coefficients based on the knowledge of the beam index to which a user is associated (per satellite) and on the satellite orbital parameters:

$$\mathbf{W}_{SS-MMSE} = \tilde{\mathbf{H}}^H\left(\tilde{\mathbf{H}}\tilde{\mathbf{H}}^H + \mathrm{diag}(\boldsymbol{\alpha})\mathbf{I}_{N_B}\right)^{-1}\tilde{\mathbf{H}}^H \tag{13}$$

where $\tilde{\mathbf{H}} = \left[\mathbf{H}^{(1)}, \ldots, \mathbf{H}^{(N_S)}\right]$ is the total channel matrix from the N_S satellites towards the N_{UT} users. In the feed space, the generic (i,n)-th coefficient between the i-th beam center and the n-th feed on-board the s-th satellite is estimated based on the above mentioned information as follows:

$$\tilde{h}_{i,n}^{(feed,s)} = g_{i,n}^{(tx,s)} g_{i,n}^{(rx,s)} \frac{\lambda}{4\pi d_{i,n}^{(s)}} \sqrt{\frac{1}{\kappa B T_i}} e^{-j\frac{2\pi}{\lambda} d_{i,n}^{(s)}} \tag{14}$$

where $d_{i,n}^{(s)}$ is the slant range between the i-th beam center and the n-th feed on-board the s-th satellite, which can be assumed to depend only on the satellite and user indexes. In the beam space, we have a similar channel with the only exception being that the coefficients are computed per beam, *i.e.*, between the i-th beam center and the j-th beam generated from the s-th satellite:

$$\tilde{h}_{i,j}^{(beam,s)} = g_{i,j}^{(tx,s)} g_{i,j}^{(rx,s)} \frac{\lambda}{4\pi d_{i,j}^{(s)}} \sqrt{\frac{1}{\kappa B T_i}} e^{-j\frac{2\pi}{\lambda} d_{i,j}^{(s)}} \tag{15}$$

In the above estimated channel coefficients, it can be noticed that all the terms can be obtained by knowing the beam center location, the satellite orbital parameters, and topography information for the currently covered portion of the Earth's surface. Finally, with this algorithm all of the normalisations defined in D3.2 are required:

- Sum Power Constraint (SPC)

$$\breve{\mathbf{W}}_{SS-MMSE} = \sqrt{\frac{N_S P_t}{\mathrm{tr}(\mathbf{W}_{SS-MMSE}\mathbf{W}_{SS-MMSE}^H)}}\mathbf{W}_{SS-MMSE} \tag{16}$$

- Maximum Power Constraint (MPC)

$$\breve{\mathbf{W}}_{SS-MMSE} = \sqrt{\frac{N_S P_t}{N_S K \max\limits_{k=1,\dots,K}\left\|\mathbf{w}_{k,:}\right\|^2}}\mathbf{W}_{SS-MMSE} \tag{17}$$

- Per Antenna Constraint (PAC)

$$\breve{\mathbf{W}}_{SS-MMSE} = \sqrt{\frac{P_t}{K}}\,\mathrm{diag}\left(\frac{1}{\left\|\mathbf{w}_{1,:}\right\|},\dots,\frac{1}{\left\|\mathbf{w}_{K,:}\right\|}\right)\mathbf{W}_{SS-MMSE} \tag{18}$$

In the above normalisations, K is either equal to N_F or to N_B, for feed space and beam space precoding, respectively. In addition, when multiple satellites are considered, two additional normalisations were introduced in D3.2:

- satellite-SPC (sSPC): SPC guarantees that the total power emitted from the N_S satellites does not exceed $N_S P_t$, but there is no upper bound to the power emitted by a single satellite in the swarm, which can be larger than P_t. Thus, observing that the precoding matrix in (13) contains can be factorised as $\mathbf{W}_{SS-MMSE} = \left[\mathbf{W}_{SS-MMSE}^{(1)};\dots;\mathbf{W}_{SS-MMSE}^{(N_S)}\right]$, with $\mathbf{W}_{SS-MMSE}^{(s)}$ representing the precoding coefficients from the s-th satellite, the SPC normalisation is applied on a satellite-basis:

$$\breve{\mathbf{W}}_{SS-MMSE}^{(s)} = \sqrt{\frac{P_t}{\mathrm{tr}\left(\mathbf{W}_{SS-MMSE}^{(s)}\left(\mathbf{W}_{SS-MMSE}^{(s)}\right)^H\right)}}\mathbf{W}_{SS-MMSE}^{(s)}, s = 1,\dots,N_S \tag{19}$$

- satellite-MPC (sMPC): following the same approach, also the MPC normalisation can be applied on a satellite basis, so as to guarantee that each satellites emits, from at least one beam/feed, the maximum power per beam/feed. Thus:

$$\breve{\mathbf{W}}_{SS-MMSE}^{(s)} = \sqrt{\frac{P_t}{K \max\limits_{k=1,\dots,K}\left\|\mathbf{w}_{k,:}^{(s)}\right\|^2}}\mathbf{W}_{SS-MMSE}^{(s)} \tag{20}$$

Figure 8 shows the EIRP allocations, with the same parameters considered for the stand-alone scenario, with two satellites. On the left, with SPC, MPC, and PAC, we can notice the same behaviour as that reported in Figure 7, with the only exception being the number of beams: in this case, although the on-ground coverage contains $N_B = 91$ beams, we are transmitting from $N_S N_B = 182$ equivalent antennas on-board two satellites. On the right, the sSPC and sMPC normalisations are shown; it can be noticed that the power allocations are different for each beam, but not the same as those for SPC and MPC: in this case, we are normalising on a satellite-basis and, thus, the orthogonality in the optimal MMSE solution is slightly disrupted (the orthogonality is maintained on a satellite-basis).

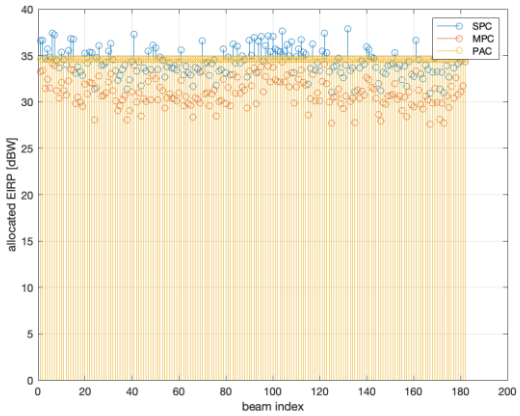

(c) SPC, MPC, PAC

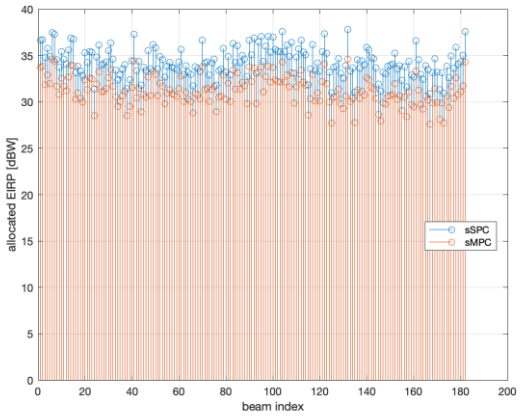

(d) sSPC, sMPC

Figure 8 - EIRP allocations with beam space SS-MMSE precoding per beam with multiple satellites.

2.1.3 System deployment

This block implements a Monte Carlo simulation for the numerical assessment in the scenario identified in the previous steps. The numerical assessment is provided with MB and SS-MMSE precoding and the performance benchmark is the one obtained with MMSE precoding and ideal CSI estimates at the transmitter side. In the following paragraphs, we thoroughly describe each step that is performed at each iteration.

2.1.3.1 Users' deployment

In the coverage area defined by the desired beam lattice, $N_{UE} = \lceil \delta_{UT} A_{cov} \rceil$ users are uniformly distributed in latitude and longitude coordinates. The users are strictly located inside the beams identified in the beam lattice, *i.e.*, no user is experiencing a radiation pattern value that is below $-\Delta G_{edge}$ dB compared to that at beam center. Figure 9 shows an example with $\delta_{UE} = 1$ users/km^2 and $n_{tier} = 5$, which leads to $N_{UE} = 57155$ users in the coverage area (clearly, with uniformly distributed users in different iterations there might be a different number of users); it can be noticed that indeed no user is located outside of the desired coverage area. This example is shown in Figure 5 for a stand-alone satellite.

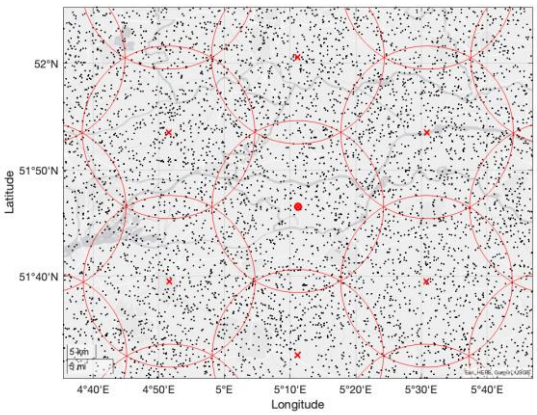

(a)

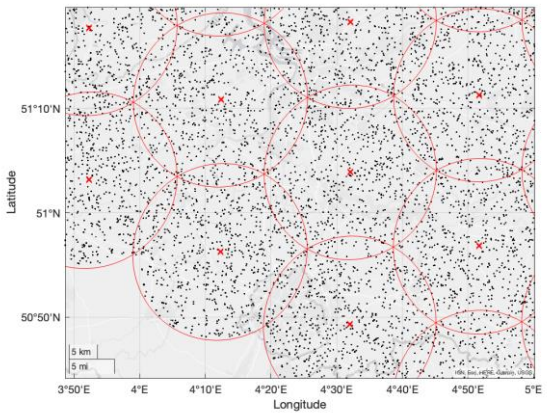

(b)

Figure 9 - Example of users' deployment with $\delta_{UE} = 1$ users/km^2 and a stand-alone satellite.

For each user, the following set of additional parameters, based on their locations and on the SSPs' positions, is obtained: i) the elevation angle, $\varepsilon_i^{(s)} = \cos^{-1}\left(\frac{\sqrt{\left(u_i^{(s)}\right)^2+\left(v_i^{(s)}\right)^2}}{\rho^{(s)}}\right)$; ii) the Earth central angle, $\lambda_i^{(s)} = 90° - \varepsilon_i^{(s)} - \sin^{-1}\left(\sqrt{\left(u_i^{(s)}\right)^2 + \left(v_i^{(s)}\right)^2}\right)$; iii) the slant range, $d_i^{(s)} = R_E \frac{\lambda_i^{(s)}}{\sqrt{\left(u_i^{(s)}\right)^2+\left(v_i^{(s)}\right)^2}}$; iv) the latitude and longitude coordinates; and v) the $\left(\vartheta^{(s)}, \varphi^{(s)}\right)$ coordinates to compute the radiating element pattern.

Based on these additional parameters, the antenna gain from each feed (feed space precoding) or beam (beam space precoding) is computed for each satellite, *i.e.*, $g_{i,j}^{(tx,s)}$. Figure 10 provides an example of beamformed antenna gain in the considered scenario, in the beam space, for beams 4 and 37. Figure 11 shows the two satellites scenario. Then, the best serving beam from the best satellite is identified for each user as the one providing the largest gain, leading to the largest received signal power.

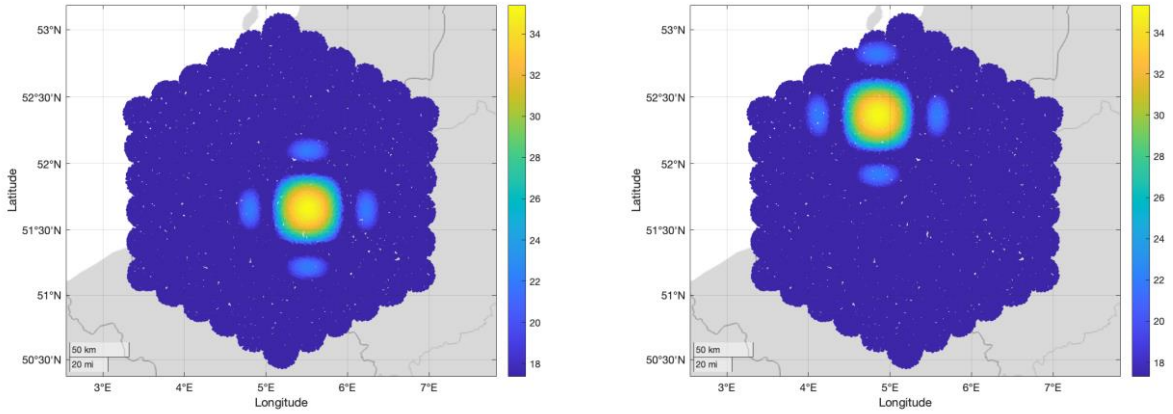

(a) beam 4 *(b) beam 37*

Figure 10 - Example of beamformed antenna gain with $\delta_{UE} = 1$ users/km² and a stand-alone satellite.

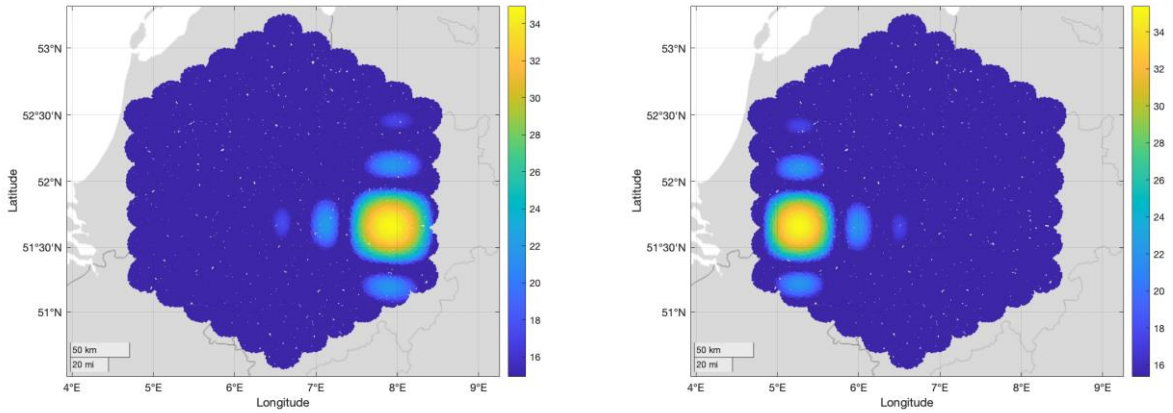

(a) beam 9 *(b) beam 81*

Figure 11 - Example of beamformed antenna gain with $\delta_{UE} = 1$ users/km² and a two satellites.

2.1.3.2 Estimation phase

In this step, two critical operations are performed: i) the users are scheduled for being served; and ii) the CSI vectors for MMSE precoding are computed.

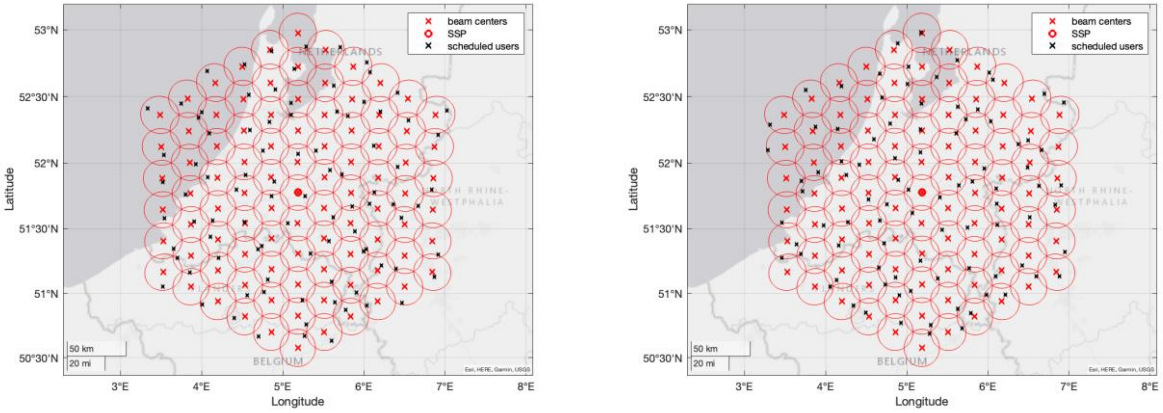

(a) time frame 1 *(b) time frame 2*

Figure 12 -Example of scheduled users in two time frames for the stand-alone satellite scenario.

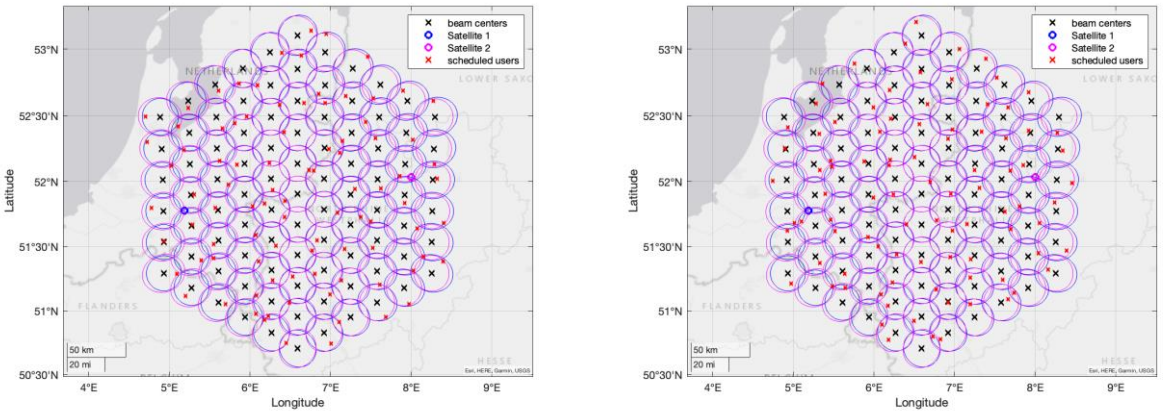

(a) time frame 1 *(b) time frame 2*

Figure 13 - Example of scheduled users in two time frames for the two satellites scenario.

With respect to scheduling, it shall be noticed that, in this preliminary evaluation of the short-term MU-MIMO techniques: i) no advanced RRM algorithm is considered; and ii) all users are assumed to request the same amount of traffic, *i.e.*, the traffic distribution is uniform. Based on these two assumptions, the users are randomly scheduled. In particular, at each time frame one user from each beam is randomly selected to be served and the total number of time frames is computed so as to guarantee that all users are served. Since in each beam there is a variable number of users, when all users from a beam have been served, they are again included in the pool of available users. Clearly, this is a simplified assumption[4] and in future releases of this document, based on the DYNASAT study outcomes, proper RRM algorithms will be included together with

[4] These assumptions are in line with the full buffer traffic model also adopted in 3GPP studies.

a non-uniform traffic request as, for instance, the one proposed in [4]. Figure 12 and Figure 13 show an example of scheduling in the stand-alone and two satellites scenarios, respectively.

As for the CSI estimation, which is required only for MMSE precoding and it is thus assumed to be ideal to provide a comparison with an optimal benchmark solution, the following channel coefficients are estimated from each satellite for the feed and beam spaces, respectively:

$$h_{i,n}^{(feed,s)} = g_{i,n}^{(tx,s)} g_{i,n}^{(rx,s)} \frac{\lambda}{4\pi d_{i,n}^{(s)}} \sqrt{\frac{L_{i,n}^{(s)}}{\kappa B T_i}} e^{-j\frac{2\pi}{\lambda} d_{i,n}^{(s)}} e^{j\varphi_i^{(s)}}, n = 1, \dots, N_F \quad (21)$$

$$h_{i,j}^{(beam,s)} = g_{i,j}^{(tx,s)} g_{i,j}^{(rx,s)} \frac{\lambda}{4\pi d_{i,j}^{(s)}} \sqrt{\frac{L_{i,j}^{(s)}}{\kappa B T_i}} e^{-j\frac{2\pi}{\lambda} d_{i,j}^{(s)}} e^{j\varphi_i^{(s)}}, j = 1, \dots, N_B \quad (22)$$

where, differently from the terms that have been introduced above for the beam centers and MB/SS-MMSE precoding, we are now computing the channel coefficients at each user's location; in addition, $L_{i,n}^{(s)}$ and $L_{i,j}^{(s)}$ represent the additional losses between the i-th user and the n-th feed or j-th beam of the s-th satellite, respectively, that were not taken into account before since they cannot be known in advance[5]. The additional losses included in this software are based on TR 38.821 and TR 38.811 and take into account: i) the shadow fading, as a long-normal random variable; ii) the Clutter Loss (CL), when the terminal is in NLOS conditions; iii) the scintillation loss; and iv) the gaseous absorption. The large scale losses are computed as per Section 6.6 in TR 38.811, summarised below for the sake of completeness referring to the generic i-th user:

the LOS probability is a function of the user's elevation angle and the environment in which it is located. Thus, for each satellite, the elevation angle is first used as an entry for

- Table 7 to identify the probability with which the user is in LOS or NLOS conditions. If the user is in LOS conditions, then the large scale loss only includes a shadow fading term, computed as a realisation of a log-normal random variable with a standard deviation σ_{SF} defined by the elevation angle and the propagation environment; if the user is in NLOS conditions, in addition to the shadow fading term, there is also a CL term, again computed as a function of the elevation angle and the environment. The CL and shadow fading standard deviation are reported in Table 8;

Table 7 - LoS probability as a function of the elevation angle and the propagation environment, [3].

Elevation angle	Dense urban	Urban	Sub-urban/rural
10°	28.2%	24.6%	78.2%
20°	33.1%	38.6%	86.9%
30°	39.8%	49.3%	91.9%
40°	46.8%	61.3%	92.9%
50°	53.7%	72.6%	93.5%
60°	61.2%	80.5%	94.0%
70°	73.8%	91.9%	94.9%
80°	82.0%	96.8%	95.2%
90°	98.1%	99.2%	99.8%

[5] The possibility to also adopt techniques to predict the additional losses, as those due to atmospheric events, can be considered for future activities.

Table 8 - Shadow fading and clutter loss for dense-urban, urban, and sub-urban/rural scenarios, [3].

Scenario	Elevation angle	S-band			Ka-band		
		LOS	NLOS		LOS	NLOS	
		σ_{SF}[dB]	σ_{SF}[dB]	CL[dB]	σ_{SF}[dB]	σ_{SF}[dB]	CL[dB]
dense urban	10°	3.5	15.5	34.3	2.9	17.1	44.3
	20°	3.4	13.9	30.9	2.4	17.1	39.9
	30°	2.9	12.4	29.0	2.7	15.6	37.5
	40°	3.0	11.7	27.7	2.4	14.6	35.8
	50°	3.1	10.6	26.8	2.4	14.2	34.6
	60°	2.7	10.5	26.2	2.7	12.6	33.8
	70°	2.5	10.1	25.8	2.6	12.1	33.3
	80°	2.3	9.2	25.5	2.8	12.3	33.0
	90°	1.2	9.2	25.5	0.6	12.3	32.9
urban	10°	4	6	34.3	4	6	44.3
	20°	4	6	30.9	4	6	39.9
	30°	4	6	29.0	4	6	37.5
	40°	4	6	27.7	4	6	35.8
	50°	4	6	26.8	4	6	34.6
	60°	4	6	26.2	4	6	33.8
	70°	4	6	25.8	4	6	33.3
	80°	4	6	25.5	4	6	33.0
	90°	4	6	25.5	4	6	32.9
sub- urban/rural	10°	1.79	8.93	19.52	1.9	10.7	29.5
	20°	1.14	9.08	18.17	1.6	10.0	24.6
	30°	1.14	8.78	18.42	1.9	11.2	21.9
	40°	0.92	10.25	18.28	2.3	11.6	20.0
	50°	1.42	10.56	18.63	2.7	11.8	18.7
	60°	1.56	10.74	17.68	3.1	10.8	17.8
	70°	0.85	10.17	16.50	3.0	10.8	17.2
	80°	0.72	11.52	16.30	3.6	10.8	16.9
	90°	0.72	11.52	16.30	0.4	10.8	16.8

- as for scintillation, the procedure in Section 6.6 of TR 38.811 is considered, as also reported in D2.1 for link budget computations;
- with respect to the gaseous absorption, ITU-R Recommendation P. 676 is used to compute the zenith attenuation, which is then adjusted based on the elevation angle:

$$A_i^{(gas)} = \frac{A_{zenith}}{\sin \varepsilon_i}$$

The computation of these terms is defined as *estimation phase* since it is the moment in which the users estimate their CSI and/or their reference beam index, so as to correctly implement the considered precoding techniques. It is separated from the *transmission phase*, in which the precoded symbols are sent from the satellite to the scheduled users, because the satellites moved along their orbits and, for moving users, also the users' locations are changed. Consequently, both the stochastic and the non-stochastic (depending on the elevation angle) terms in the additional losses can be significantly different from those used in the estimation phase, leading to a performance loss due to the misalignment between the transmission conditions and the precoding matrices. Finally, $\varphi_i^{(s)}$ models a random phase offset to take into account any difference

in the synchronisation between the satellites' oscillators, distributed as a uniform random variable between 0 and 2π.

2.1.3.3 Users and satellites movement

In this section of the software tool, the movement of the users and the satellites in the considered system is taken into account. In particular, as described in D3.2, we have to take into account that the pre-computed precoding matrices (MB and SS-MMSE) and the CSI-based precoding matrix (MMSE) are based on the estimates that users perform at a time instant t_0, for the deployment considered above and shown in the figures. As extensively discussed in D3.2, the estimated information then has to be sent back to the gNB-CU for Centralised Precoding Computation (CPC) or to the on-board gNB-DU for Distributed Precoding Computation (DPC), in order to compute the precoding and scheduling matrices. Thus, the delay between the estimation instant and that in which precoding actually happens is given by:

$$\Delta t = t_{ut,max} + 2t_{feeder} + 2t_r + t_p \tag{23}$$

where $t_{ut,max}$ is the maximum propagation delay for the user terminals requesting connectivity in the coverage area towards the farthest satellite, t_{feeder} is the delay on the feeder link between the satellite (perhaps in another swarm) connected to the GW (and, thus, to the reference gNB-CU) for CPC, t_r is the latency related to routing of the information through the ISLs, and t_p is the processing delay to compute the precoding matrix. When DPC is implemented, the latency to obtain the users' information and compute the precoding matrix is given by $t_{ut,max} + t_p$ only; however, in order to also obtain the users' symbols to be precoded, the other terms have to be considered and, thus, no difference arises between CPC and DPC from this point of view.

Assuming a negligible impact of the routing and processing delays[6], users that can see the satellites with an elevation as low as $30°$, and that the GW is seen by the satellite physically connected to the network at $10°$ (worst case assumption), we obtain $\Delta t = 0.0167$ s for the dual satellite scenario previously introduced; clearly, other values can be obtained in case a different number of satellites is taken into account and when including the routing and processing delays, but this value already provides a realistic performance assessment when taking into account the difference between the channel matrix in the estimation phase and that in the transmission phase. In this time interval, both the users and the satellites moved and, thus: i) the best serving beam for a user might not be the estimated one; and ii) the estimated CSI vectors might be different from the estimated ones. With respect to the latter, apart from the different slant ranges and antenna gains, a different realisation of the random variables defining the large scale and scintillation losses. Finally, it shall be noticed that, since the satellite is moving, also the on-ground beam lattice will be moved accordingly.

With respect to the users, their movement is modelled based on the speed reported in Table 4. To this aim, we assume that each user is moving in a random direction distributed as a uniform random variable between $0°$ and $360°$ with respect to the z-axis in an Earth-Centered Earth-Fixed (ECEF) reference system, *i.e.*, with respect to the North Pole. Let us denote by ψ_i the random direction and by $v_{UT,i}$ the speed in km/h for the generic i-th user; in the time interval Δt, this user moves from a location $\tilde{\mathbf{p}}_{t_0,i} = \left(\mathrm{lat}_{t_0,i}, \mathrm{lon}_{t_0,i}\right)$ to a new location $\tilde{\mathbf{p}}_{\Delta t,i} = \left(\mathrm{lat}_{\Delta t,i}, \mathrm{lon}_{\Delta t,i}\right)$ that are separated by an angle with respect to the Earth center given by:

$$\delta_i = \frac{180}{\pi}\frac{\Delta t \cdot v_{UE,i}}{3.6R_E}\ [\mathrm{deg}] \tag{24}$$

Let us denote by $\tilde{\mathbf{p}}_{t_0,i}^{(ECEF)}$ and $\tilde{\mathbf{p}}_{\Delta t,i}^{(ECEF)}$ the starting and final locations of the user in ECEF coordinates, where:

[6] A detailed analysis on these aspects will be provided in the next phase of the study, *i.e.*, D3.5 or D3.6.

$$\tilde{\mathbf{p}}_{t_0,i}^{(ECEF)} = \begin{bmatrix} \cos \text{lat}_{t_0,i} \cos \text{lon}_{t_0,i} \\ \cos \text{lat}_{t_0,i} \sin \text{lon}_{t_0,i} \\ \sin \text{lat}_{t_0,i} \end{bmatrix}$$
$$\tilde{\mathbf{p}}_{\Delta t,i}^{(ECEF)} = \begin{bmatrix} \cos \text{lat}_{\Delta t,i} \cos \text{lon}_{\Delta t,i} \\ \cos \text{lat}_{\Delta t,i} \sin \text{lon}_{\Delta t,i} \\ \sin \text{lat}_{\Delta t,i} \end{bmatrix} \quad (25)$$

It can be shown that:

$$\tilde{\mathbf{p}}_{\Delta t,i}^{(ECEF)} = \begin{bmatrix} -\sin \delta_i \left(\sin \text{lat}_{\Delta t,i} \cos \text{lon}_{t_0,i} \cos \psi_i + \sin \text{lon}_{t_0,i} \sin \psi_i \right) + \cos \delta_i \cos \text{lat}_{\Delta t,i} \cos \text{lon}_{t_0,i} \\ -\sin \delta_i \left(\sin \text{lat}_{\Delta t,i} \sin \text{lon}_{t_0,i} \cos \psi_i - \cos \text{lon}_{t_0,i} \sin \psi_i \right) + \cos \delta_i \cos \text{lat}_{\Delta t,i} \sin \text{lon}_{t_0,i} \\ \sin \delta_i \cos \text{lat}_{\Delta t,i} \cos \psi_i + \cos \delta_i \sin \text{lat}_{\Delta t,i} \end{bmatrix} \quad (26)$$

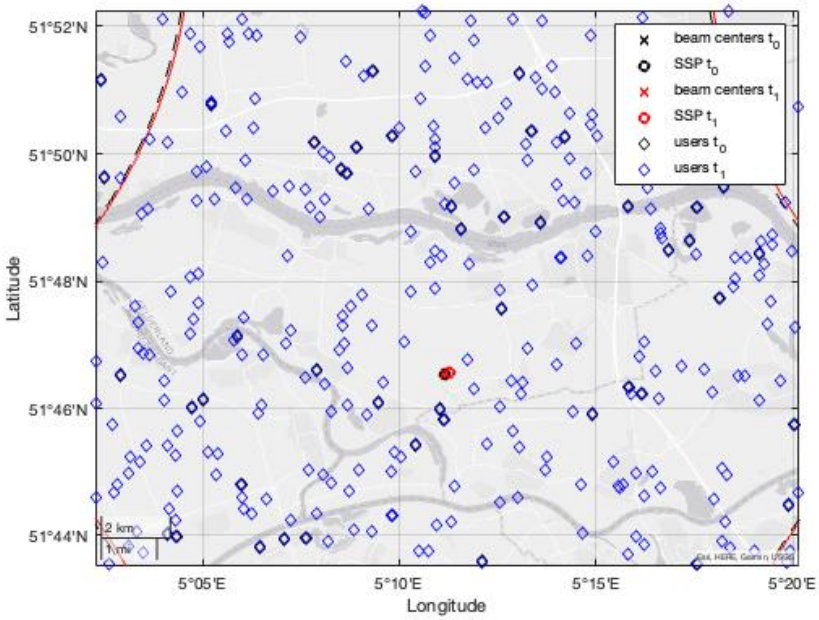

Figure 14 - Beam centers, SSP, and user locations at t_0 and $t_1 = t_0 + \Delta t$ in the stand-alone scenario.

From the above coordinates, it is straightforward to obtain the latitude and longitude coordinates:

$$\text{lat}_{\Delta t,i} = \sin^{-1} \tilde{\text{p}}_{\Delta t,i}^{(ECEF,z)}$$
$$\text{lon}_{\Delta t,i} = \text{atan2} \left(\tilde{\text{p}}_{\Delta t,i}^{(ECEF,y)}, \tilde{\text{p}}_{\Delta t,i}^{(ECEF,x)} \right) \quad (27)$$

Figure 14 shows an example of users and satellite locations after $\Delta t = 0.0167$ s; in this figure, the aircraft receiver type was assumed, with $v_{UE} = 1000$ km/h. While the new beam edges and the SSP locations can be observed, the users are almost in the same position. This is reasonable, since, in this limited time interval, an aircraft travelled for 4.6 m, approximately. Thus, we can expect that the user movement, in this context, does not significantly affect the system performance, while the satellite movement might have a more relevant impact.

2.1.3.4 Transmission phase

In this step, the actual user channel vectors are computed so as to assess the system performance. Thus, the new coordinates obtained in the previous phase are exploited in order to obtain the actual radiation pattern values, new slant ranges, and current additional losses (large scale and scintillation). The channel coefficients are obtained from the same equations provided above and reported here for the sake of clarity:

$$\tilde{h}_{i,n}^{(feed,s)} = g_{i,n}^{(tx,s)} g_{i,n}^{(rx,s)} \frac{\lambda}{4\pi d_{i,n}^{(s)}} \sqrt{\frac{L_{i,n}^{(s)}}{\kappa B T_i}} e^{-j\frac{2\pi}{\lambda} d_{i,n}^{(s)}} e^{j\varphi_i^{(s)}}, n = 1, \dots, N_F \quad (28)$$

$$\tilde{h}_{i,j}^{(beam,s)} = g_{i,j}^{(tx,s)} g_{i,j}^{(rx,s)} \frac{\lambda}{4\pi d_{i,j}^{(s)}} \sqrt{\frac{L_{i,j}^{(s)}}{\kappa B T_i}} e^{-j\frac{2\pi}{\lambda} d_{i,j}^{(s)}} e^{j\varphi_i^{(s)}}, j = 1, \dots, N_B \quad (29)$$

where the tilde highlights that these are different channels compared to those obtained in the estimation phase (for MMSE) and in the system configuration phase (for MB and SS-MMSE). Notably, this misalignment might have a significant impact on the MMSE performance, in particular when the additional losses are included in the scenario; as for MB and SS-MMSE, they are based on approximated channels coefficients computed for the beam centers and, thus, they are expected to be less sensitive to such impairments.

As previously mentioned, for the time being no advanced RRM algorithm is implemented and the users are randomly scheduled. In particular, at each time frame one user per beam is randomly selected and the number of time frames is computed so as to ensure that all users in all beams have been served at least once. It shall be also noticed that, for MMSE in the feed space, there would be no need for a beam lattice generation; however, for the sake of a fair comparison with MB and SS-MMSE, which require the lattice also in the feed space, we still consider the random user selection on a beam-basis. Moreover, this approach also gives the implicit advantage of limiting the time frames in which two users too close to each other are scheduled together, which is detrimental for the precoding performance as detailed in [5]. The random scheduling algorithm, denoted by $\mathcal{S}$, thus defines a $N_B \times N_{tf}$ matrix $\mathbf{Q}$ in which the generic j-th column contains the indexes of the users to be served in the j-th time frame. In future WP3 activities, advanced RRM algorithms will be considered.

Table 9 - Summary of possible precoding-normalisation combinations for the numerical assessment.

Space	Precoding	Normalisations
feed	MMSE	SPC, MPC, PAC (sSPC, sMPC)
	MB	SPC
	SS-MMSE	SPC, MPC, PAC (sSPC, sMPC)
beam	MMSE	SPC, MPC, PAC (sSPC, sMPC)
	SS-MMSE	SPC, MPC, PAC (sSPC, sMPC)

Focusing on the generic time frame, the signal received at the corresponding user terminals can be written as reported in D3.2:

$$\begin{aligned} \mathbf{y}^{(j)} &= \mathbf{H}^{(feed)} \mathbf{W}_x^{(q)} \mathbf{s}^{(q)} + \mathbf{z}^{(q)}: \text{feed space} \\ \mathbf{y}^{(j)} &= \mathbf{H}^{(beam)} \mathbf{W}_x^{(q)} \mathbf{s}^{(q)} + \mathbf{z}^{(q)}: \text{beam space} \end{aligned} \quad (30)$$

where x denotes the combination of precoding algorithm and normalisation exploited at the transmitter side. The possible combinations are summarised in Table 9.

2.1.4 Key Performance Indicators

Based on the received symbols, the Key Performance Indicators (KPI) of each user scheduled in the j-th time frame can be obtained. In particular, the $N_B \times N_B$ power transfer matrix is obtained:

$$\mathbf{A}^{(q)} = \left| \mathbf{H}^{(feed)} \mathbf{W}_x^{(q)} \right|^2 : \text{feed space}$$

$$\mathbf{A}^{(q)} = \left|\mathbf{H}^{(beam)}\mathbf{W}_{x}^{(q)}\right|^{2} : \text{beam space} \tag{31}$$

As extensively discussed in D3.2, this matrix contains the intended users' power on the diagonal elements, while the off-diagonal elements contain the interference received from each of the other users' signals. Based on this matrix, it is thus possible to easily compute the received Signal-to-Noise Ratio (SNR) and Interference-to-Noise Ratio (INR):

$$\begin{aligned} SNR_k^{(q)} &= a^{(q)}(k,k) \\ INR_k^{(q)} &= \sum_{\substack{i=1 \\ i\neq k}}^{N_B} a^{(q)}(k,i) \end{aligned} \tag{32}$$

From these values, we are able to also obtain:

- the SINR, $SINR_k^{(q)} = {SNR_k^{(q)}}\Big/{\left(1 + INR_k^{(q)}\right)}$, since the noise power is already included in the channel coefficients, as previously discussed;
- the Signal-to-Interference Ratio (SIR), $SIR_k^{(q)} = {SNR_k^{(q)}}\Big/{INR_k^{(q)}}$.

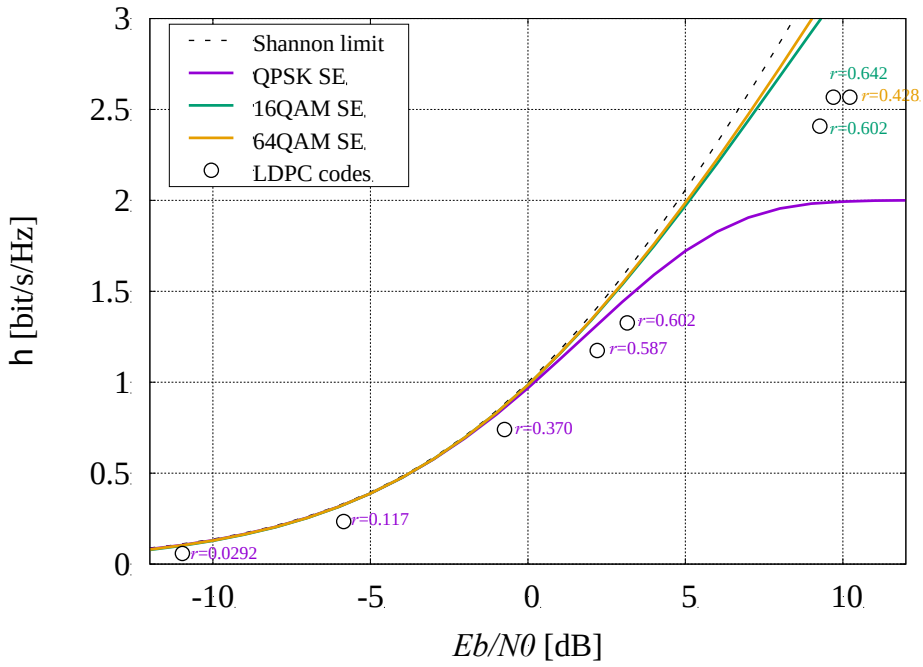

Figure 15 - 5G ModCods spectral efficiency values compared to the Shannon bound.

Finally, the spectral efficiency with which each user in each time frame is served is obtained through the Shannon bound formula:

$$\eta_k^{(q)} = \log_2\left(1 + SINR_k^{(q)}\right) \tag{33}$$

With respect to the spectral efficiency, it shall be highlighted that the Shannon formula provides the theoretical upper bound for a given SINR level. However, there are advanced ModCod techniques that lead to spectral efficiency values that are extremely close to the Shannon bound. This is the case of 5G systems or DVB-S2X systems. Figure 15 shows the Shannon limit and the theoretical spectral efficiency curves of finite modulations for AWGN channel. In the same figure, we report the spectral efficiency of ModCods for 5G systems based on LDPC codes of different rate, obtained by computer simulations based on the software described in Annex A. In particular, the points correspond to the SINR needed to achieve a bit error rate of 10^{-4} in the hypothesis of

AWGN channel. The results show that the spectral efficiency of these ModCods is extremely close to the upper bound. Another important aspect is that the 5G system ModCods have a fine granularity due to the availability of many codes with different rate. For this reason, we use equation (33) to obtain the maximum spectral efficiency that the users would obtain in AWGN channel in order to have a general analysis that is not dependent on the specific ModCod or amount of allocated resources/signalling in the 5G time-frequency resource grid. It is worth noticing that a loss in spectral efficiency should be expected in real systems due to the overhead of the cyclic prefix and to the signalling to manage, for example, system aspects and mobility.

From the performance of each user in each time frame, for each of the numerical iterations considered in the assessment, the average KPIs are computed:

$$\begin{aligned}\overline{SNR} &= \mathbb{E}_{k,q,m}\left\{SNR_k^{(q,m)}\right\}\\ \overline{INR} &= \mathbb{E}_{k,q,m}\left\{INR_k^{(q,m)}\right\}\\ \overline{SINR} &= \mathbb{E}_{k,q,m}\left\{SINR_k^{(q,m)}\right\}\\ \overline{SIR} &= \mathbb{E}_{k,q,m}\left\{SIR_k^{(q,m)}\right\}\\ \bar{\eta} &= \mathbb{E}_{k,q,m}\left\{\eta_k^{(q,m)}\right\}\end{aligned} \tag{33}$$

where the additional index m refers to the Monte Carlo iteration. In addition to the average performance, in order to obtain a more detailed overview of the system performance, we also derive the CDF functions of the above metrics, for each scenario and technique-normalisation. Clearly, the finite packet length prevents the system from achieving the maximum theoretical performance; while this aspect will be taken into account in the next activities, these results already allow to identify the most relevant trends in the system performance.

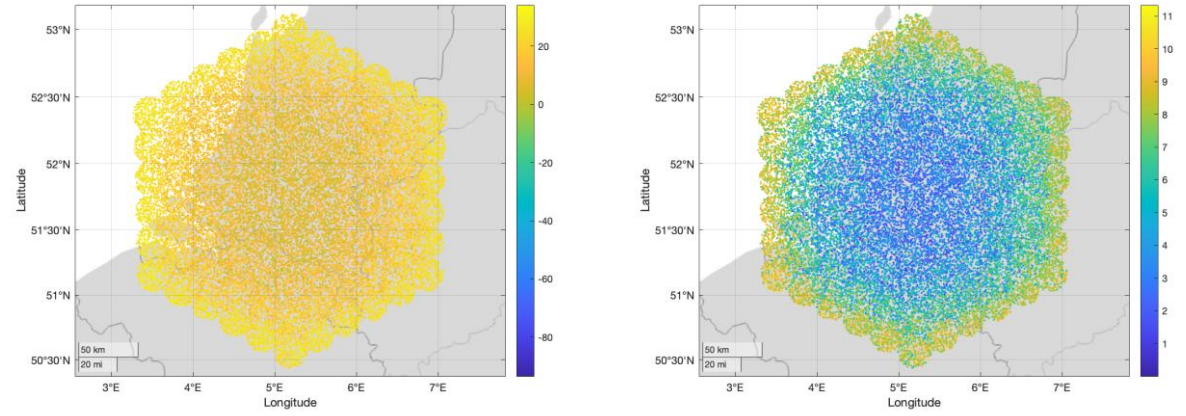

(a) SINR [dB] (b) spectral efficiency [bit/s/Hz]

Figure 16 - Example of MMSE-SPC precoding: SINR and spectral efficiency.

Figure 16, Figure 17, and Figure 18 show an example of feed space precoding with MMSE SPC, PAC, and MPC normalisations, respectively. These examples were obtained for fixed VSAT terminals in the stand-alone scenario operating in S-band and they refer to a single iteration of the Monte Carlo simulation. The propagation scenario is LOS in a dense urban environment, with $P_{t,dens} = 4$ dBW and $n_{tier} = 5$. In line with the exhaustive discussion in the next section, SPC provides the best performance, with MPC quite close to this optimum; as for PAC, the system suffers from the extended interference caused by the disruption of the orthogonality in the precoding matrix columns.

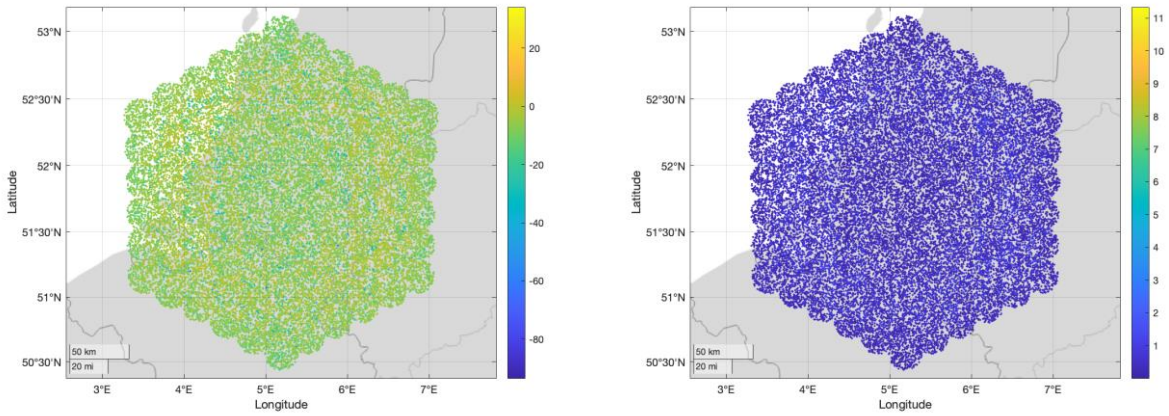

(a) SINR [dB] (b) spectral efficiency [bit/s/Hz]

Figure 17 - Example of MMSE-PAC precoding: SINR and spectral efficiency.

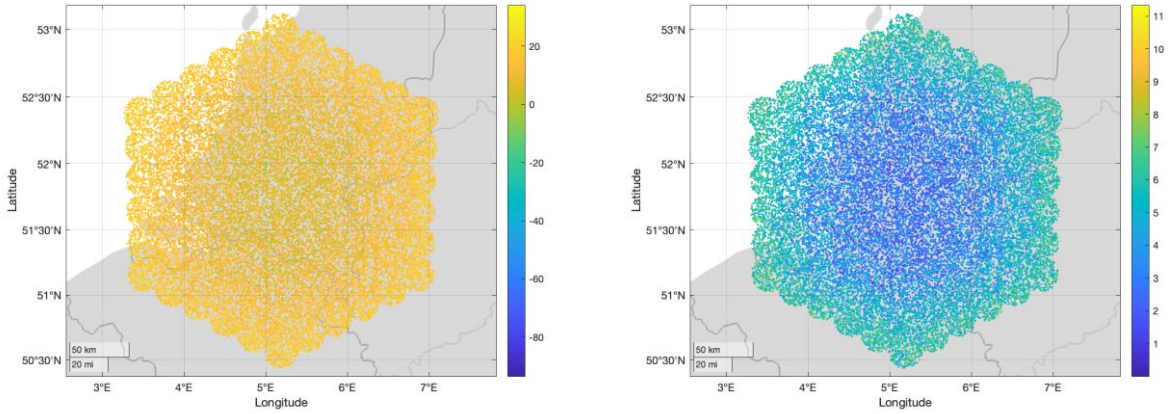

(a) SINR [dB] (b) spectral efficiency [bit/s/Hz]

Figure 18 - Example of MMSE-MPC precoding: SINR and spectral efficiency.

2.2 Performance assessment

In this section, we report the outcomes of the extensive numerical assessment performed for the system defined above. The list of scenarios is reported in Table 10. For each scenario, fixed and public safety ($v_{UE} = 250$ km/h) terminals are considered; moreover, both the stand-alone and the dual satellite hot-spot scenario are evaluated, with more satellites to be considered in future activities. With respect to the precoding technique, the considered combinations are those previously reported in Table 9. For each scenario, the KPIs discussed above are computed and evaluated: average values and CDFs of the SNR, SINR, SIR, INR, and achievable spectral efficiency. The parameters of the numerical simulations are reported in Table 11. While the user density might seem limited, it shall be recalled that we are not considering scheduling algorithms and, thus, the user density does not impact the overall performance, as long as the number of Monte Carlo iterations guarantees the system convergence.

Table 10 - List of scenarios for the numerical assessment.

Propagation	Environment	Space	Terminal
pLOS	-	beam	VSAT
			handheld

		feed	VSAT
			handheld
LOS	dense urban	beam	VSAT
			handheld
		feed	VSAT
			handheld
	urban	beam	VSAT
			handheld
		feed	VSAT
			handheld
	sub-urban	beam	VSAT
			handheld
		feed	VSAT
			handheld
NLOS	dense urban	beam	VSAT
			handheld
		feed	VSAT
			handheld
	urban	beam	VSAT
			handheld
		feed	VSAT
			handheld
	sub-urban	beam	VSAT
			handheld
		feed	VSAT
			handheld

Table 11 - Parameters of the numerical assessment.

Parameter	Range
System band	S
Beamforming space	feed, beam
Receiver type	VSAT, handheld
Receiver scenario	fixed, public safety
Propagation scenario	pLOS, LOS, NLOS
Total on-board power density $P_{t,dens}$	$0, 4, 8, 12$ dBW/MHz
Number of tiers n_{tier}	5
User density δ_{UE}	0.5 users/km^2
Radiation pattern at beam edge ΔG_{edge}	3 dB
Monte Carlo iterations	70

2.2.1 Stand-alone satellite scenario

For the stand-alone scenario, the precoding algorithms are MMSE (benchmark) and SS-MMSE for beam space precoding, while in the feed space we also include MB (which has the same performance of the non-precoded system in the beam space). In terms of normalisations, SPC, MPC, and PAC are considered for the MMSE and SS-MMSE algorithms; as shown in D3.2, with the MB approach all normalisations lead to the same precoding matrix.

2.2.1.1 Fixed terminals

We first focus on the pure LOS scenario, in which, as described above, the channel coefficients do no include any additional loss as per TR 38.821 and TR 38.811, but it only accounts for free space loss, noise, and phase rotation due to the slant range. Figure 19 shows the average spectral efficiency and Table 12 reports the corresponding values in a heatmap, to give a clear overview of the major trends. In general, the following behaviours can be observed:

- MMSE precoding provides a better performance compared to SS-MMSE and the non-precoded scenario, as expected. However, with low power and handheld terminals the SS-MMSE approach is relatively close to the performance of MMSE. This is motivated by observing that, when the power increases and in particular with VSAT terminals that have a large receiving antenna gain, there is a more critical need for a better interference limitation, *i.e.*, to avoid any approximation in the precoding matrix, and thus the MMSE precoder provides significantly better results. In scenarios with a reduced need for interference limitation, the SS-MMSE is a good solution;

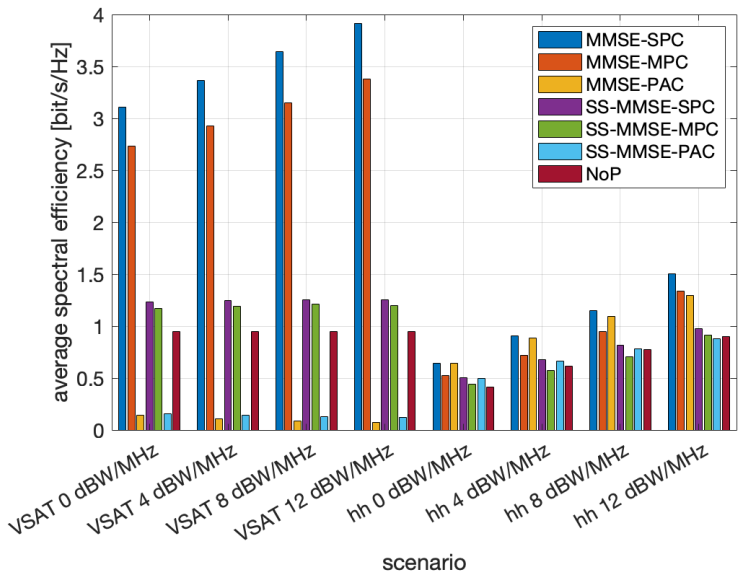

Figure 19 - Average spectral efficiency [bit/s/Hz] *for the pLOS scenario in the beam space, stand-alone satellite.*

- in terms of normalisations, SPC always provides the best performance as expected. However, this approach does not guarantee that an antenna or feed does not exceed the power it can emit and, thus, the MPC and PAC solutions should be preferred. Comparing them, it can be noticed that the MPC is significantly better when the interference in the system is larger, *i.e.*, for VSAT terminals with large antenna gains (all antennas are ideally pointed towards the co-located feeds on-board the satellite): in this case, it is fundamental to keep the orthogonality in the precoding matrix columns. With handheld terminals, both for MMSE and SS-MMSE, as long as the power is limited, it is more important to increase the SNR and, thus, PAC is better: this solution guarantees that each feed or antenna emits the same power level, while perturbing the precoding orthogonality. When the power is increased, interference becomes more impacting and MPC is again the best option;

Table 12 - Average spectral efficiency [bit/s/Hz] *for the pLOS scenario in the beam space, stand-alone satellite.*

Scenario	MMSE SPC	MMSE MPC	MMSE PAC	SS-MMSE SPC	SS-MMSE MPC	SS-MMSE PAC	NoP
VSAT 0 dBW/MHz	3.1111	2.7334	0.1457	1.2331	1.1724	0.1540	0.9457
VSAT	3.3670	2.9290	0.1046	1.2436	1.1897	0.1395	0.9457

4 dBW/MHz							
VSAT 8 dBW/MHz	3.6412	3.1492	0.0860	1.2521	1.2106	0.1317	0.9457
VSAT 12 dBW/MHz	3.9163	3.3797	0.0760	1.2540	1.1985	0.1190	0.9451
Handheld 0 dBW/MHz	0.6434	0.5249	0.6391	0.5024	0.4386	0.4985	0.4139
Handheld 4 dBW/MHz	0.9049	0.7193	0.8860	0.6797	0.5738	0.6655	0.6157
Handheld 8 dBW/MHz	1.1460	0.9489	1.0909	0.8167	0.7076	0.7839	0.7722
Handheld 12 dBW/MHz	1.5061	1.3371	1.2962	0.9741	0.9141	0.8808	0.9025

- comparing the two considered user equipment types, VSATs provide a much better performance thanks to the significantly larger antenna gain compared to handheld terminals. In this scenario, it is worth noticing that there is no advantage of VSATs related to interference rejection with the directive radiation pattern, since it is assumed that all of the UEs' antennas are ideally pointed towards the single satellite, with the legit assumption of co-located antenna feeds;
- finally, observing the trends as a function of the transmission power[7], a larger power allocation leads to larger average rate values. However, this does not apply for VSAT terminals in the absence of precoding: in this case, the intended and interfering power levels change accordingly and, as a consequence, the SINR level is almost constant, with a slight decrease at $P_{t,dens} = 12$ dBW/MHz; with handheld terminals, more limited in terms of receiving antenna gain, larger power levels lead to larger spectral efficiencies.

The above trends are substantiated by the results shown in Figure 20, which reports the CDFs for the SNR, SIR, and SINR in the pLOS scenario for VSAT terminals in the beam space. It can be noticed that SPC provides a larger SNR value and that, for increasing transmission power levels, the SIR increases accordingly, leading to a better SINR. As for PAC, a larger transmission power leads to a worse SINR curve (*i.e.*, on the left of the low-power case), denoting a significant sensitivity to the loss of orthogonality in the precoding matrix columns in scenarios with increased interference. This is also evident by observing the SIR and SNR trends, which highlight some interesting behaviours. For an increased transmission power, the SNR is always increased, but this is significantly more evident with PAC (and even more without precoding) compared to SPC and MPC. In this case, the satellite is increasing the transmission power of each antenna feed by the same amount; an increased SNR level is also present for MPC and SPC, but more limited: in this case, the precoder is actually exploiting the increased power and, at the same time, trying to limit interference by preserving the orthogonality in the precoding matrix columns. Thus, despite the SNR in figure (c) for SPC and MPC is significantly below that obtained with PAC (and even more compared to the non-precoded case), the performance is improved since the SIR is much better. In fact, looking at figure (b), MPC and SPC have a significantly better performance in limiting interference compared to both the non-precoded and PAC cases. Actually, the PAC normalisation leads to a performance that is even worse than the non-precoded case with VSATs, highlighting the poor interference rejection obtained with this approach in scenarios with a significant co-channel interference.

It is also worth mentioning that, for MPC and SPC, the SIR plots are overlapped: in fact, the SIR does not depend on a scalar multiplicative factor and, consequently, it is exactly the same in both normalisations. Finally, it is also interesting to note that SPC and MPC provide a fairer power

[7] Despite the performance is provided as a function of the transmission power density, we often refer to the transmission power since in all scenarios the user bandwidth is the same; thus, from a conceptual point of view, these two terms can be used interchangeably.

allocation to the users, as the SNR CDFs show a significantly steeper behaviour compared to PAC: in this case, since the power allocation is uniform and independent of the channel, users in good propagation conditions will be privileged compared to users in bad conditions, which will be further penalised by this normalisation.

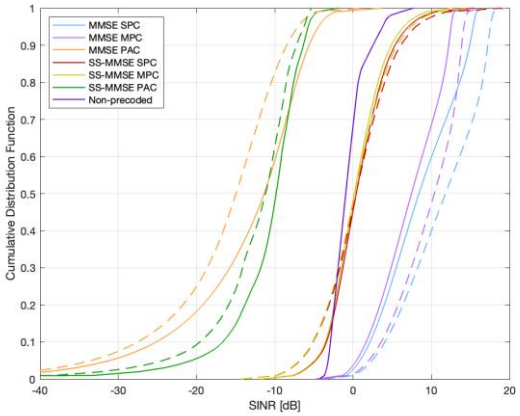

(a) SINR [dB]

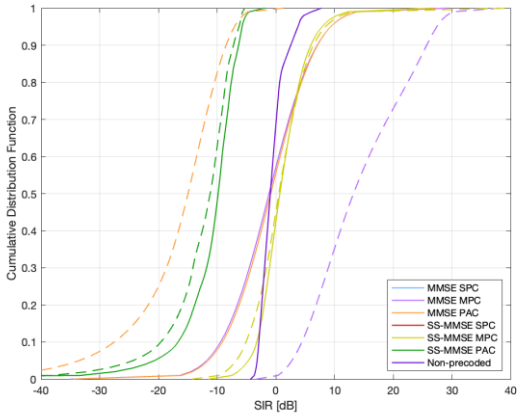

(b) SIR [dB]

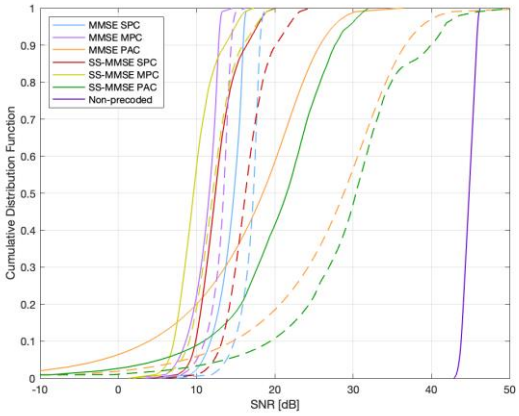

(c) SNR [dB]

Figure 20 - SINR, SIR, and SNR CDFs for VSAT terminals in the pLOS scenario for beam space precoding, $P_{t,dens} = 0$ dBW/MHz (solid line) and $P_{t,dens} = 12$ dBW/MHz (dashed line).

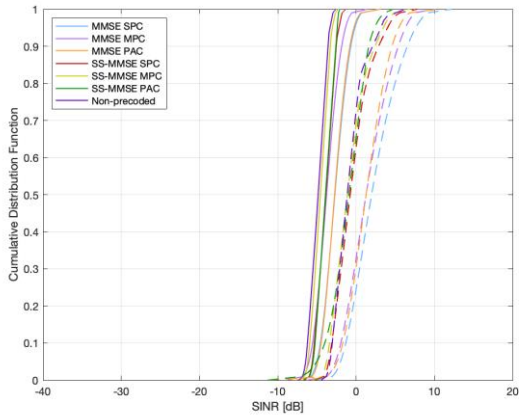

(a) SINR [dB]

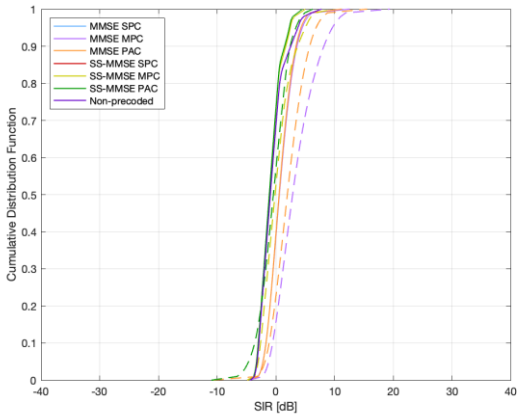

(b) SIR [dB]

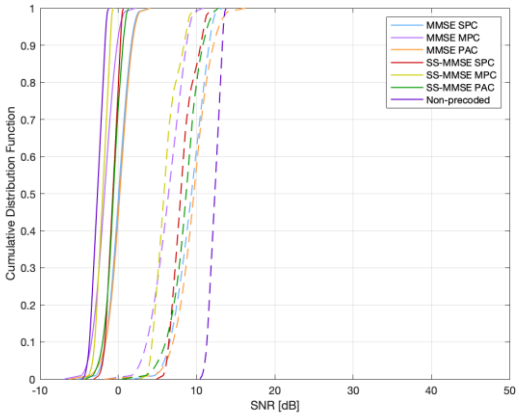

(c) SNR [dB]

Figure 21 - SINR, SIR, and SNR CDFs for handheld terminals in the pLOS scenario for beam space precoding, $P_{t,dens} = 0$ dBW/MHz (solid line) and $P_{t,dens} = 12$ dBW/MHz (dashed line).

Figure 21 shows the CDF plots when handheld terminals are considered:

- the performance of the PAC normalisation is improved since, as previously discussed, in scenarios with a more limited interference, guaranteeing an equal transmission power level while also disrupting the orthogonality of the precoding matrix is more acceptable;
- the performance with larger transmission power is always better, again due to a more limited interference because of the receiving antenna gain equal to 0 dBi. This is also evident thanks to the SIR in figure (b), where it can be noticed that for all precoding approaches, a very similar SIR is obtained, *i.e.*, the system is less sensible to a loss in the orthogonality of the precoder columns;
- also in terms of the intended power, the different normalisation approaches do not have a significant impact, as shown in the SNR CDFs in figure (c).

Figure 22 and Table 13 report the results for feed space precoding, in which MB precoding is included. It shall be noticed that the performance without precoding is not shown; in fact, in the feed space it is not meaningful to implement a non-precoded and non-beamformed system, which would lead to an extremely poor performance. A fair comparison is with a beamformed system

without precoding, which is the result obtained with MB in the feed space. As already mentioned, the MB performance in the feed space is completely equivalent to the non-precoded performance in the beam space: this technique approximates the columns of the precoding matrix with those of the beamforming matrix and, without an illumination plan (beam-hopping) related to a proper scheduling, it is equivalent to a non-precoded scheme.

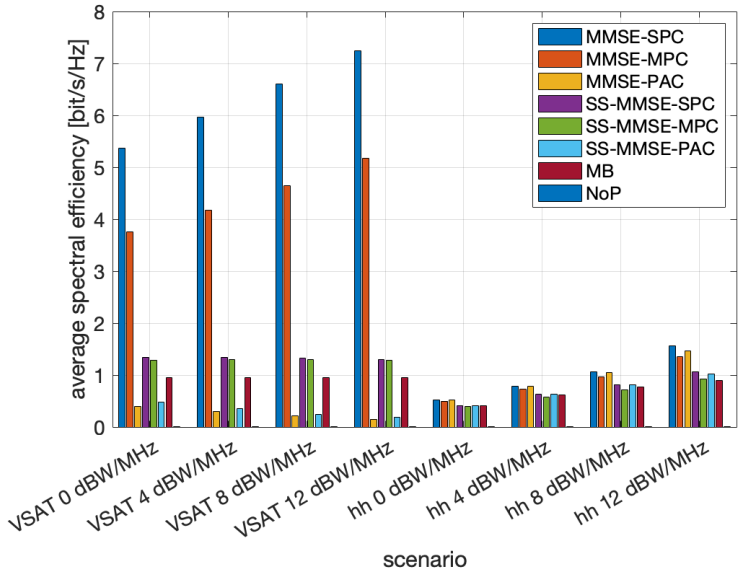

Figure 22 - Average spectral efficiency [bit/s/Hz] *for the pLOS scenario in the feed space, stand-alone satellite.*

Table 13 - Average spectral efficiency [bit/s/Hz] *for the pLOS scenario in the feed space, stand-alone satellite.*

Scenario	MMSE SPC	MMSE MPC	MMSE PAC	SS-MMSE SPC	SS-MMSE MPC	SS-MMSE PAC	MB
VSAT 0 dBW/MHz	5.3660	3.7578	0.3952	1.3384	1.2787	0.4768	0.9457
VSAT 4 dBW/MHz	5.9711	4.1793	0.2944	1.3350	1.2952	0.3570	0.9457
VSAT 8 dBW/MHz	6.5975	4.6512	0.2121	1.3214	1.2934	0.2458	0.9457
VSAT 12 dBW/MHz	7.2407	5.1717	0.1472	1.3003	1.2797	0.1931	0.9451
Handheld 0 dBW/MHz	0.5167	0.4911	0.5159	0.4158	0.3897	0.4157	0.4139
Handheld 4 dBW/MHz	0.7889	0.7307	0.7851	0.6289	0.5703	0.6270	0.6157
Handheld 8 dBW/MHz	1.0648	0.9630	1.0503	0.8179	0.7220	0.8103	0.7727
Handheld 12 dBW/MHz	1.5574	1.3550	1.4706	1.0571	0.9174	1.0251	0.9025

The trends previously highlighted for the beam space approach are still clear:

- MMSE precoding is always providing the best performance, followed by the SS-MMSE approach. However, while this is always true for the SPC and MPC normalisations, when PAC is considered the MB precoding is better: this is motivated by the loss in terms of interference limitation of the PAC normalisation, discussed above, which leads to a better performance implementing beamforming only (MB);

- the performance of precoding in the feed space is better for larger power levels as long as the SPC and MPC normalisations are used with VSATs and in all cases for handheld terminals. However, when PAC is used for VSATs, the performance becomes worse. This is motivated by the fact that PAC perturbs the orthogonality in the precoder columns and, thus, is sensible to the increased interference level. This behaviour is not present with handheld terminals: in this case, the absence of an antenna gain at the receiver makes the increased transmission power always a beneficial effect;

Table 14 - Relative gain [%] *of feed space precoding compared to beam space approach, pLOS scenario.*

Scenario	MMSE SPC	MMSE MPC	MMSE PAC	SS-MMSE SPC	SS-MMSE MPC	SS-MMSE PAC
VSAT 0 dBW/MHz	72,48	37,48	171,24	8,54	9,07	209,61
VSAT 4 dBW/MHz	77,34	42,69	181,45	7,35	8,87	155,91
VSAT 8 dBW/MHz	81,19	47,69	146,63	5,53	6,84	86,64
VSAT 12 dBW/MHz	84,89	53,02	93,68	3,69	6,78	62,27
Handheld 0 dBW/MHz	-19,69	-6,44	-19,28	-17,24	-11,15	-16,61
Handheld 4 dBW/MHz	-12,82	1,58	-11,39	-7,47	-0,61	-5,79
Handheld 8 dBW/MHz	-7,09	1,49	-3,72	0,15	2,04	3,37
Handheld 12 dBW/MHz	3,41	1,34	13,45	8,52	0,36	16,38

Table 14 shows the relative gain in terms of average spectral efficiency of feed space precoding over the beam space approach. It can be noticed that feed space precoding performs significantly better than beam space precoding for VSAT terminals. Moreover, for VSATs, this gain increases for increasing power levels when MMSE with the SPC or MPC normalisations is used, while it decreases for MMSE with PAC and SS-MMSE precoding: i) in the former case, this behaviour is motivated by the increased interference and the fact that PAC disrupts the orthogonality in the precoder columns; and ii) in the latter, it can be explained by recalling that the SS-MMSE precoding approach is an approximation based on a pre-defined beam lattice and, as such, it is sub-optimal in dealing with the increased interference level. For handheld terminals, the gain of the feed space approach is more limited and, with low power levels, it seems that precoding solutions in the beam space provide a slight advantage. This can be motivated by the significant limitation of the handheld terminals in terms of receiving antenna gain: with a low transmission power from the satellite, the formation of pre-defined beams provides an advantage in terms of directivity compared to working only in the feed space, thus leading to a slightly better performance. When the transmission power is increased, with all precoding and normalisation solutions the feed space approach becomes better than the beam space one.

To further highlight the above trends, Figure 23 and Figure 24 show the average SNR and SIR for beam and feed space precoding, respectively. Focusing on VSATs, it can be noticed that with PAC normalisations, an increased power leads to an increased SNR but a decreased SIR, thus worsening the overall SINR performance. With SPC and MPC, both the SNR and the SIR (they are overlapped as already motivated above) increase, thus providing a better performance. With handheld terminals, also with PAC the SIR tends to increase up to what seems to be a saturation point, thus leading to a performance increase. Comparing the two figures, it can be noticed that the gains are more relevant in the feed space in all scenarios, apart from VSAT terminals with PAC, in which the advantage of a larger transmission power is more evident in the beam space, in line with the results in Table 14. In particular, the SIR decreases significantly for this scenario in the feed space, further highlighting the importance of a non-perturbed precoding matrix.

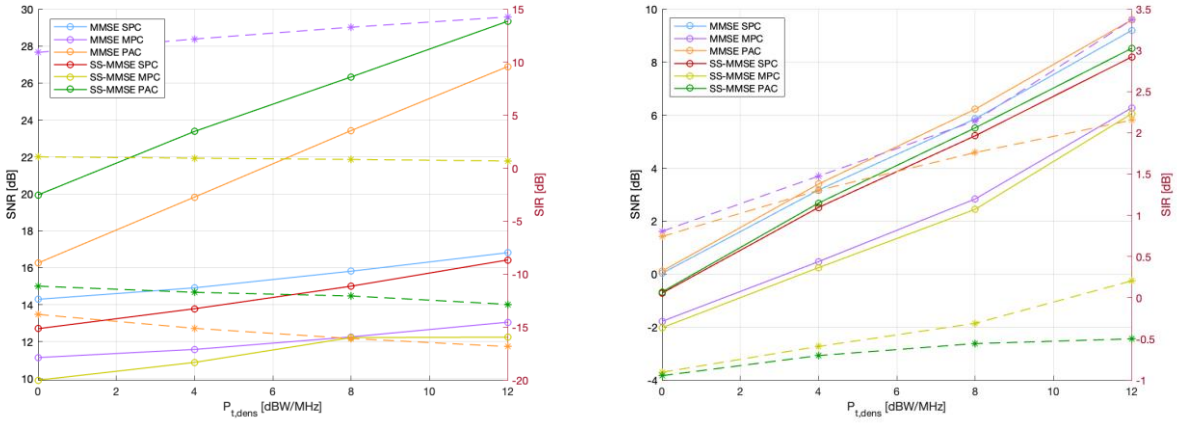

(a) VSAT (b) handheld

Figure 23 - Average SNR (left y-axis, solid line) and SIR (right y-axis, dashed line) and handheld terminals in the beam space, pLOS scenario.

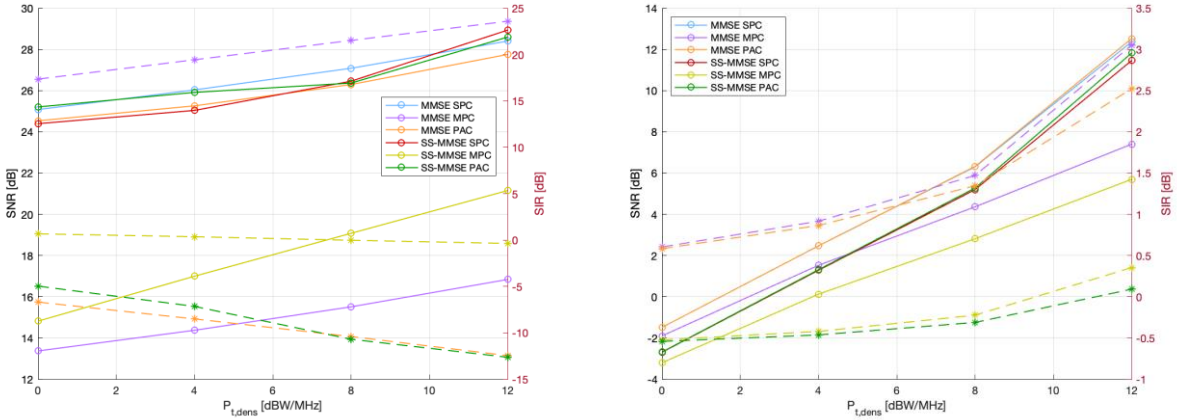

(a) VSAT (b) handheld

Figure 24 - Average SNR (left y-axis, solid line) and SIR (right y-axis, dashed line) for VSAT and handheld terminals in the feed space, pLOS scenario.

Figure 25 and Table 15 report the results obtained in the LOS scenario in the sub-urban case with beam space precoding; as a reminder, as per 3GPP specifications, in this scenario we are assuming that all users are in LOS conditions and they experience shadow fading, scintillation, and gaseous absorptions. It can be noticed that the trends are completely in line with those observed in the pure LOS scenario. However, in most cases the performance with LOS sub-urban conditions is better compared to the pure LOS scenario. This might seem confusing, since we are considering additional losses in the channel propagation and, thus, we might expect a performance degradation.

To motivate this trend, it is worth to remind that we are separating the estimation and transmission phases: the channel matrix used to compute the precoding matrix is thus misaligned compared to that encountered during the actual transmission of the precoded symbols. With MMSE and SS-MMSE precoding, this misalignment leads to a performance degradation, *i.e.*, to an increased interference level compared to that achievable with ideal CSI, because the orthogonality of the precoder columns is not perfectly matched to the channel anymore. Thus, a scenario with a slight increase in the channel losses is preferable since it slightly reduces the interfering power levels at the receiver, basically limiting the loss related to the non-ideal CSI knowledge. This is

substantiated by observing that the most relevant gains with a sub-urban LOS propagation are obtained with the MPC normalisation (up to 3.2 bit/s/Hz), which limits the SNR, while with SPC this advantage is more limited (in the order of 0.17 bit/s/Hz): with a larger power allocation per antenna (SPC), a misalignment between the channel matrix and the precoding matrix can be more disruptive and, thus, the reduced interference thanks to channel losses is less beneficial. Finally, it shall be noticed that, with handheld terminals, the gain of the sub-urban case tends to decrease for increasing power levels: in this case, the limited receiver antenna gain makes the need for a limited interfering power less critical compared to that for a larger intended power, a behaviour opposed to that of VSAT terminals.

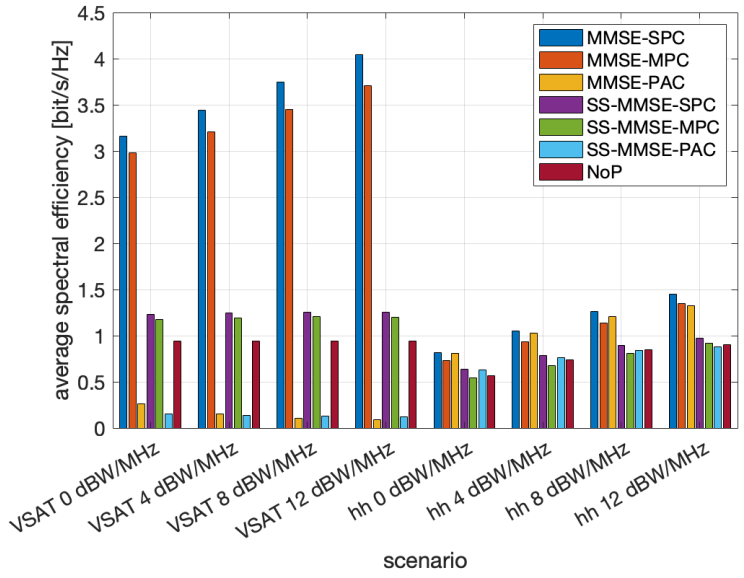

Figure 25 - Average spectral efficiency [bit/s/Hz] *for the LOS scenario in sub-urban conditions in the beam space, stand-alone satellite.*

Table 15 - Average spectral efficiency [bit/s/Hz] *for the LOS scenario in sub-urban conditions in the beam space, stand-alone satellite.*

Scenario	MMSE SPC	MMSE MPC	MMSE PAC	SS-MMSE SPC	SS-MMSE MPC	SS-MMSE PAC	NoP
VSAT 0 dBW/MHz	3.1631	2.9779	0.2602	1.2327	1.1721	0.1540	0.9452
VSAT 4 dBW/MHz	3.4447	3.2050	0.1547	1.2433	1.1893	0.1395	0.9453
VSAT 8 dBW/MHz	3.7429	3.4531	0.1085	1.2519	1.2103	0.1317	0.9453
VSAT 12 dBW/MHz	4.0423	3.7084	0.0877	1.2559	1.2002	0.1192	0.9453
Handheld 0 dBW/MHz	0.8147	0.7300	0.8082	0.6382	0.5401	0.6273	0.5673
Handheld 4 dBW/MHz	1.0513	0.9334	1.0290	0.7867	0.6742	0.7595	0.7393
Handheld 8 dBW/MHz	1.2620	1.1391	1.2057	0.8940	0.8054	0.8405	0.8474
Handheld 12 dBW/MHz	1.4519	1.3457	1.3270	0.9745	0.9144	0.8812	0.9027

Observing the results in Figure 26 and Table 16 for the feed space, we can notice that this behaviour is still present for MMSE precoding with MPC and PAC normalisations, both with VSAT and handheld terminals, with the latter in low power mode. When MMSE with SPC is considered, or we observe handheld terminals with larger transmission power, the pure LOS scenario is better. In this case, working in the feed space provides many more degrees of freedom and, thus, the precoder is able to limit the interference and compensate for the non-ideal CSI at the transmitter side. With SS-MMSE, almost the same performance is obtained, motivated by the fact that this precoding approach is based on an approximated location of the users and, thus, more limited benefits are obtained moving to the feed space.

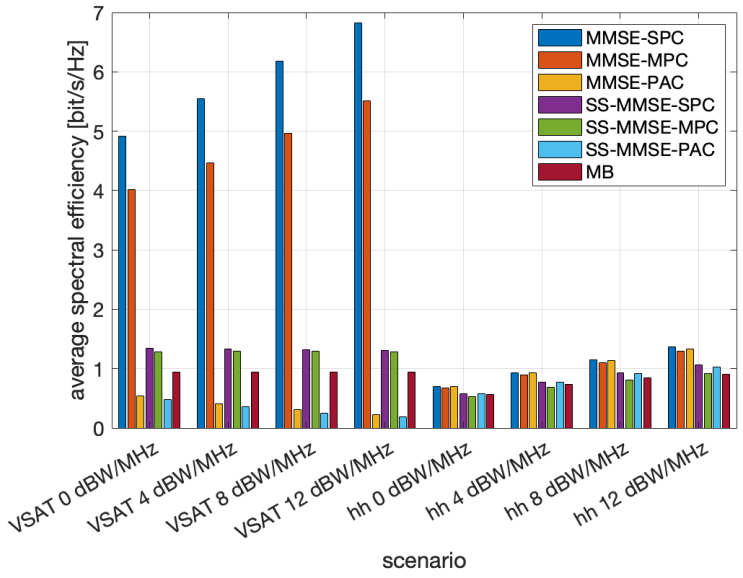

Figure 26 - Average spectral efficiency [bit/s/Hz] *for the LOS scenario in sub-urban conditions in the feed space, stand-alone satellite.*

Table 16 - Average spectral efficiency [bit/s/Hz] *for the LOS scenario in sub-urban condition in the feed space, stand-alone satellite.*

Scenario	MMSE SPC	MMSE MPC	MMSE PAC	SS-MMSE SPC	SS-MMSE MPC	SS-MMSE PAC	MB
VSAT 0 dBW/MHz	4.9218	4.0119	0.5461	1.3385	1.2786	0.4766	0.9452
VSAT 4 dBW/MHz	5.5475	4.4687	0.4101	1.3353	1.2954	0.3569	0.9453
VSAT 8 dBW/MHz	6.1801	4.9660	0.3066	1.3220	1.2938	0.2458	0.9453
VSAT 12 dBW/MHz	6.8245	5.5070	0.2226	1.3035	1.2826	0.1933	0.9453
Handheld 0 dBW/MHz	0.6943	0.6761	0.6933	0.5761	0.5266	0.5749	0.5673
Handheld 4 dBW/MHz	0.9313	0.8982	0.9272	0.7741	0.6872	0.7684	0.7393
Handheld 8 dBW/MHz	1.1452	1.0962	1.1318	0.9328	0.8136	0.9177	0.8474
Handheld 12 dBW/MHz	1.3637	1.2968	1.3266	1.0575	0.9177	1.0253	0.9027

When comparing the beam and feed space precoding approaches in the sub-urban scenario, as reported in Table 17, it can be observed that for VSATs we have a similar trend as that obtained in pure LOS conditions. However, for handheld terminals it is always better to work in the beam space for MMSE precoding; thus, in this case, it is more important to obtain an increased

directivity thanks to a pre-defined beamforming matrix rather than working with more degrees of freedom or preserve the orthogonality. More specifically, in LOS conditions the channel matrix in the estimation phase (the one used to compute the precoding matrix) is further misaligned from the channel matrix encountered during the transmission phase due to the additional losses; this introduces a priori a loss in terms of the optimal orthogonality in the precoder columns. As a consequence, in scenarios with a limited received power at the on-ground terminal it is better to compensate this loss via a pre-determined beamforming (beam space precoding), rather than trying to optimally weight the signals from all of the antenna feeds. This advantage becomes more limited for increasing power levels, in particular with MPC and PAC.

Table 17 - Relative gain [%] *of feed space precoding compared to beam space approach, LOS scenario in sub-urban conditions.*

Scenario	MMSE SPC	MMSE MPC	MMSE PAC	SS-MMSE SPC	SS-MMSE MPC	SS-MMSE PAC
VSAT 0 dBW/MHz	55.60	34.72	109.88	8.58	9.09	209.48
VSAT 4 dBW/MHz	61.04	39.43	165.09	7.40	8.92	155.84
VSAT 8 dBW/MHz	65.12	43.81	182.58	5.60	6.90	86.64
VSAT 12 dBW/MHz	68.83	48.50	153.82	3.79	6.87	62.16
Handheld 0 dBW/MHz	-14.78	-7.38	-14.22	-9.73	-2.50	-8.35
Handheld 4 dBW/MHz	-11.41	-3.77	-9.89	-1.60	1.93	1.17
Handheld 8 dBW/MHz	-9.26	-3.77	-6.13	4.34	1.02	9.19
Handheld 12 dBW/MHz	-6.07	-3.63	-0.03	8.52	0.36	16.35

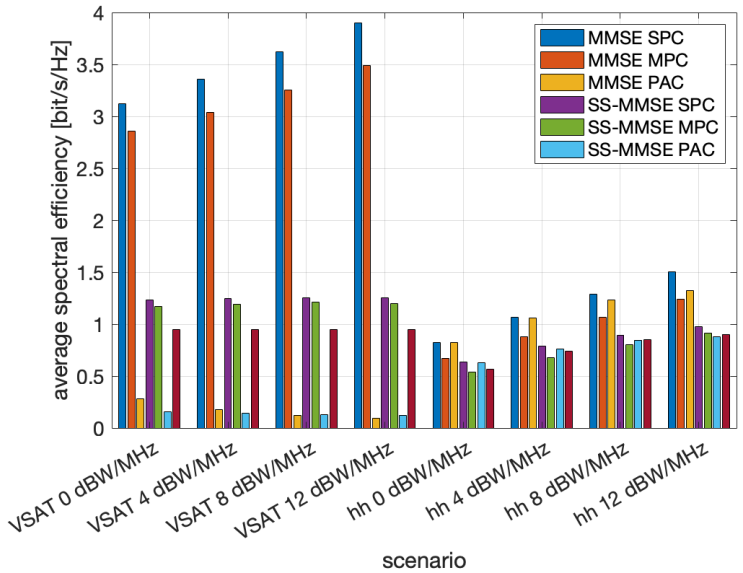

Figure 27 - Average spectral efficiency [bit/s/Hz] *for the LOS scenario in urban conditions in the beam space, stand-alone satellite.*

Figure 27, Figure 28, Table 18, and Table 19 provide the results for the LOS propagation in urban conditions. Similar trends as those reported above for the sub-urban scenario are present:

- SPC and MPC provide the best performance for VSAT terminals, with PAC performing poorly. In particular, its average spectral efficiency is significantly below the non-precoded system or the MB precoding, for the beam and feed spaces, respectively;
- with handheld terminals, PAC provides a performance as good as the MPC and SPC solutions, since in this case the limited antenna gain at the receiver makes an SNR increase more relevant for the overall performance.

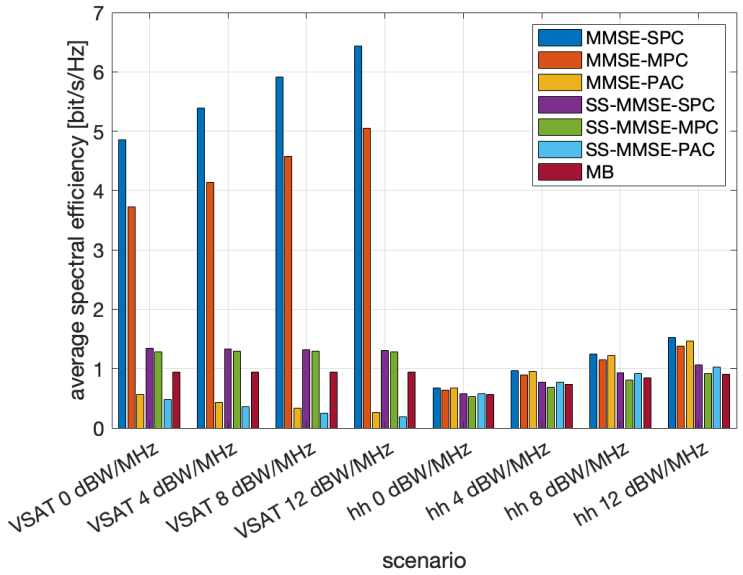

Figure 28 - Average spectral efficiency [bit/s/Hz] *for the LOS scenario in urban conditions in the feed space, stand-alone satellite.*

Table 18 - Average spectral efficiency [bit/s/Hz] *for the LOS scenario in urban condition in the beam space, stand-alone satellite.*

Scenario	MMSE SPC	MMSE MPC	MMSE PAC	SS-MMSE SPC	SS-MMSE MPC	SS-MMSE PAC	NoP
VSAT 0 dBW/MHz	3.1212	2.8577	0.2828	1.2327	1.1721	0.1540	0.9452
VSAT 4 dBW/MHz	3.3563	3.0377	0.1792	1.2433	1.1893	0.1395	0.9453
VSAT 8 dBW/MHz	3.6202	3.2537	0.1242	1.2519	1.2103	0.1317	0.9453
VSAT 12 dBW/MHz	3.9009	3.4864	0.0965	1.2559	1.2002	0.1192	0.9453
Handheld 0 dBW/MHz	0.8200	0.6683	0.8227	0.6382	0.5401	0.6273	0.5673
Handheld 4 dBW/MHz	1.0641	0.8793	1.0585	0.7867	0.6742	0.7595	0.7393
Handheld 8 dBW/MHz	1.2907	1.0642	1.2353	0.8940	0.8054	0.8405	0.8474
Handheld 12 dBW/MHz	1.5016	1.2422	1.3222	0.9745	0.9144	0.8812	0.9027

When comparing the performance with the pure LOS scenario: i) for MMSE precoding with SPC, the performance is slightly worse; ii) the gain with MPC is more limited; and iii) with PAC, the gain is slightly improved. In line with this behaviour, for handheld terminals the gains are less evident and with large transmission power levels, the pLOS scenario is better.

Table 19 - Average spectral efficiency [bit/s/Hz] *for the LOS scenario in urban condition in the feed space, stand-alone satellite.*

Scenario	MMSE SPC	MMSE MPC	MMSE PAC	SS-MMSE SPC	SS-MMSE MPC	SS-MMSE PAC	MB
VSAT 0 dBW/MHz	4.8560	3.7252	0.5607	1.3385	1.2786	0.4766	0.9452
VSAT 4 dBW/MHz	5.3905	4.1338	0.4364	1.3353	1.2954	0.3569	0.9453
VSAT 8 dBW/MHz	5.9182	4.5744	0.3401	1.3220	1.2938	0.2458	0.9453
VSAT 12 dBW/MHz	6.4350	5.0489	0.2606	1.3035	1.2826	0.1933	0.9453
Handheld 0 dBW/MHz	0.6727	0.6375	0.6711	0.5761	0.5266	0.5749	0.5673
Handheld 4 dBW/MHz	0.9603	0.8968	0.9542	0.7741	0.6872	0.7684	0.7393
Handheld 8 dBW/MHz	1.2422	1.1456	1.2225	0.9328	0.8136	0.9177	0.8474
Handheld 12 dBW/MHz	1.5207	1.3788	1.4618	1.0575	0.9177	1.0253	0.9027

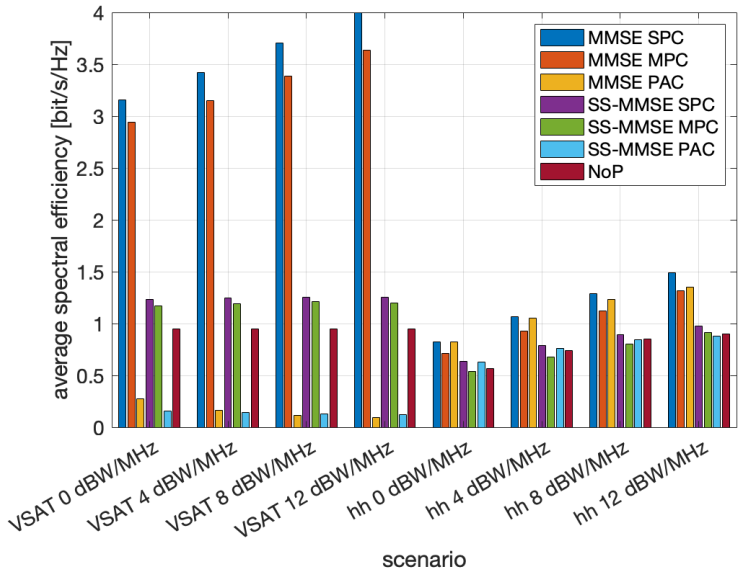

Figure 29 - Average spectral efficiency [bit/s/Hz] *for the LOS scenario in dense-urban conditions in the beam space, stand-alone satellite.*

Comparing the beam and the feed space performance for VSAT terminals, the performance is much better in the feed space; for handheld terminals with large transmission power, the improvement is still present, but limited. Finally, when handheld terminals are considered with low transmission power levels, the directivity obtained with beamforming makes the beam space approach more suitable, as already observed.

To conclude the numerical assessment for LOS conditions, we report the results the beam and feed space precoding in the dense-urban scenario. The overall trend is aligned with the observations provided above for the urban and sub-urban scenarios.

Table 20 - Average spectral efficiency [bit/s/Hz] *for the LOS scenario in dense urban condition in the beam space, stand-alone satellite.*

Scenario	MMSE SPC	MMSE MPC	MMSE PAC	SS-MMSE SPC	SS-MMSE MPC	SS-MMSE PAC	NoP
VSAT 0 dBW/MHz	3.1539	2.9393	0.2711	1.2327	1.1721	0.1540	0.9452
VSAT 4 dBW/MHz	3.4176	3.1489	0.1639	1.2433	1.1893	0.1395	0.9453
VSAT 8 dBW/MHz	3.7033	3.3857	0.1140	1.2519	1.2103	0.1317	0.9453
VSAT 12 dBW/MHz	3.9959	3.6335	0.0908	1.2559	1.2002	0.1192	0.9453
Handheld 0 dBW/MHz	0.8249	0.7126	0.8200	0.6382	0.5401	0.6273	0.5673
Handheld 4 dBW/MHz	1.0687	0.9284	1.0516	0.7867	0.6742	0.7595	0.7393
Handheld 8 dBW/MHz	1.2888	1.1230	1.2358	0.8940	0.8054	0.8405	0.8474
Handheld 12 dBW/MHz	1.4884	1.3164	1.3509	0.9745	0.9144	0.8812	0.9027

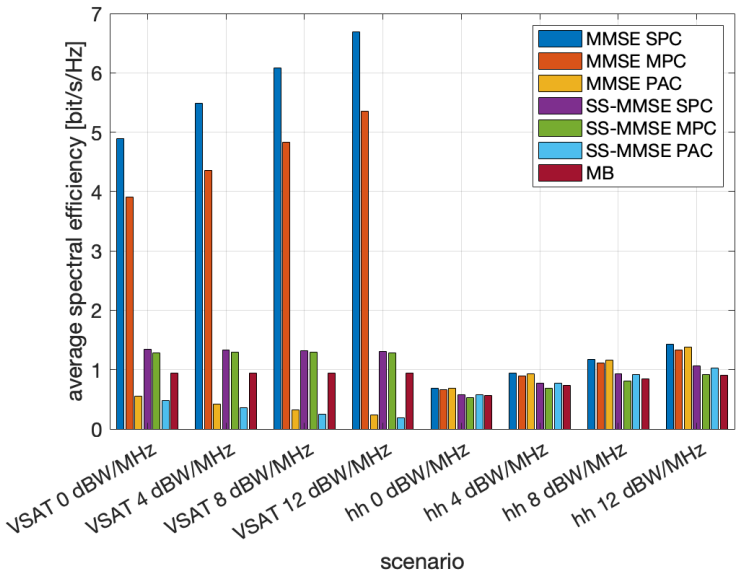

Figure 30 - Average spectral efficiency [bit/s/Hz] *for the LOS scenario in dense-urban conditions in the feed space, stand-alone satellite.*

Another interesting aspect to be highlighted is that the performance in dense-urban conditions is slightly better compared to the urban case and worse compared to the sub-urban case; while the latter observation makes sense, the former is related to the standard deviation values from TR 38.811 that have to be used for these scenarios, as reported in Table 8: for a urban scenario, this is always equal to 4 dB, while in the dense-urban case it varies with the elevation angle, but it is always below this value.

Table 21 - Average spectral efficiency [bit/s/Hz] *for the LOS scenario in dense urban condition in the feed space, stand-alone satellite.*

Scenario	MMSE	MMSE	MMSE	SS-MMSE	SS-MMSE	SS-MMSE	MB

	SPC	MPC	PAC	SPC	MPC	PAC	
VSAT 0 dBW/MHz	4.8940	3.9110	0.5538	1.3385	1.2786	0.4766	0.9452
VSAT 4 dBW/MHz	5.4863	4.3511	0.4216	1.3353	1.2954	0.3569	0.9453
VSAT 8 dBW/MHz	6.0830	4.8310	0.3199	1.3220	1.2938	0.2458	0.9453
VSAT 12 dBW/MHz	6.6867	5.3548	0.2361	1.3035	1.2826	0.1933	0.9453
Handheld 0 dBW/MHz	0.6827	0.6605	0.6816	0.5761	0.5266	0.5749	0.5673
Handheld 4 dBW/MHz	0.9369	0.8962	0.9322	0.7741	0.6872	0.7684	0.7393
Handheld 8 dBW/MHz	1.1785	1.1171	1.1634	0.9328	0.8136	0.9177	0.8474
Handheld 12 dBW/MHz	1.4238	1.3363	1.3806	1.0575	0.9177	1.0253	0.9027

To conclude the assessment for fixed terminals in the stand-alone satellite scenario, we also consider NLOS propagation conditions in sub-urban, urban, and dense-urban environments. In this case, the users are not forced to be in LOS conditions, but they might be in NLOS propagation with a probability related to the environment and the elevation angle, as reported in Table 7. When the user is in NLOS conditions, in addition to the impairments already present for the LOS scenario, it also experiences a Clutter Loss.

Table 22 and Table 23 provide the average spectral efficiency for the sub-urban environment in NLOS conditions, with feed and beam space precoding, respectively. It can be noticed that:

- the performance is significantly worse compared to beam and feed space precoding in pure LOS conditions, with losses in the order of 2 bit/s/Hz and 4-5 bit/s/Hz, respectively. Also compared to the LOS conditions, this scenario is significantly penalising since the clutter losses provided in TR 38.811 introduce a significant additional attenuation term;
- as already observed in other scenarios, MMSE and SS-MMSE precoding with SPC and MPC normalisations improving the performance with larger power levels;
- with the PAC normalisation, differently from the previous cases, the MMSE precoding provides a good performance, relatively close to the MPC. When including the clutter losses, the benefit of increasing the SNR is more impactful compared to the loss in the precoder orthogonality. This trend is not present for SS-MMSE precoding with PAC, which still shows a poor spectral efficiency; in this case, the further approximation of the channel matrix with that at beam center makes the SNR improvement negligible with respect to the orthogonality loss;
- with handheld terminals, the PAC approach is even better than the SPC. This behaviour is motivated by the extremely harsh propagation conditions: the inclusion of clutter losses in the order of tens of dBs makes the misalignment between the channel matrix and the precoding matrix significant. Consequently, with such large losses and without any gain at the receiver, it is better to equally allocate the power to the users, since the orthogonality is already disrupted. Moreover, in the feed space, the SPC and MPC approaches are even worse compared to MB (*i.e.*, non-precoded performance in the beam space) at low power levels: this further highlights that, in very low SNR regimes at the receiver, it is more important to increase the SNR rather than properly weighting the symbols for their linear combination at the transmitter side.

Table 22 - Average spectral efficiency [bit/s/Hz] *for the NLOS scenario in sub-urban condition in the beam space, stand-alone satellite.*

Scenario	MMSE SPC	MMSE MPC	MMSE PAC	SS-MMSE SPC	SS-MMSE MPC	SS-MMSE PAC	NoP
VSAT 0 dBW/MHz	1.6437	1.6417	1.4143	1.2328	1.1722	0.1541	0.9454
VSAT 4 dBW/MHz	1.8163	1.8147	1.4462	1.2434	1.1894	0.1395	0.9454
VSAT 8 dBW/MHz	2.0199	2.0186	1.4336	1.2518	1.2103	0.1317	0.9454
VSAT 12 dBW/MHz	2.2480	2.2468	1.3365	1.2557	1.2001	0.1192	0.9454
Handheld 0 dBW/MHz	0.5848	0.2545	0.6823	0.6383	0.5402	0.6274	0.5673
Handheld 4 dBW/MHz	0.7182	0.3992	0.8030	0.7868	0.6743	0.7596	0.7394
Handheld 8 dBW/MHz	0.8057	0.5805	0.8734	0.8942	0.8055	0.8407	0.8475
Handheld 12 dBW/MHz	0.8596	0.7592	0.9145	0.9747	0.9146	0.8815	0.9028

Table 23 - Average spectral efficiency [bit/s/Hz] *for the NLOS scenario in sub-urban condition in the feed space, stand-alone satellite.*

Scenario	MMSE SPC	MMSE MPC	MMSE PAC	SS-MMSE SPC	SS-MMSE MPC	SS-MMSE PAC	MB
VSAT 0 dBW/MHz	1.5118	1.5108	1.4372	1.3381	1.2784	0.4765	0.9454
VSAT 4 dBW/MHz	1.7372	1.7357	1.5784	1.3348	1.2950	0.3567	0.9454
VSAT 8 dBW/MHz	2.0248	2.0230	1.7178	1.3212	1.2932	0.2456	0.9454
VSAT 12 dBW/MHz	2.3735	2.3716	1.7575	1.3025	1.2819	0.1931	0.9454
Handheld 0 dBW/MHz	0.5450	0.5450	0.5450	0.5762	0.5267	0.5750	0.5673
Handheld 4 dBW/MHz	0.7355	0.7354	0.7355	0.7742	0.6873	0.7685	0.7394
Handheld 8 dBW/MHz	0.8808	0.8807	0.8807	0.9329	0.8137	0.9178	0.8475
Handheld 12 dBW/MHz	0.9747	0.9745	0.9746	1.0577	0.9178	1.0255	0.9028

Finally, it is interesting to notice that the performance in the feed space is much closer to that in the beam space. This is again motivated by the presence of the clutter loss: with such a difficult propagation environment, which also deeply perturbs the orthogonality in the precoding matrix, generating directive beams in desired directions is almost as beneficial as exploiting many more degrees of freedom in the precoding weights computation. This aspect is particularly relevant in the urban and dense-urban scenarios, as discussed below.

Table 24 - Average spectral efficiency [bit/s/Hz] *for the NLOS scenario in urban condition in the beam space, stand-alone satellite.*

Scenario	MMSE SPC	MMSE MPC	MMSE PAC	SS-MMSE SPC	SS-MMSE MPC	SS-MMSE PAC	NoP
VSAT	1.1418	1.1418	1.1679	1.2328	1.1722	0.1541	0.9454

0 dBW/MHz							
VSAT 4 dBW/MHz	1.2986	1.2986	1.2907	1.2434	1.1894	0.1395	0.9454
VSAT 8 dBW/MHz	1.4731	1.4731	1.4162	1.2518	1.2103	0.1317	0.9454
VSAT 12 dBW/MHz	1.6528	1.6528	1.5049	1.2557	1.2001	0.1192	0.9454
Handheld 0 dBW/MHz	0.5953	0.3013	0.6842	0.6383	0.5402	0.6274	0.5673
Handheld 4 dBW/MHz	0.7050	0.4570	0.8078	0.7868	0.6743	0.7596	0.7394
Handheld 8 dBW/MHz	0.7691	0.6010	0.8759	0.8942	0.8055	0.8407	0.8475
Handheld 12 dBW/MHz	0.8011	0.7064	0.9083	0.9747	0.9146	0.8815	0.9028

Table 25 - Average spectral efficiency [bit/s/Hz] *for the NLOS scenario in urban condition in the feed space, stand-alone satellite.*

Scenario	MMSE SPC	MMSE MPC	MMSE PAC	SS-MMSE SPC	SS-MMSE MPC	SS-MMSE PAC	MB
VSAT 0 dBW/MHz	1.0687	1.0687	1.0675	1.3381	1.2784	0.4765	0.9454
VSAT 4 dBW/MHz	1.1243	1.1243	1.1214	1.3348	1.2950	0.3567	0.9454
VSAT 8 dBW/MHz	1.2223	1.2223	1.2151	1.3212	1.2932	0.2456	0.9454
VSAT 12 dBW/MHz	1.3736	1.3736	1.3549	1.3025	1.2819	0.1931	0.9454
Handheld 0 dBW/MHz	0.5738	0.5738	0.5738	0.5762	0.5267	0.5750	0.5673
Handheld 4 dBW/MHz	0.7549	0.7549	0.7549	0.7742	0.6873	0.7685	0.7394
Handheld 8 dBW/MHz	0.8831	0.8831	0.8831	0.9329	0.8137	0.9178	0.8475
Handheld 12 dBW/MHz	0.9563	0.9563	0.9563	1.0577	0.9178	1.0255	0.9028

Table 24 and Table 25 show the performance for a urban scenario, in the beam and feed spaces, respectively. It can be noticed that, despite the typical behaviours observed so far, the beam space solution provides a slightly better spectral efficiency with MMSE precoding and VSAT terminals, while with handheld terminals we have an opposite trend. With SS-MMSE precoding the performance in the beam and feed spaces are very close. This behaviour can be motivated by observing that, when the received power is large (large transmitted power and VSAT terminals), the misalignment between the precoding and channel matrices (estimation and transmission phases, respectively) has a deeper impact on the performance, which can be slightly mitigated by the exploitation of pre-determined beams in fixed desired directions, *i.e.*, the advantage of having more degrees of freedom in the feed space is not useful. When the received power is more limited, as for handheld terminals, or the precoding algorithm is based on an approximation, as with SS-MMSE, this trend is not present and the feed space approach is the best option, even though only slightly.

Table 26 - Average spectral efficiency [bit/s/Hz] *for the NLOS scenario in dense-urban condition in the beam space, stand-alone satellite.*

Scenario	MMSE SPC	MMSE MPC	MMSE PAC	SS-MMSE SPC	SS-MMSE MPC	SS-MMSE PAC	NoP
VSAT 0 dBW/MHz	1.1539	1.1537	1.1547	1.2328	1.1722	0.1541	0.9454
VSAT 4 dBW/MHz	1.2891	1.2889	1.2446	1.2434	1.1894	0.1395	0.9454
VSAT 8 dBW/MHz	1.4440	1.4439	1.3383	1.2518	1.2103	0.1317	0.9454
VSAT 12 dBW/MHz	1.6092	1.6091	1.4158	1.2557	1.2001	0.1192	0.9454
Handheld 0 dBW/MHz	0.5187	0.1753	0.6585	0.6383	0.5402	0.6274	0.5673
Handheld 4 dBW/MHz	0.6361	0.2901	0.7813	0.7868	0.6743	0.7596	0.7394
Handheld 8 dBW/MHz	0.7136	0.4236	0.8512	0.8942	0.8055	0.8407	0.8475
Handheld 12 dBW/MHz	0.7581	0.5531	0.8865	0.9747	0.9146	0.8815	0.9028

Table 27 - Average spectral efficiency [bit/s/Hz] *for the NLOS scenario in dense-urban condition in the feed space, stand-alone satellite.*

Scenario	MMSE SPC	MMSE MPC	MMSE PAC	SS-MMSE SPC	SS-MMSE MPC	SS-MMSE PAC	MB
VSAT 0 dBW/MHz	1.0911	1.0911	1.0888	1.3381	1.2784	0.4765	0.9454
VSAT 4 dBW/MHz	1.1606	1.1606	1.1560	1.3348	1.2950	0.3567	0.9454
VSAT 8 dBW/MHz	1.2578	1.2577	1.2470	1.3212	1.2932	0.2456	0.9454
VSAT 12 dBW/MHz	1.3914	1.3914	1.3626	1.3025	1.2819	0.1931	0.9454
Handheld 0 dBW/MHz	0.4811	0.4811	0.4811	0.5762	0.5267	0.5750	0.5673
Handheld 4 dBW/MHz	0.6570	0.6570	0.6570	0.7742	0.6873	0.7685	0.7394
Handheld 8 dBW/MHz	0.7970	0.7970	0.7970	0.9329	0.8137	0.9178	0.8475
Handheld 12 dBW/MHz	0.8870	0.8870	0.8870	1.0577	0.9178	1.0255	0.9028

Table 26 and Table 27 show the results in terms of average spectral efficiency for the dense-urban scenario. The same trend introduced above for the urban scenario is present: with a large received power level, the beam space approach is better compared to the feed space.

A final observation related to the NLOS scenarios is that, differently from LOS propagation, the harsher is the environment, the worse becomes the performance. In fact, in this case the standard deviation in urban scenarios is smaller compared to that in dense-urban ones; thus, in NLOS the dense-urban scenario is the worst and the sub-urban scenario is the best.

2.2.1.2 Public Safety terminals

In this section, we report the numerical results obtained with moving UEs in the same configurations and scenarios as those reported above for fixed terminals.

In particular, we consider a scenario with Public Safety terminals that move at $v_{UE} = 250$ km/h. In the limited time interval between the estimation and the transmission phase with CPC, which

is expected to be even lower with a DPC architecture[8] where the precoding coefficients are computed on-board, there is a position error that leads to a further misalignment in the channel matrix used in the estimation phase and that in the transmission phase. With this type of terminals, the distance travelled in this interval is equal to 1.156 meters. It is thus reasonable to expect that the impact of the users' movement is negligible on the system performance compared to the other sources of non-ideal CSI (in particular the different realisations of the stochastic terms). As reported below, this is indeed the outcome of the analysis with Public Safety terminals.

For the sake of completeness, below we report the performance tables in the beam and feed spaces for pLOS and NLOS propagation conditions (the two extreme propagation conditions). By comparing these results with the corresponding tables in the fixed terminal section, the Public Safety terminals provide a performance that is at most equal to that of fixed terminals or, in the worst case, with a rate degradation in the order of 10^{-4} bit/s/Hz, thus substantiating the above observations.

Table 28 - Average spectral efficiency [bit/s/Hz] *for the pLOS scenario in the beam space with Public Safety terminals, stand-alone satellite.*

Scenario	MMSE SPC	MMSE MPC	MMSE PAC	SS-MMSE SPC	SS-MMSE MPC	SS-MMSE PAC	NoP
VSAT 0 dBW/MHz	3.1105	2.7331	0.1456	1.2313	1.1708	0.1539	0.9451
VSAT 4 dBW/MHz	3.3663	2.9283	0.1044	1.2417	1.1879	0.1394	0.9451
VSAT 8 dBW/MHz	3.6402	3.1478	0.0858	1.2501	1.2087	0.1316	0.9451
VSAT 12 dBW/MHz	3.9163	3.3797	0.0760	1.2540	1.1985	0.1190	0.9451
Handheld 0 dBW/MHz	0.8403	0.6671	0.8265	0.6381	0.5400	0.6271	0.5671
Handheld 4 dBW/MHz	1.0884	0.8893	1.0453	0.7864	0.6740	0.7592	0.7391
Handheld 8 dBW/MHz	1.3078	1.1250	1.2030	0.8937	0.8051	0.8402	0.8472
Handheld 12 dBW/MHz	1.5061	1.3371	1.2962	0.9741	0.9141	0.8808	0.9025

Table 29 - Average spectral efficiency [bit/s/Hz] *for the pLOS scenario in the feed space with Public Safety terminals, stand-alone satellite.*

Scenario	MMSE SPC	MMSE MPC	MMSE PAC	SS-MMSE SPC	SS-MMSE MPC	SS-MMSE PAC	MB
VSAT 0 dBW/MHz	5.3619	3.7546	0.3947	1.3360	1.2765	0.4767	0.9451
VSAT 4 dBW/MHz	5.9666	4.1748	0.2939	1.3325	1.2929	0.3568	0.9451
VSAT	6.5930	4.6456	0.2116	1.3189	1.2909	0.2456	0.9451

[8] These aspects are extensively discussed in D3.2.

8 dBW/MHz							
VSAT 12 dBW/MHz	7.2407	5.1716	0.1472	1.3003	1.2797	0.1931	0.9451
Handheld 0 dBW/MHz	0.7192	0.6705	0.7166	0.5760	0.5265	0.5748	0.5671
Handheld 4 dBW/MHz	0.9960	0.9059	0.9854	0.7739	0.6870	0.7682	0.7391
Handheld 8 dBW/MHz	1.2701	1.1302	1.2366	0.9325	0.8134	0.9175	0.8472
Handheld 12 dBW/MHz	1.5574	1.3550	1.4706	1.0571	0.9174	1.0251	0.9025

Table 30 - Average spectral efficiency [bit/s/Hz] *for the NLOS scenario in sub-urban condition in the beam space with Public Safety terminals, stand-alone satellite.*

Scenario	MMSE SPC	MMSE MPC	MMSE PAC	SS-MMSE SPC	SS-MMSE MPC	SS-MMSE PAC	NoP
VSAT 0 dBW/MHz	1.6437	1.6417	1.4143	1.2328	1.1722	0.1541	0.9454
VSAT 4 dBW/MHz	1.8163	1.8147	1.4462	1.2434	1.1894	0.1395	0.9454
VSAT 8 dBW/MHz	2.0199	2.0186	1.4336	1.2518	1.2103	0.1317	0.9454
VSAT 12 dBW/MHz	2.2480	2.2468	1.3365	1.2557	1.2001	0.1192	0.9454
Handheld 0 dBW/MHz	0.5848	0.2545	0.6823	0.6383	0.5402	0.6274	0.5673
Handheld 4 dBW/MHz	0.7182	0.3992	0.8030	0.7868	0.6743	0.7596	0.7394
Handheld 8 dBW/MHz	0.8057	0.5805	0.8734	0.8942	0.8055	0.8407	0.8475
Handheld 12 dBW/MHz	0.8596	0.7592	0.9145	0.9747	0.9146	0.8815	0.9028

Table 31 - Average spectral efficiency [bit/s/Hz] *for the NLOS scenario in sub-urban condition in the feed space with Public Safety terminals, stand-alone satellite.*

Scenario	MMSE SPC	MMSE MPC	MMSE PAC	SS-MMSE SPC	SS-MMSE MPC	SS-MMSE PAC	MB
VSAT 0 dBW/MHz	1.5118	1.5108	1.4372	1.3381	1.2784	0.4765	0.9454
VSAT 4 dBW/MHz	1.7372	1.7357	1.5784	1.3348	1.2950	0.3567	0.9454
VSAT 8 dBW/MHz	2.0248	2.0230	1.7178	1.3212	1.2932	0.2456	0.9454
VSAT	2.3735	2.3716	1.7575	1.3025	1.2819	0.1931	0.9454

12 dBW/MHz							
Handheld 0 dBW/MHz	0.5450	0.5450	0.5450	0.5762	0.5267	0.5750	0.5673
Handheld 4 dBW/MHz	0.7355	0.7354	0.7355	0.7742	0.6873	0.7685	0.7394
Handheld 8 dBW/MHz	0.8808	0.8807	0.8807	0.9329	0.8137	0.9178	0.8475
Handheld 12 dBW/MHz	0.9747	0.9745	0.9746	1.0577	0.9178	1.0255	0.9028

Table 32 - Average spectral efficiency [bit/s/Hz] *for the NLOS scenario in urban condition in the beam space with Public Safety terminals, stand-alone satellite.*

Scenario	MMSE SPC	MMSE MPC	MMSE PAC	SS-MMSE SPC	SS-MMSE MPC	SS-MMSE PAC	NoP
VSAT 0 dBW/MHz	1.1418	1.1418	1.1679	1.2328	1.1722	0.1541	0.9454
VSAT 4 dBW/MHz	1.2986	1.2986	1.2907	1.2434	1.1894	0.1395	0.9454
VSAT 8 dBW/MHz	1.4731	1.4731	1.4162	1.2518	1.2103	0.1317	0.9454
VSAT 12 dBW/MHz	1.6528	1.6528	1.5049	1.2557	1.2001	0.1192	0.9454
Handheld 0 dBW/MHz	0.5953	0.3013	0.6842	0.6383	0.5402	0.6274	0.5673
Handheld 4 dBW/MHz	0.7050	0.4570	0.8078	0.7868	0.6743	0.7596	0.7394
Handheld 8 dBW/MHz	0.7691	0.6010	0.8759	0.8942	0.8055	0.8407	0.8475
Handheld 12 dBW/MHz	0.8011	0.7064	0.9083	0.9747	0.9146	0.8815	0.9028

Table 33 - Average spectral efficiency [bit/s/Hz] *for the NLOS scenario in urban condition in the feed space with Public Safety terminals, stand-alone satellite.*

Scenario	MMSE SPC	MMSE MPC	MMSE PAC	SS-MMSE SPC	SS-MMSE MPC	SS-MMSE PAC	MB
VSAT 0 dBW/MHz	1.0687	1.0687	1.0675	1.3381	1.2784	0.4765	0.9454
VSAT 4 dBW/MHz	1.1243	1.1243	1.1214	1.3348	1.2950	0.3567	0.9454
VSAT 8 dBW/MHz	1.2223	1.2223	1.2151	1.3212	1.2932	0.2456	0.9454
VSAT 12 dBW/MHz	1.3736	1.3736	1.3549	1.3025	1.2819	0.1931	0.9454

Handheld 0 dBW/MHz	0.5738	0.5738	0.5738	0.5762	0.5267	0.5750	0.5673
Handheld 4 dBW/MHz	0.7549	0.7549	0.7549	0.7742	0.6873	0.7685	0.7394
Handheld 8 dBW/MHz	0.8831	0.8831	0.8831	0.9329	0.8137	0.9178	0.8475
Handheld 12 dBW/MHz	0.9563	0.9563	0.9563	1.0577	0.9178	1.0255	0.9028

Table 34 - Average spectral efficiency [bit/s/Hz] *for the NLOS scenario in dense-urban condition in the beam space with Public Safety terminals, stand-alone satellite.*

Scenario	MMSE SPC	MMSE MPC	MMSE PAC	SS-MMSE SPC	SS-MMSE MPC	SS-MMSE PAC	NoP
VSAT 0 dBW/MHz	1.1539	1.1537	1.1547	1.2328	1.1722	0.1541	0.9454
VSAT 4 dBW/MHz	1.2891	1.2889	1.2446	1.2434	1.1894	0.1395	0.9454
VSAT 8 dBW/MHz	1.4440	1.4439	1.3383	1.2518	1.2103	0.1317	0.9454
VSAT 12 dBW/MHz	1.6092	1.6091	1.4158	1.2557	1.2001	0.1192	0.9454
Handheld 0 dBW/MHz	0.5187	0.1753	0.6585	0.6383	0.5402	0.6274	0.5673
Handheld 4 dBW/MHz	0.6361	0.2901	0.7813	0.7868	0.6743	0.7596	0.7394
Handheld 8 dBW/MHz	0.7136	0.4236	0.8512	0.8942	0.8055	0.8407	0.8475
Handheld 12 dBW/MHz	0.7581	0.5531	0.8865	0.9747	0.9146	0.8815	0.9028

Table 35 - Average spectral efficiency [bit/s/Hz] *for the NLOS scenario in dense-urban condition in the feed space with Public Safety terminals, stand-alone satellite.*

Scenario	MMSE SPC	MMSE MPC	MMSE PAC	SS-MMSE SPC	SS-MMSE MPC	SS-MMSE PAC	MB
VSAT 0 dBW/MHz	1.0911	1.0911	1.0888	1.3381	1.2784	0.4765	0.9454
VSAT 4 dBW/MHz	1.1606	1.1606	1.1560	1.3348	1.2950	0.3567	0.9454
VSAT 8 dBW/MHz	1.2578	1.2577	1.2470	1.3212	1.2932	0.2456	0.9454
VSAT 12 dBW/MHz	1.3914	1.3914	1.3626	1.3025	1.2819	0.1931	0.9454
Handheld 0 dBW/MHz	0.4811	0.4811	0.4811	0.5762	0.5267	0.5750	0.5673

Handheld 4 dBW/MHz	0.6570	0.6570	0.6570	0.7742	0.6873	0.7685	0.7394
Handheld 8 dBW/MHz	0.7970	0.7970	0.7970	0.9329	0.8137	0.9178	0.8475
Handheld 12 dBW/MHz	0.8870	0.8870	0.8870	1.0577	0.9178	1.0255	0.9028

2.2.1.3 Observations

The extensive numerical assessment performed with a stand-alone satellites provides a valuable insight on the performance of SS-MMSE and MB precoding compared to the optimal MMSE solution. In particular, many trade-offs have been identified, which can be summarised as follows:

- **Precoding algorithm**
  - MMSE is always providing the largest spectral efficiency values;
  - SS-MMSE precoding shows an acceptable performance, also considering that it is based on pre-computed channel coefficients, *i.e.*, it does not need a continuous reporting of CSI vectors from the UEs to the gNB. Almost independently from the propagation scenario (pure LOS, LOS, NLOS) and environment (sub-urban, urban, dense-urban), SS-MMSE precoding always leads to an average spectral efficiency in the order of: i) $1.2 - 1.25$ bit/s/Hz in the beam space with SPC and MPC, while with PAC it is in the order of $0.1 - 0.15$ bit/s/Hz; ii) $1.3 - 1.33$ bit/s/Hz in the beam space with SPC and MPC, $0.2 - 0.5$ bit/s/Hz with PAC;
  - MB precoding in the feed space and the non-precoded system in the beam space are completely equivalent, as long as no beam-hopping scheme is implemented. In terms of average spectral efficiency, these algorithms perform better only of the SS-MMSE solution with PAC, with $0.5 - 0.95$ bit/s/Hz.
- **Normalisation**
  - SPC and MPC normalisations provide the best solution in scenarios characterised by a large power at the receiver, *i.e.*, scenarios where interference is significant; these scenarios are those with VSAT terminals and pLOS or LOS propagation. In fact, in these situations the orthogonality of the precoding matrix is fundamental to properly manage the significant interference at each user terminal;
  - in scenarios with a limited received power (NLOS or handheld with low transmission power), the PAC normalisation provides a good solution with MMSE. In these conditions, rather than preserving the orthogonality, it is more impacting the enhancement of the intended signal power, independently from the channel conditions, guaranteed by a PAC approach.

In general, for the stand-alone scenario we can conclude that MMSE precoding (or other similar solutions) is worth to be further investigated because SS-MMSE precoding is significantly degrading the performance in many relevant scenarios. As for the normalisations, MPC and PAC provide, depending on the scenarios as discussed above, a performance close to that of SPC. They are to be preferred since they guarantee that each antenna feed is not emitting a transmission power above its maximum.

2.2.2 Dual satellite scenario

In this Section, we perform the numerical assessment in the same scenarios as the stand-alone case, with two satellites covering the same service area as shown in Figure 3. It shall be recalled that, with more than one satellite, two additional normalisation schemes were introduced in D3.2 and briefly outlined in the previous sections: the satellite-based SPC and MPC, denoted as sSPC and sMPC, respectively. These schemes were introduced to take into account that, for a swarm of satellites, the application of the traditional SPC and MPC approaches is not realistic: in that

case, in fact ,the satellites in the swarm should be able to exchange power. Taking this aspect into account, in the following we do not report the results with SPC and MPC, but only those with sSPC and sMPC (in addition to PAC, which can be implemented without modifications).

Finally, in order to guarantee a fair comparison in terms of allocated power, the results reported below are still as a function of $P_{t,dens}$, which now represents the power density allocated to the entire swarm. Thus, the maximum power density available from one satellite is $P_{t,dens} - 10\log_{10} N_S$, with N_S being the number of satellites, and the total power density from the entire swarm is equal to that of a single satellite.

2.2.2.1 Fixed terminals

As for the stand-alone scenario, we first evaluate the performance in pure LOS conditions, *i.e.*, without scintillation, shadow fading, gaseous absorption, and clutter losses. Figure 31 shows the average spectral efficiency and Table 36 reports the corresponding values in a heatmap for beam space precoding. The following trends can be identified:

- MMSE precoding always provides the best performance, followed by the SS-MMSE and MB algorithms. In particular, the gap between MMSE and SS-MMSE is significantly larger for VSATs, while with handheld terminals there are very close. This trend is in line with the stand-alone case;
- with respect to the normalisations, sSPC is always the best option as SPC was in the stand-alone scenario. sMPC provides a performance quite close to that of sSPC and PAC is closer to them only for handheld terminals. Again, as observed with one satellite, a normalisation which preserves as much as possible the orthogonality is to be preferred when interference is large, while PAC provides a close, or even better, performance when the received power is low and an increased SNR level is needed. Differently from the stand-alone scenario, PAC with VSAT terminals provides a slightly better performance;
- in terms of transmission power, it is interesting to note that with VSAT there is no significant benefit in increasing it and with handheld terminals the advantage rapidly saturates the maximum achievable spectral efficiency. This behaviour is motivated by the peculiarity of the scenario geometry; in fact, we are considering a service area which is approximately in the middle of the two satellites coverage areas. In this scenario, users are seen from one satellite with a reduced angular distance and, moreover, there is a symmetry in the channel coefficients from the two satellites that poses some issues in the matrix inversions required to compute precoding; thus, when the precoder tries to improve a generic user's signal, it is more difficult to simultaneously limit the interference it generates towards other users. As a consequence, the precoder can increase the SINR for an increasing transmission power to a certain limit, after which the performance basically saturates and, if the power is further increased, it might also worsen.

The above trend is further substantiated by observing that, often, the performance with PAC is much better in the dual satellite scenario compared to the stand-alone case. As mentioned for the stand-alone scenario, this normalisation starts to be effective when interference is less relevant compared to the need of an increased SNR; in this case, the precoder is not able to further limit interference and, thus, the increase in the SNR is beneficial.

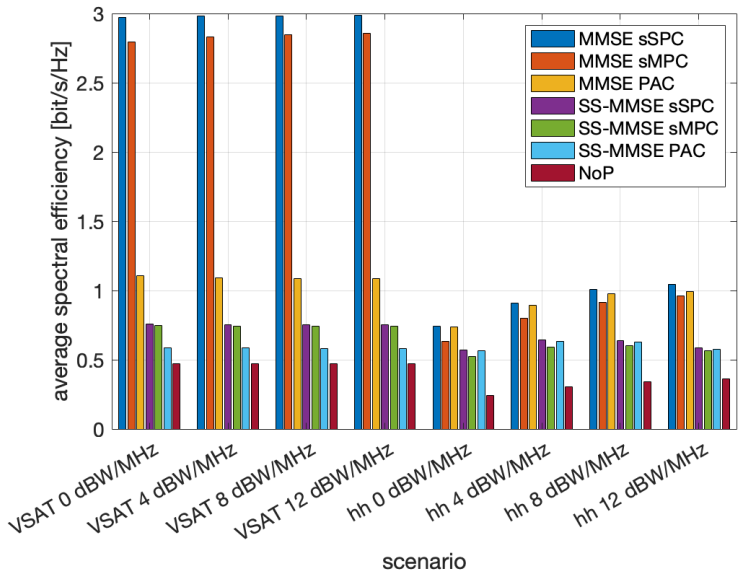

Figure 31 - Average spectral efficiency [bit/s/Hz] *for the pLOS scenario in the beam space, dual satellite scenario.*

Table 36 - Average spectral efficiency [bit/s/Hz] *for the pLOS scenario in the beam space, dual satellite scenario.*

Scenario	MMSE sSPC	MMSE sMPC	MMSE PAC	SS-MMSE sSPC	SS-MMSE sMPC	SS-MMSE PAC	NoP
VSAT 0 dBW/MHz	2.9734	2.7940	1.1048	0.7573	0.7453	0.5883	0.4691
VSAT 4 dBW/MHz	2.9792	2.8290	1.0929	0.7540	0.7428	0.5841	0.4691
VSAT 8 dBW/MHz	2.9827	2.8484	1.0881	0.7527	0.7418	0.5825	0.4691
VSAT 12 dBW/MHz	2.9844	2.8580	1.0862	0.7522	0.7414	0.5818	0.4691
Handheld 0 dBW/MHz	0.7437	0.6351	0.7367	0.5708	0.5234	0.5651	0.2443
Handheld 4 dBW/MHz	0.9085	0.8019	0.8925	0.6421	0.5916	0.6323	0.3068
Handheld 8 dBW/MHz	1.0066	0.9165	0.9783	0.6380	0.6032	0.6265	0.3425
Handheld 12 dBW/MHz	1.0456	0.9611	0.9947	0.5878	0.5661	0.5758	0.3595

When comparing the performance of the dual satellite scenario with the stand-alone scenario, there are some interesting trends to be commented:

- in high interference condition (VSAT terminals and handheld terminals with $P_{t,dens} > 4$ dBW/MHz), the stand-alone scenario provides a better performance with SPC and MPC. In particular, for larger transmission power levels and VSAT terminals, the gap in the average spectral efficiency can be as large as 1 bit/s/Hz (MMSE SPC). For handheld terminals, it can be approximately half of this value. For VSATs and PAC, the dual satellite scenario is significantly better (approximately one order of magnitude);
- in low interference conditions (handheld terminals with $P_{t,dens} \leq 4$ dBW/MHz), the dual satellite scenario provides a slight advantage, in the order of $0.1 - 0.2$ bit/S/Hz;
- when no precoding is implemented, the performance in the dual satellite scenario is always half of that obtained in the stand-alone case.

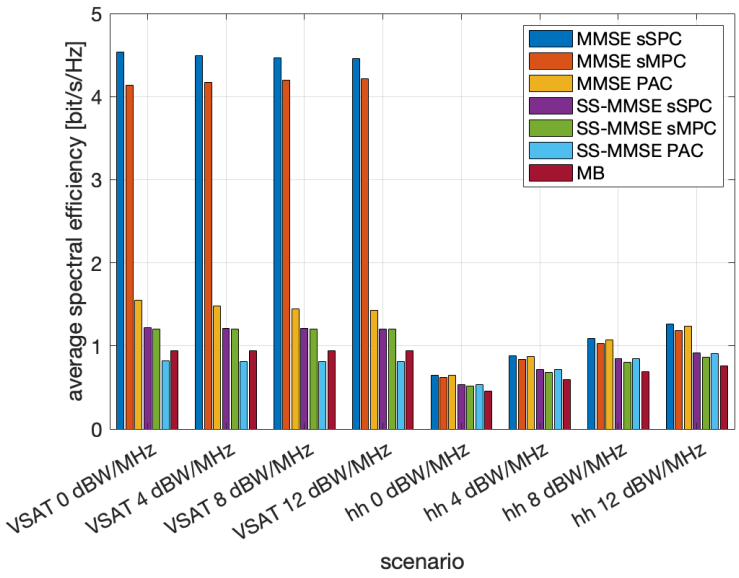

Figure 32 - Average spectral efficiency [bit/s/Hz] *for the pLOS scenario in the feed space, dual satellite scenario.*

Table 37 - Average spectral efficiency [bit/s/Hz] *for the pLOS scenario in the feed space, dual satellite scenario.*

Scenario	MMSE sSPC	MMSE sMPC	MMSE PAC	SS-MMSE sSPC	SS-MMSE sMPC	SS-MMSE PAC	MB
VSAT 0 dBW/MHz	4.5362	4.1402	1.5454	1.2211	1.2063	0.8246	0.9430
VSAT 4 dBW/MHz	4.4904	4.1727	1.4762	1.2120	1.2056	0.8159	0.9430
VSAT 8 dBW/MHz	4.4656	4.1984	1.4450	1.2081	1.2055	0.8122	0.9430
VSAT 12 dBW/MHz	4.4542	4.2150	1.4319	1.2065	1.2054	0.8107	0.9430
Handheld 0 dBW/MHz	0.6453	0.6213	0.6442	0.5342	0.5123	0.5337	0.4542
Handheld 4 dBW/MHz	0.8781	0.8349	0.8737	0.7157	0.6774	0.7133	0.5912
Handheld 8 dBW/MHz	1.0885	1.0268	1.0760	0.8499	0.7995	0.8442	0.6920
Handheld 12 dBW/MHz	1.2649	1.1878	1.2350	0.9159	0.8640	0.9066	0.7556

These performance trends are present in the feed space as well, for which the results are summarised in Figure 32 and Table 37. The better performance of sSPC and sMPC compared to PAC confirm that, in high interference scenarios, the preservation of the orthogonality of the precoder columns is critical. However, the fact that in these scenarios the stand-alone satellite provides a better performance is interesting, as discussed above.

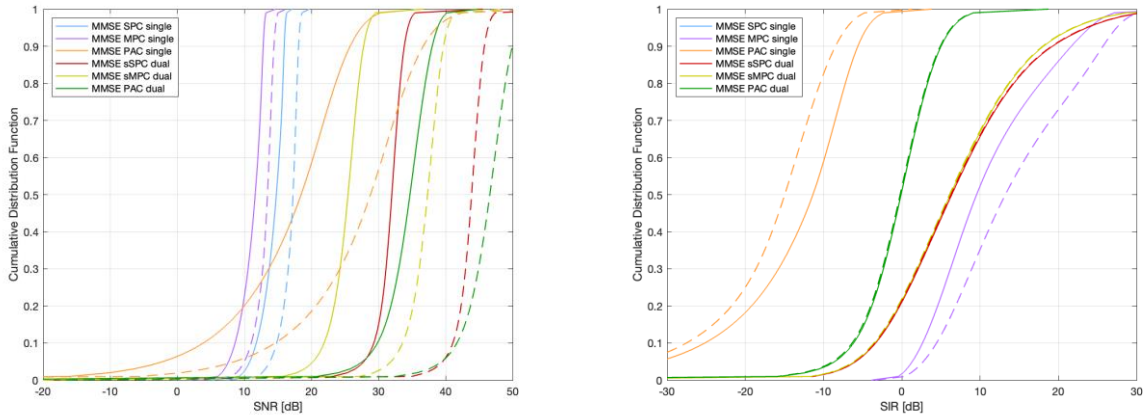

(a) SNR [dB] (b) SIR [dB]

Figure 33 – Comparison of stand-alone and dual satellite scenarios: SNR and SIR CDFs with VSATs in the beam space and MMSE precoding.

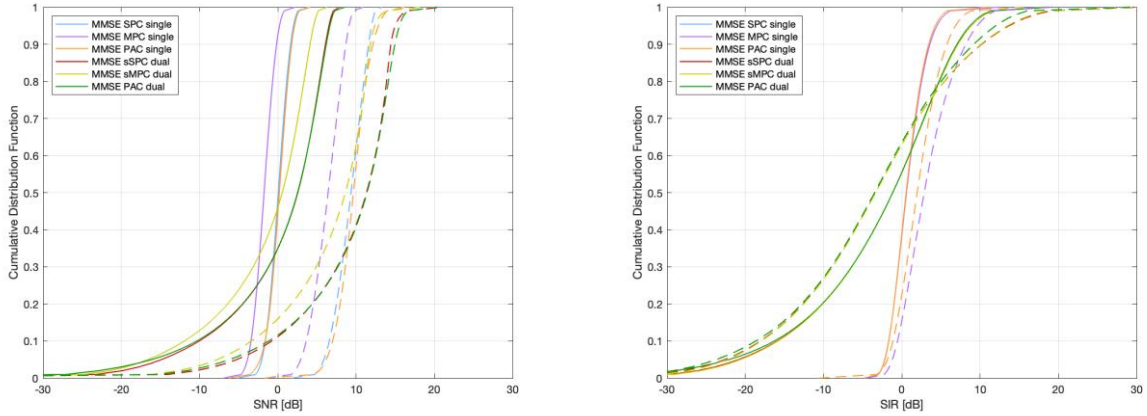

(a) SNR [dB] (b) SIR [dB]

Figure 34 - Comparison of stand-alone and dual satellite scenarios: SNR and SIR CDFs with handheld terminals in the beam space and MMSE precoding.

To substantiate these considerations, Figure 33 and Figure 34 compare the SNR and SIR for the stand-alone and dual satellite scenarios in the beam space with VSATs; for the sake of clarity, we only report the CDFs for the MMSE algorithm, but for the SS-MMSE solution similar trends can be obtained. It can be noticed that, in terms of SNR, the dual satellite scenario provides a better performance, in particular with VSAT receivers; however, the SIR performance is poorer compared to the stand-alone scenario for sSPC and sMPC: given the geometry of the system (and also partially due to the slight loss in orthogonality with these normalisations), the dual satellite scenario is more critical in terms of interference limitation.

We can now focus on the LOS scenario. The average spectral efficiency in sub-urban conditions is provided in Figure 35, Table 38, and Table 39. The trends are in line with those reported above for the pure LOS scenario; the only difference is that the performance with handheld terminals is always better with the stand-alone satellite. Clearly, in LOS conditions the performance is worse compared to the pure LOS scenario. The same trends can be observed for the feed space.

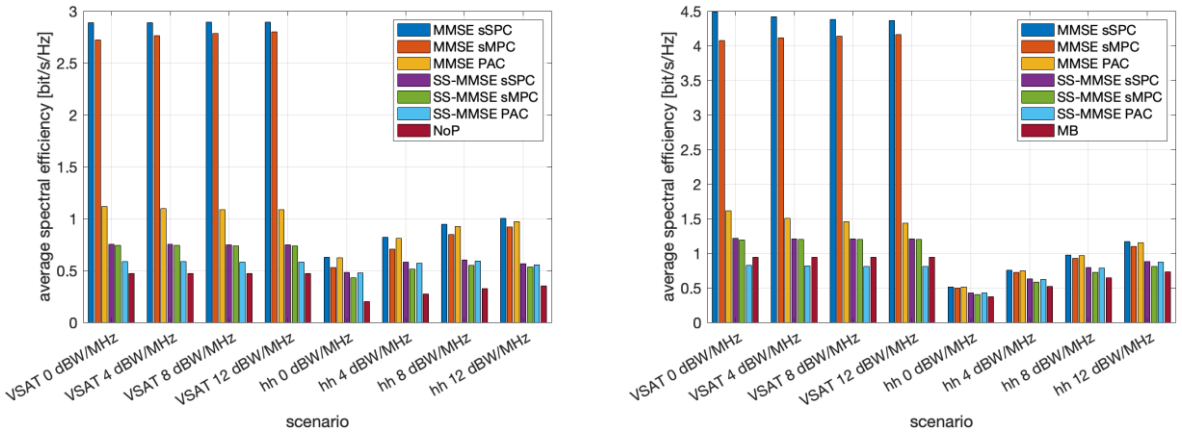

(a) beam space

(b) feed space

Figure 35 - Average spectral efficiency [bit/s/Hz] *for the LOS scenario in sub-urban conditions in the beam (left) and feed (right) spaces, dual satellite scenario.*

Table 38 - Average spectral efficiency [bit/s/Hz] *for the LOS scenario in sub-urban conditions in the beam space, dual satellite scenario.*

Scenario	MMSE sSPC	MMSE sMPC	MMSE PAC	SS-MMSE sSPC	SS-MMSE sMPC	SS-MMSE PAC	NoP
VSAT 0 dBW/MHz	2.8872	2.7195	1.1146	0.7530	0.7411	0.5881	0.4695
VSAT 4 dBW/MHz	2.8891	2.7610	1.0954	0.7501	0.7396	0.5840	0.4695
VSAT 8 dBW/MHz	2.8913	2.7857	1.0875	0.7489	0.7390	0.5824	0.4695
VSAT 12 dBW/MHz	2.8925	2.7984	1.0844	0.7484	0.7387	0.5817	0.4695
Handheld 0 dBW/MHz	0.6276	0.5283	0.6240	0.4827	0.4299	0.4787	0.2005
Handheld 4 dBW/MHz	0.8186	0.7070	0.8078	0.5788	0.5156	0.5706	0.2759
Handheld 8 dBW/MHz	0.9461	0.8476	0.9262	0.5991	0.5520	0.5889	0.3263
Handheld 12 dBW/MHz	1.0034	0.9209	0.9712	0.5650	0.5340	0.5543	0.3526

Table 39 - Average spectral efficiency [bit/s/Hz] *for the LOS scenario in sub-urban conditions in the feed space, dual satellite scenario.*

Scenario	MMSE sSPC	MMSE sMPC	MMSE PAC	SS-MMSE sSPC	SS-MMSE sMPC	SS-MMSE PAC	MB
VSAT 0 dBW/MHz	4.4878	4.0778	1.6103	1.2187	1.1949	0.8235	0.9430
VSAT 4 dBW/MHz	4.4200	4.1104	1.5072	1.2100	1.1996	0.8149	0.9430
VSAT 8 dBW/MHz	4.3801	4.1382	1.4584	1.2062	1.2019	0.8113	0.9431
VSAT 12 dBW/MHz	4.3608	4.1584	1.4372	1.2047	1.2029	0.8098	0.9431
Handheld 0 dBW/MHz	0.5148	0.4995	0.5144	0.4278	0.4055	0.4276	0.3709
Handheld 4 dBW/MHz	0.7515	0.7190	0.7493	0.6259	0.5802	0.6243	0.5218
Handheld 8 dBW/MHz	0.9750	0.9231	0.9678	0.7900	0.7224	0.7853	0.6453
Handheld 12 dBW/MHz	1.1685	1.1000	1.1498	0.8818	0.8068	0.8734	0.7305

Figure 36 shows the results in the beam space (on the left) and the feed space (on the right) in the LOS scenario with urban conditions. The heatmaps with the corresponding spectral efficiency values are provided in Table 40 and Table 41. While the general trends are the same as those discussed for pure LOS and LOS in sub-urban conditions, in this case the advantage of the stand-alone satellite is larger; this can be motivated by observing that in LOS conditions, the urban scenario has larger values of the standard deviation of the shadow fading, which are also independent of the elevation angle. Thus, the impact on the SNR (which is where the dual satellite system has an advantage) is extremely detrimental and the gap from the stand-alone scenario is more evident. It is also interesting to notice that, in the feed space, the performance is particularly bad for low transmission power levels and then it rapidly increases.

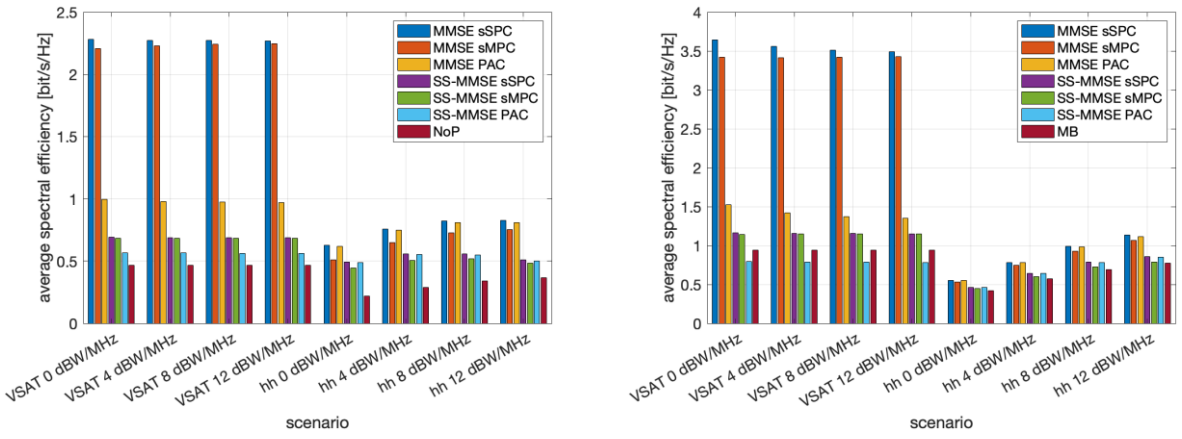

(a) beam space

(b) feed space

Figure 36 - Average spectral efficiency [bit/s/Hz] *for the LOS scenario in urban conditions in the beam (left) and feed (right) spaces, dual satellite scenario.*

Table 40 - Average spectral efficiency [bit/s/Hz] *for the LOS scenario in urban conditions in the beam space, dual satellite scenario.*

Scenario	MMSE sSPC	MMSE sMPC	MMSE PAC	SS-MMSE sSPC	SS-MMSE sMPC	SS-MMSE PAC	NoP
VSAT 0 dBW/MHz	2.2801	2.2060	0.9956	0.6911	0.6851	0.5682	0.4673
VSAT 4 dBW/MHz	2.2729	2.2280	0.9791	0.6882	0.6836	0.5643	0.4674
VSAT 8 dBW/MHz	2.2704	2.2413	0.9723	0.6871	0.6830	0.5627	0.4674
VSAT 12 dBW/MHz	2.2696	2.2482	0.9696	0.6866	0.6828	0.5621	0.4674
Handheld 0 dBW/MHz	0.6261	0.5098	0.6188	0.4907	0.4453	0.4868	0.2189
Handheld 4 dBW/MHz	0.7590	0.6468	0.7486	0.5587	0.5068	0.5517	0.2902
Handheld 8 dBW/MHz	0.8236	0.7286	0.8101	0.5566	0.5193	0.5483	0.3397
Handheld 12 dBW/MHz	0.8271	0.7550	0.8074	0.5093	0.4857	0.5014	0.3673

Table 41 - Average spectral efficiency [bit/s/Hz] *for the LOS scenario in urban conditions in the feed space, dual satellite scenario.*

Scenario	MMSE sSPC	MMSE sMPC	MMSE PAC	SS-MMSE sSPC	SS-MMSE sMPC	SS-MMSE PAC	MB
VSAT 0 dBW/MHz	3.6453	3.4190	1.5214	1.1663	1.1412	0.7984	0.9425
VSAT 4 dBW/MHz	3.5569	3.4141	1.4190	1.1571	1.1462	0.7896	0.9425
VSAT 8 dBW/MHz	3.5092	3.4185	1.3698	1.1532	1.1486	0.7859	0.9426
VSAT 12 dBW/MHz	3.4871	3.4250	1.3483	1.1516	1.1497	0.7844	0.9426
Handheld 0 dBW/MHz	0.5538	0.5335	0.5530	0.4652	0.4446	0.4648	0.4212
Handheld 4 dBW/MHz	0.7828	0.7433	0.7797	0.6439	0.6031	0.6420	0.5717
Handheld 8 dBW/MHz	0.9885	0.9300	0.9797	0.7863	0.7264	0.7811	0.6925
Handheld 12 dBW/MHz	1.1344	1.0652	1.1145	0.8577	0.7914	0.8489	0.7735

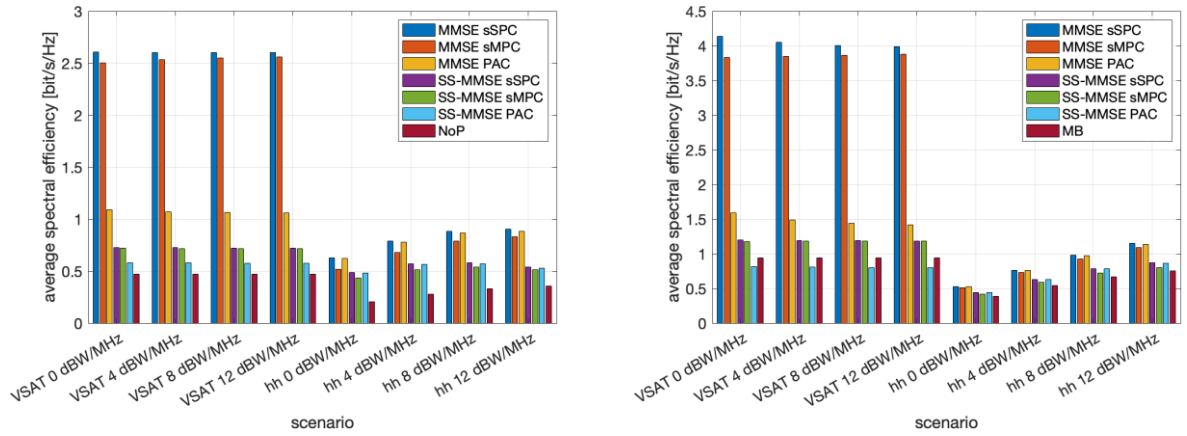

(a) beam space

(b) feed space

Figure 37 - Average spectral efficiency [bit/s/Hz] *for the LOS scenario in dense-urban conditions in the beam (left) and feed (right) spaces, dual satellite scenario.*

Figure 37, Table 42, and Table 43 report the results in the LOS dense-urban scenario. The trends are similar to that already discussed for the sub-urban and urban scenarios.

Table 42 - Average spectral efficiency [bit/s/Hz] *for the LOS scenario in dense-urban conditions in the beam space, dual satellite scenario.*

Scenario	MMSE sSPC	MMSE sMPC	MMSE PAC	SS-MMSE sSPC	SS-MMSE sMPC	SS-MMSE PAC	NoP
VSAT 0 dBW/MHz	2.6074	2.5045	1.0901	0.7277	0.7192	0.5824	0.4689
VSAT 4 dBW/MHz	2.6029	2.5342	1.0723	0.7247	0.7176	0.5783	0.4690
VSAT 8 dBW/MHz	2.6017	2.5516	1.0650	0.7235	0.7170	0.5767	0.4690
VSAT 12 dBW/MHz	2.6014	2.5605	1.0620	0.7231	0.7167	0.5761	0.4690
Handheld 0 dBW/MHz	0.6261	0.5172	0.6202	0.4856	0.4354	0.4815	0.2068
Handheld 4 dBW/MHz	0.7906	0.6773	0.7789	0.5709	0.5122	0.5629	0.2812
Handheld 8 dBW/MHz	0.8835	0.7868	0.8665	0.5812	0.5386	0.5717	0.3317
Handheld 12 dBW/MHz	0.9055	0.8312	0.8817	0.5402	0.5130	0.5307	0.3586

Table 43 - Average spectral efficiency [bit/s/Hz] *for the LOS scenario in dense-urban conditions in the feed space, dual satellite scenario.*

Scenario	MMSE sSPC	MMSE sMPC	MMSE PAC	SS-MMSE sSPC	SS-MMSE sMPC	SS-MMSE PAC	MB
VSAT 0 dBW/MHz	4.1338	3.8330	1.5923	1.2012	1.1775	0.8158	0.9429
VSAT 4 dBW/MHz	4.0511	3.8481	1.4906	1.1922	1.1819	0.8071	0.9429
VSAT 8 dBW/MHz	4.0062	3.8649	1.4426	1.1884	1.1841	0.8034	0.9430
VSAT 12 dBW/MHz	3.9853	3.8782	1.4217	1.1868	1.1851	0.8019	0.9430
Handheld 0 dBW/MHz	0.5287	0.5119	0.5281	0.4407	0.4189	0.4405	0.3888
Handheld 4 dBW/MHz	0.7633	0.7286	0.7608	0.6328	0.5887	0.6311	0.5423
Handheld 8 dBW/MHz	0.9806	0.9269	0.9728	0.7890	0.7243	0.7841	0.6679
Handheld 12 dBW/MHz	1.1533	1.0859	1.1342	0.8724	0.8011	0.8638	0.7535

To conclude the analysis for fixed terminals in the dual satellite scenario, we also consider NLOS propagation conditions in the sub-urban, urban, and dense-urban environments, which include the clutter loss in addition to the impairments in LOS propagation.

Table 44 and Table 45 show the performance in sub-urban conditions. The trends in terms of normalisations and precoding algorithms are aligned with those in other. However, the comparison with the stand-alone system is now different:

- MMSE precoding with the sSPC and sMPC normalisations provides a better performance in the dual satellite scenario, in particular for VSATs;
- MMSE with PAC is worse with VSATs and handheld terminals with low transmission power;
- with SS-MMSE precoding, the stand-alone satellite scenario is again better with sSPC and sMPC with both terminals, and with handheld terminals for PAC solutions.

Table 44 - Average spectral efficiency [bit/s/Hz] *for the NLOS scenario in sub-urban conditions in the beam space, dual satellite scenario.*

Scenario	MMSE sSPC	MMSE sMPC	MMSE PAC	SS-MMSE sSPC	SS-MMSE sMPC	SS-MMSE PAC	NoP
VSAT 0 dBW/MHz	2.7421	2.5800	1.0752	0.7418	0.7307	0.5828	0.4685
VSAT 4 dBW/MHz	2.7409	2.6165	1.0558	0.7389	0.7292	0.5788	0.4685
VSAT 8 dBW/MHz	2.7415	2.6384	1.0478	0.7377	0.7285	0.5771	0.4686
VSAT 12 dBW/MHz	2.7421	2.6498	1.0446	0.7373	0.7283	0.5765	0.4686
Handheld 0 dBW/MHz	0.6226	0.5219	0.6180	0.4837	0.4320	0.4796	0.2038
Handheld 4 dBW/MHz	0.8031	0.6898	0.7906	0.5755	0.5139	0.5674	0.2784
Handheld 8 dBW/MHz	0.9191	0.8183	0.8976	0.5926	0.5468	0.5825	0.3287
Handheld 12 dBW/MHz	0.9660	0.8832	0.9326	0.5566	0.5267	0.5461	0.3552

Table 45 - Average spectral efficiency [bit/s/Hz] *for the NLOS scenario in sub-urban conditions in the feed space, dual satellite scenario.*

Scenario	MMSE sSPC	MMSE sMPC	MMSE PAC	SS-MMSE sSPC	SS-MMSE sMPC	SS-MMSE PAC	MB
VSAT 0 dBW/MHz	4.2933	3.9253	1.5878	1.2059	1.1821	0.8171	0.9421
VSAT 4 dBW/MHz	4.2132	3.9428	1.4806	1.1972	1.1868	0.8085	0.9422
VSAT 8 dBW/MHz	4.1665	3.9610	1.4288	1.1934	1.1891	0.8049	0.9422
VSAT 12 dBW/MHz	4.1439	3.9759	1.4060	1.1919	1.1901	0.8035	0.9422
Handheld 0 dBW/MHz	0.5202	0.5029	0.5196	0.4341	0.4122	0.4338	0.3796
Handheld 4 dBW/MHz	0.7544	0.7200	0.7520	0.6288	0.5839	0.6272	0.5293
Handheld 8 dBW/MHz	0.9709	0.9182	0.9635	0.7897	0.7232	0.7849	0.6520
Handheld 12 dBW/MHz	1.1532	1.0859	1.1346	0.8783	0.8046	0.8699	0.7363

Similar considerations hold also for the urban environment shown in Table 46 and Table 47 for the beam and feed spaces, respectively. The only difference compared to the sub-urban case is that the PAC normalisation is always performing slightly better with a stand-alone satellite in the beam space, but not in the feed space.

Table 46 - Average spectral efficiency [bit/s/Hz] *for the NLOS scenario in urban conditions in the beam space, dual satellite scenario.*

Scenario	MMSE sSPC	MMSE sMPC	MMSE PAC	SS-MMSE sSPC	SS-MMSE sMPC	SS-MMSE PAC	NoP
VSAT 0 dBW/MHz	2.2632	2.1897	0.9891	0.6889	0.6829	0.5670	0.4670
VSAT 4 dBW/MHz	2.2559	2.2116	0.9726	0.6860	0.6815	0.5631	0.4670
VSAT 8 dBW/MHz	2.2534	2.2249	0.9658	0.6849	0.6809	0.5616	0.4671
VSAT 12 dBW/MHz	2.2525	2.2318	0.9630	0.6844	0.6806	0.5609	0.4671
Handheld 0 dBW/MHz	0.6254	0.5085	0.6180	0.4909	0.4458	0.4870	0.2198
Handheld 4 dBW/MHz	0.7569	0.6442	0.7464	0.5581	0.5064	0.5509	0.2909
Handheld 8 dBW/MHz	0.8205	0.7250	0.8068	0.5553	0.5182	0.5469	0.3403
Handheld 12 dBW/MHz	0.8234	0.7509	0.8037	0.5077	0.4842	0.4997	0.3679

Table 47 - Average spectral efficiency [bit/s/Hz] *for the NLOS scenario in urban conditions in the feed space, dual satellite scenario.*

Scenario	MMSE sSPC	MMSE sMPC	MMSE PAC	SS-MMSE sSPC	SS-MMSE sMPC	SS-MMSE PAC	MB
VSAT 0 dBW/MHz	3.6193	3.3956	1.5154	1.1635	1.1383	0.7974	0.9420
VSAT 4 dBW/MHz	3.5304	3.3898	1.4124	1.1543	1.1434	0.7886	0.9421
VSAT 8 dBW/MHz	3.4824	3.3937	1.3629	1.1504	1.1458	0.7849	0.9421
VSAT 12 dBW/MHz	3.4601	3.3999	1.3412	1.1488	1.1469	0.7834	0.9421
Handheld 0 dBW/MHz	0.5546	0.5340	0.5537	0.4666	0.4461	0.4662	0.4232
Handheld 4 dBW/MHz	0.7829	0.7431	0.7798	0.6445	0.6040	0.6426	0.5733
Handheld 8 dBW/MHz	0.9876	0.9288	0.9786	0.7861	0.7265	0.7809	0.6937
Handheld 12 dBW/MHz	1.1321	1.0629	1.1122	0.8569	0.7908	0.8480	0.7744

Similar considerations hold for the dense-urban scenario, which is reported in Table 48 and Table 49 for the beam and feed spaces, respectively.

The better performance in NLOS conditions with MMSE precoding is related to the above mentioned geometry of this type of coverage. In particular, the relative position of the users with respect to the two satellites and the smaller separation in the angular domain among the users lead to channel matrices that show some slight correlation among their rows. This leads to a worse performance compared to the stand-alone case, in general. However, when there are impairments that disrupt this built-in symmetry, the performance with multiple satellites is improved. This does not apply to the SS-MMSE precoding, but it shall not be surprising: this algorithm is based on an approximation of the user CSI with that of the beam center; with two satellites, we are doubling the CSI elements in both the beam and the feed space and, thus, the misalignment with respect to the real channel matrix is too large.

Table 48 - Average spectral efficiency [bit/s/Hz] *for the NLOS scenario in dense-urban conditions in the beam space, dual satellite scenario.*

Scenario	MMSE sSPC	MMSE sMPC	MMSE PAC	SS-MMSE sSPC	SS-MMSE sMPC	SS-MMSE PAC	NoP
VSAT 0 dBW/MHz	2,3008	2,2096	0,9917	0,6944	0,6874	0,5639	0,4659
VSAT 4 dBW/MHz	2,2921	2,2328	0,9737	0,6915	0,6859	0,5600	0,4659
VSAT 8 dBW/MHz	2,2889	2,2471	0,9662	0,6904	0,6853	0,5585	0,4659
VSAT 12 dBW/MHz	2,2877	2,2546	0,9632	0,6899	0,6851	0,5578	0,4659
Handheld 0 dBW/MHz	0,6188	0,5050	0,6107	0,4887	0,4424	0,4845	0,2182
Handheld 4 dBW/MHz	0,7590	0,6419	0,7434	0,5603	0,5066	0,5526	0,2895
Handheld 8 dBW/MHz	0,8319	0,7317	0,8093	0,5612	0,5225	0,5522	0,3391
Handheld 12 dBW/MHz	0,8405	0,7653	0,8107	0,5157	0,4911	0,5071	0,3667

Table 49 - Average spectral efficiency [bit/s/Hz] *for the NLOS scenario in dense-urban conditions in the feed space, dual satellite scenario.*

Scenario	MMSE sSPC	MMSE sMPC	MMSE PAC	SS-MMSE sSPC	SS-MMSE sMPC	SS-MMSE PAC	MB
VSAT 0 dBW/MHz	3.6727	3.4393	1.5204	1.1619	1.1378	0.7946	0.9408
VSAT 4 dBW/MHz	3.5758	3.4265	1.4116	1.1529	1.1424	0.7860	0.9409
VSAT 8 dBW/MHz	3.5219	3.4255	1.3576	1.1491	1.1447	0.7823	0.9410
VSAT 12 dBW/MHz	3.4962	3.4290	1.3334	1.1475	1.1457	0.7809	0.9410
Handheld 0 dBW/MHz	0.5495	0.5262	0.5486	0.4620	0.4414	0.4616	0.4171
Handheld 4 dBW/MHz	0.7770	0.7356	0.7739	0.6420	0.6006	0.6401	0.5649
Handheld 8 dBW/MHz	0.9760	0.9181	0.9673	0.7869	0.7260	0.7818	0.6856
Handheld 12 dBW/MHz	1.1223	1.0551	1.1029	0.8605	0.7932	0.8516	0.7676

2.2.2.2 Public Safety terminals

In this section, we report the numerical results obtained with Public Safety UEs in the same configurations and scenarios as those reported above for fixed terminals.

Differently from the behaviour observed with the stand-alone satellite, in this case there is a slight benefit (in the order of 10^{-3} at most) in having a moving user. This trend, documented by the tables below showing the performance in the beam and feed spaces with pure LOS and NLOS conditions, further substantiates the considerations for the dual satellite scenario: given the geometry of the system, which leads to a limited correlation in the channel matrices compared to the stand-alone scenario, any impairment or phenomenon that introduces a misalignment might be beneficial to the system.

Table 50 - Average spectral efficiency [bit/s/Hz] *for the pLOS scenario in the beam space with Public Safety terminals, dual satellite scenario.*

Scenario	MMSE sSPC	MMSE sMPC	MMSE PAC	SS-MMSE sSPC	SS-MMSE sMPC	SS-MMSE PAC	NoP
VSAT 0 dBW/MHz	2.9776	2.7977	1.1052	0.7583	0.7462	0.5887	0.4691
VSAT 4 dBW/MHz	2.9836	2.8329	1.0933	0.7550	0.7437	0.5845	0.4691
VSAT 8 dBW/MHz	2.9871	2.8524	1.0885	0.7537	0.7427	0.5828	0.4691
VSAT 12 dBW/MHz	2.9889	2.8620	1.0866	0.7532	0.7423	0.5821	0.4691
Handheld 0 dBW/MHz	0.7447	0.6360	0.7378	0.5713	0.5238	0.5656	0.2443
Handheld 4 dBW/MHz	0.9102	0.8034	0.8942	0.6429	0.5923	0.6331	0.3068
Handheld 8 dBW/MHz	1.0090	0.9186	0.9805	0.6390	0.6041	0.6274	0.3425
Handheld 12 dBW/MHz	1.0485	0.9637	0.9972	0.5890	0.5672	0.5769	0.3595

Table 51 - Average spectral efficiency [bit/s/Hz] *for the pLOS scenario in the feed space with Public Safety terminals, dual satellite scenario.*

Scenario	MMSE sSPC	MMSE sMPC	MMSE PAC	SS-MMSE sSPC	SS-MMSE sMPC	SS-MMSE PAC	MB
VSAT 0 dBW/MHz	4.5412	4.1441	1.5458	1.2219	1.2071	0.8247	0.9429
VSAT 4 dBW/MHz	4.4955	4.1769	1.4766	1.2128	1.2065	0.8160	0.9430
VSAT 8 dBW/MHz	4.4708	4.2027	1.4454	1.2089	1.2063	0.8124	0.9430
VSAT 12 dBW/MHz	4.4594	4.2194	1.4322	1.2074	1.2063	0.8109	0.9430
Handheld 0 dBW/MHz	0.6460	0.6219	0.6448	0.5346	0.5127	0.5340	0.4547
Handheld 4 dBW/MHz	0.8790	0.8358	0.8747	0.7161	0.6778	0.7138	0.5917
Handheld 8 dBW/MHz	1.0899	1.0281	1.0773	0.8505	0.8001	0.8448	0.6924
Handheld 12 dBW/MHz	1.2668	1.1896	1.2370	0.9167	0.8648	0.9075	0.7560

Table 52 - Average spectral efficiency [bit/s/Hz] *for the NLOS scenario in sub-urban condition in the beam space with Public Safety terminals, dual satellite scenario.*

Scenario	MMSE sSPC	MMSE sMPC	MMSE PAC	SS-MMSE sSPC	SS-MMSE sMPC	SS-MMSE PAC	NoP
VSAT 0 dBW/MHz	2.7442	2.5823	1.0760	0.7430	0.7318	0.5830	0.4685
VSAT 4 dBW/MHz	2.7428	2.6188	1.0566	0.7401	0.7303	0.5789	0.4685
VSAT 8 dBW/MHz	2.7433	2.6407	1.0486	0.7389	0.7297	0.5773	0.4686
VSAT 12 dBW/MHz	2.7439	2.6521	1.0454	0.7385	0.7294	0.5766	0.4686
Handheld 0 dBW/MHz	0.6241	0.5232	0.6195	0.4839	0.4322	0.4799	0.2038
Handheld 4 dBW/MHz	0.8049	0.6914	0.7925	0.5759	0.5142	0.5679	0.2784
Handheld 8 dBW/MHz	0.9211	0.8201	0.8996	0.5932	0.5474	0.5832	0.3287
Handheld 12 dBW/MHz	0.9680	0.8851	0.9347	0.5574	0.5274	0.5470	0.3552

Table 53 - Average spectral efficiency [bit/s/Hz] *for the NLOS scenario in sub-urban condition in the feed space with Public Safety terminals, dual satellite scenario.*

Scenario	MMSE sSPC	MMSE sMPC	MMSE PAC	SS-MMSE sSPC	SS-MMSE sMPC	SS-MMSE PAC	MB

VSAT 0 dBW/MHz	4.2962	3.9282	1.5885	1.2071	1.1832	0.8173	0.9421
VSAT 4 dBW/MHz	4.2160	3.9457	1.4814	1.1984	1.1880	0.8087	0.9422
VSAT 8 dBW/MHz	4.1691	3.9639	1.4295	1.1947	1.1903	0.8051	0.9422
VSAT 12 dBW/MHz	4.1464	3.9788	1.4067	1.1931	1.1914	0.8036	0.9422
Handheld 0 dBW/MHz	0.5213	0.5040	0.5208	0.4343	0.4124	0.4340	0.3797
Handheld 4 dBW/MHz	0.7560	0.7216	0.7537	0.6291	0.5841	0.6275	0.5295
Handheld 8 dBW/MHz	0.9729	0.9202	0.9655	0.7900	0.7235	0.7852	0.6521
Handheld 12 dBW/MHz	1.1556	1.0882	1.1370	0.8787	0.8049	0.8702	0.7364

Table 54 - Average spectral efficiency [bit/s/Hz] *for the NLOS scenario in urban condition in the beam space with Public Safety terminals, dual satellite scenario.*

Scenario	MMSE sSPC	MMSE sMPC	MMSE PAC	SS-MMSE sSPC	SS-MMSE sMPC	SS-MMSE PAC	NoP
VSAT 0 dBW/MHz	2.2644	2.1912	0.9896	0.6898	0.6838	0.5673	0.4670
VSAT 4 dBW/MHz	2.2570	2.2130	0.9731	0.6870	0.6824	0.5634	0.4670
VSAT 8 dBW/MH	2.2544	2.2261	0.9663	0.6858	0.6818	0.5618	0.4671
VSAT 12 dBW/MHz	2.2535	2.2330	0.9636	0.6853	0.6815	0.5612	0.4671
Handheld 0 dBW/MHz	0.6268	0.5097	0.6195	0.4913	0.4461	0.4874	0.2198
Handheld 4 dBW/MHz	0.7585	0.6457	0.7480	0.5585	0.5069	0.5514	0.2909
Handheld 8 dBW/MHz	0.8223	0.7265	0.8086	0.5559	0.5188	0.5476	0.3403
Handheld 12 dBW/MHz	0.8252	0.7525	0.8054	0.5085	0.4849	0.5005	0.3679

Table 55 - Average spectral efficiency [bit/s/Hz] *for the NLOS scenario in urban condition in the feed space with Public Safety terminals, dual satellite scenario.*

Scenario	MMSE sSPC	MMSE sMPC	MMSE PAC	SS-MMSE sSPC	SS-MMSE sMPC	SS-MMSE PAC	MB
VSAT 0 dBW/MHz	3.6214	3.3978	1.5161	1.1644	1.1392	0.7976	0.9420

VSAT 4 dBW/MHz	3.5324	3.3921	1.4132	1.1553	1.1443	0.7888	0.9421
VSAT 8 dBW/MH	3.4843	3.3961	1.3637	1.1514	1.1468	0.7851	0.9421
VSAT 12 dBW/MHz	3.4619	3.4023	1.3420	1.1498	1.1479	0.7836	0.9421
Handheld 0 dBW/MHz	0.5557	0.5352	0.5549	0.4669	0.4464	0.4665	0.4232
Handheld 4 dBW/MHz	0.7845	0.7446	0.7814	0.6449	0.6043	0.6430	0.5733
Handheld 8 dBW/MHz	0.9896	0.9307	0.9806	0.7865	0.7269	0.7814	0.6937
Handheld 12 dBW/MHz	1.1344	1.0650	1.1144	0.8574	0.7913	0.8486	0.7744

Table 56 - Average spectral efficiency [bit/s/Hz] *for the NLOS scenario in dense-urban condition in the beam space with Public Safety terminals, dual satellite scenario.*

Scenario	MMSE sSPC	MMSE sMPC	MMSE PAC	SS-MMSE sSPC	SS-MMSE sMPC	SS-MMSE PAC	NoP
VSAT 0 dBW/MHz	2.3024	2.2112	0.9921	0.6953	0.6883	0.5641	0.4659
VSAT 4 dBW/MHz	2.2936	2.2343	0.9740	0.6924	0.6868	0.5602	0.4659
VSAT 8 dBW/MH	2.2904	2.2484	0.9666	0.6913	0.6863	0.5586	0.4659
VSAT 12 dBW/MHz	2.2892	2.2559	0.9636	0.6908	0.6860	0.5580	0.4659
Handheld 0 dBW/MHz	0.6202	0.5062	0.6122	0.4890	0.4427	0.4848	0.2182
Handheld 4 dBW/MHz	0.7607	0.6433	0.7452	0.5607	0.5070	0.5530	0.2895
Handheld 8 dBW/MHz	0.8338	0.7333	0.8112	0.5617	0.5230	0.5528	0.3391
Handheld 12 dBW/MHz	0.8424	0.7670	0.8125	0.5164	0.4918	0.5078	0.3667

Table 57 - Average spectral efficiency [bit/s/Hz] *for the NLOS scenario in dense-urban condition in the feed space with Public Safety terminals, dual satellite scenario.*

Scenario	MMSE sSPC	MMSE sMPC	MMSE PAC	SS-MMSE sSPC	SS-MMSE sMPC	SS-MMSE PAC	MB
VSAT 0 dBW/MHz	3.6747	3.4412	1.5209	1.1628	1.1387	0.7947	0.9408
VSAT 4 dBW/MHz	3.5779	3.4285	1.4120	1.1539	1.1433	0.7861	0.9410

VSAT 8 dBW/MH	3.5241	3.4275	1.3580	1.1501	1.1457	0.7825	0.9410
VSAT 12 dBW/MHz	3.4983	3.4310	1.3339	1.1485	1.1467	0.7810	0.9410
Handheld 0 dBW/MHz	0.5506	0.5273	0.5497	0.4622	0.4417	0.4618	0.4170
Handheld 4 dBW/MHz	0.7786	0.7371	0.7755	0.6423	0.6009	0.6404	0.5649
Handheld 8 dBW/MHz	0.9779	0.9200	0.9693	0.7873	0.7264	0.7822	0.6855
Handheld 12 dBW/MHz	1.1246	1.0573	1.1052	0.8609	0.7936	0.8521	0.7675

2.2.2.3 Observations

Based on the exhaustive numerical assessment performed in the dual satellite scenario with the shared service area, several interesting trade-offs have been identified, as summarised hereafter:

- **Precoding algorithm**
  - MMSE is always providing the largest spectral efficiency values;
  - SS-MMSE precoding shows an acceptable performance, also considering that it is based on pre-computed channel coefficients, *i.e.*, it does not need a continuous reporting of CSI vectors from the UEs to the gNB. With slight variations related to the considered propagation scenario, SS-MMSE precoding provides an average spectral efficiency in the order of: i) $0.5 - 0.75$ bit/s/Hz in the beam space with sSPC and sMPC, while with PAC it is in the order of $0.5 - 0.6$ bit/s/Hz; ii) $1.1 - 1.2$ bit/s/Hz in the feed space with sSPC and sMPC and $0.7 - 0.8$ bit/s/Hz for VSAT terminals, $0.45 - 0.9$ bit/s/Hz for handheld terminals;
  - MB precoding in the feed space and the non-precoded system in the beam space are not equivalent as in the stand-alone case, but still a non-precoded system in the feed space is not meaningful. In terms of the average spectral efficiency, only in the feed space the MB solution provides a performance better that SS-MMSE precoding with PAC.
- **Normalisation**
  - The sSPC and sMPC normalisations provide the best solution in scenarios characterised by a large power at the receiver, *i.e.*, scenarios where interference is significant, up to the maximum interference that can be managed by the precoder. As seen for the stand-alone case, in these situations the orthogonality of the precoding matrix is fundamental to properly manage the significant interference at each user terminal. When the precoder cannot manage the increased interference level, the performance saturates;
  - in scenarios with a limited received power, *i.e.*, handheld terminals, the PAC normalisation provides a performance close to that of sSPC and sMPC, and, in some cases, even better. In these conditions, rather than preserving the orthogonality, it is more impacting the enhancement of the intended signal power, independently from the channel conditions, guaranteed by a PAC approach.

In general, also for the dual satellite scenario we can conclude that MMSE precoding (or other similar solutions) is worth to be further investigated because SS-MMSE precoding is significantly degrading the performance in many relevant scenarios. As for the normalisations, MPC and PAC provide, depending on the scenarios as discussed above, a performance close to that of SPC. They are to be preferred since they guarantee that each antenna feed is not emitting a transmission power above its maximum.

Finally, comparing the stand-alone and dual satellite scenarios, the latter provides a significantly better performance in pure LOS and LOS propagation conditions. This is motivated by the peculiarity of the dual satellite scenario, discussed above, which leads to a more difficult interference limitation procedure for the precoder, due to the implicit symmetry in the geometry and, in particular, due to the reduced angular distance between different users. In this context, other scenarios exploiting more than one satellite shall be taken into account in the next steps so as to exhaustively characterise this type of system. In particular, the hot-spot scenarios introduced in Figure 4 for the stand-alone case can be considered with multiple satellites as well; in addition, also a scenario in which each satellite in the swarm is covering its own service area, instead of a shared one, will be considered. In these scenarios, it is expected that the issues leading to a worsening in the performance will be limited.

3 MULTI-CONNECTIVITY TECHNIQUES: PRELIMINARY RESULTS

In this section, we briefly report the preliminary results for the multi-connectivity techniques selected to be demonstrated in the DYNASAT project. The used simulator is also briefly described with assumptions. We report the preliminary results produced with the current implemented simulator within a simple scenario. The simple scenario is for Proof-of-Concept (PoC) and testing purposes. More results are produced with new versions of the simulator presented later in project and reported in D3.5 and D3.6, when simulator and scenario modelling are more advanced.

3.1 Simulator description

The multi-connectivity performance is evaluated by means of dynamic system level simulations. A so called 5G NTN system level simulator based on ns-3 has been used which models:

- The system from PHY to application layer
- End-to-end system
- 5G TN/NTN air interface
- A network of nodes (UEs, gNBs, satellites) and their connectivity
- With a packet level resolution

The system level simulator is described in [6]. The modelling relies heavily on 3GPP NTN specifications in [1] and [3]. The system level simulator is also explained in the D5.1. The extension done to the simulator in this project

3.1.1 Assumptions

- Transparent satellite payload (gNB on ground)
- Priority for NTN-NTN MC (no TN-NTN)
- Both inter-beam single satellite NTN-NTN MC and inter-satellite NTN-NTN MC candidate use cases
- Multi-connectivity targeting at increased data rate at the terminal (instead of *e.g.*, reliability)
- MC for handheld terminals
- S-band frequencies
- MC is assumed to use different frequency bands
- Two satellites in case of NTN-NTN are considered as a sufficient simulation scenario size
- Stationary (non-mobile) UEs
- eMBB traffic types, *e.g.*, “full buffer” -type traffic
- LEO satellites – Note, that LEO satellites are in fact moving with respect to earth, but we consider the LEO satellites to be stationary. The reason for this is that if assuming moving LEO satellites, we would need to multiple additional aspects as well: e.g., mobility management, multiple LEO satellites. This should not be a major problem assuming quite short simulation durations.

3.1.2 The simple scenario

The simple scenario, *i.e.*, the PoC simulation scenario (see Figure 38) consists of one satellite with two beams. The beams are overlapping and have different frequencies. Furthermore, 20 stationary UEs are initially connected only to the satellite’s beam 0.

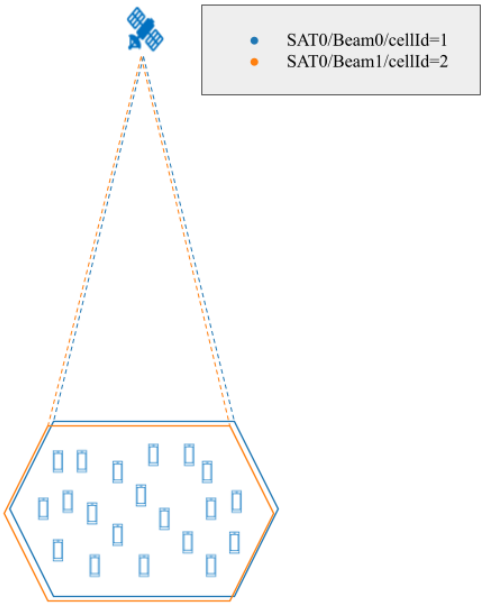

Figure 38. Simulation scenario with a single satellite having two overlapping beams and 20 UEs initially connected to beam 0.

The reasonings behind the selection of this scenario are manifold. Firstly, it can be used to clearly show that the throughput can be improved when the unutilized second beam is used as an SN for the UEs. Secondly, when testing more advanced MC algorithms that bring their own complexities to the simulations and their results' analysis, a simple scenario can reduce unnecessary complexity. Finally, as a simple scenario, it is well suitable to be used in regression testing. Simulations will be run with 1) MC off and 2) MC on. That is, in the second case, the UEs will have a secondary connection to the second beam. In the scenario's traffic model, a remote host sends UDP traffic, that traverses through the satellite, to the UEs. 2000 UDP packets, each of size 100 B is sent to each user within 2 s of simulation time (after 1 s of warmup time). Moreover, the simulations with MC off and on will be run with five drops each, i.e., with different random number generator seeds used in the generation of random values in the simulation, e.g., where the UEs are placed.

TR 38.821 [1] provides calibration cases for System Level Simulators (SLS). In the simulations, case 10 from Table 6.1.1.1-9 that uses satellite parameter set 1 (see Table 6.1.1.1-1), is considered.

3.1.3 Preliminary results

One of the Key Performance Indicators (KPI) that can be used to estimate the performance enhancements in the DYNASAT project include experienced data rate. Downlink application call throughput in kbps per UE and the corresponding CDF can be seen in Figure 39 and Figure 40, respectively. It can be observed that the throughput for each UE increases when MC is turned on (*i.e.*, every other packet is sent by the MN and every other is directed to the SN and sent by it to the UE). Node with id 16 gained the most benefit when using MC with ~132% enhancement to throughput, from ~205 to ~475 kbps. Worst throughput gain was experienced by the Node 25: ~41%, from ~395 to ~555 kbps (note, that it already had the best throughput of all the nodes). The system's total throughput improved by ~87%, from ~5095 to ~9530 kbps. The variance in the throughput between the UEs can be explained by their different locations in the area of the beams and the differing Modulation and Coding Schemes (MCS) UEs use depending on the signal strength. MCS defines how many bits is sent in a resource element. Note, that the system is overloaded such that not all the data is received by the UE during the simulation, neither with MC turned off nor on.

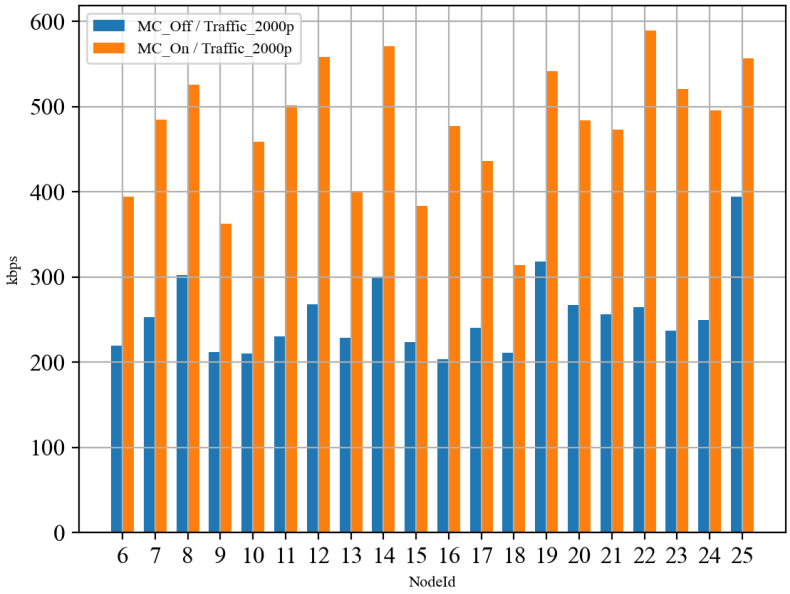

Figure 39. Downlink application call throughput (kbps) per UE, 2000 UDP packets of 100B sent to each UE.

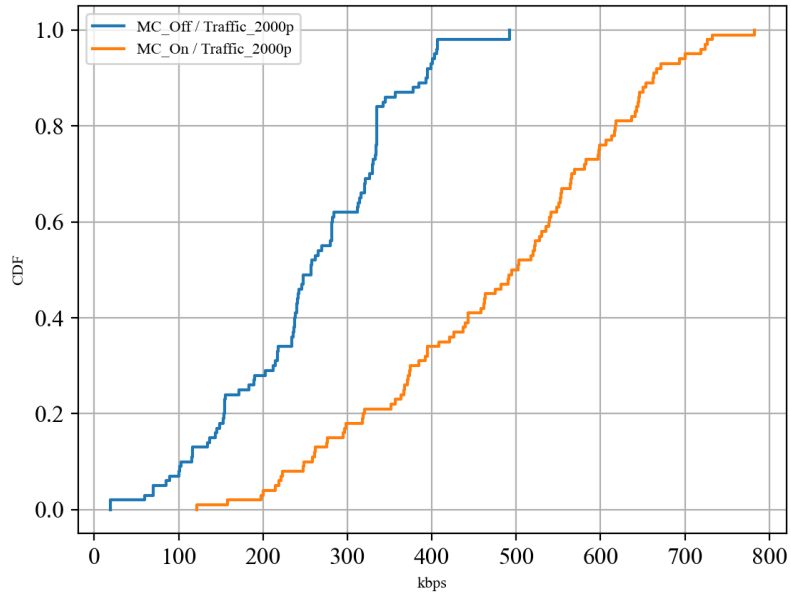

Figure 40. CDF of application call throughput, 2000 UDP packets of size 100B sent to each UE.

Another KPI of interest is the percentage of the capacity demand actually served. In the simulations, the total actual capacity demand was 32000 kb ($2000\ packets \times 100\ B \times 20\ users$). When MC was turned off, the actual capacity served was 10187.4 kb ($2\ s \times 5093.7\ kbps$), whereas when MC was turned on, it was 19062.2 kb ($2\ s \times 9531.1\ kbps$). So, the percentage of the capacity demand actually served went up from 31.8% to 59.6%.

3.1.4 Performance scenarios

Three potential MC scenarios have been identified for the multi-connectivity performance evaluations, see Figure 41.

1. Single satellite neighbouring multi-beam MC

2. Multi-satellite overlapping coverage FRF1 MC
3. Multi-satellite overlapping coverage FRF3 MC

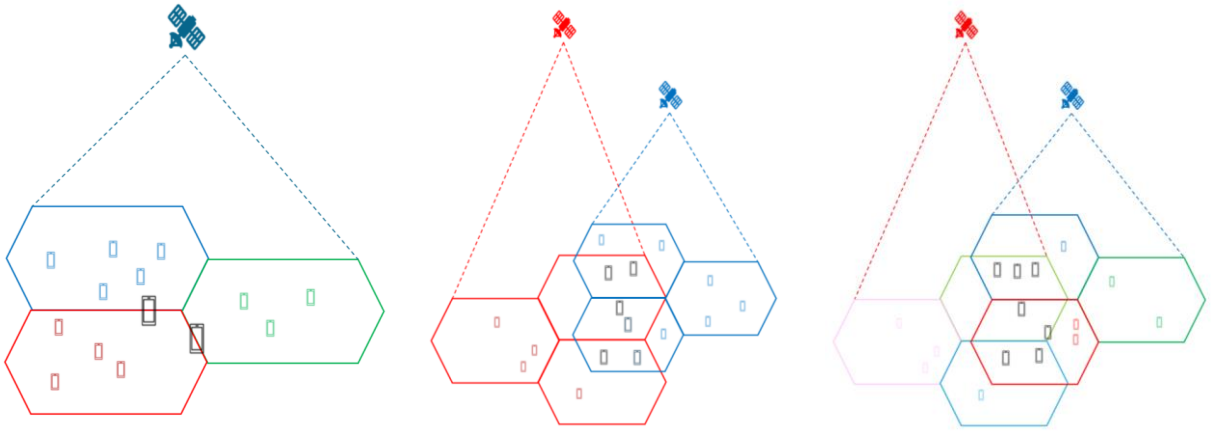

Figure 41. Multi-connectivity scenarios (a) Single satellite neighbouring multi-beam MC, (b) multi-satellite overlapping coverage FRF1 MC, (c) multi-satellite overlapping coverage FRF3 MC.

The objective is to evaluate the multi-connectivity with some of these scenarios with some modifications later in the project. In the first phase evaluations are done with 'Single satellite neighbouring multi-beam MC. Later evaluations with multi-satellite scenarios are included. Results produced with these scenarios are presented later in D3.5 and D3.6.

4 CONCLUSIONS

4.1 MU-MIMO

This document provides a detailed description of the simulator structure and KPIs for the short-term and benchmark MU-MIMO techniques designed in D3.2. For the MMSE (benchmark), SS-MMSE, and MB precoding algorithms, an exhaustive simulation campaign has been performed and reported in the document, allowing to identify some interesting trends that will serve as a baseline to identify the next steps in the task activities. It is worth to recall that the simulator and the related evaluations were obtained at system-level, under the assumption of a full buffer and uniform traffic distribution, which allowed to not consider scheduling aspects, in this first preliminary assessment.

More specifically, two scenarios have been considered: a stand-alone satellite scenario, in which a single satellites implements precoding with full frequency reuse, and a dual satellite scenario, in which two satellites cover the same service area (the same beam centers, in particular) with precoding and full frequency reuse. In general, the following trends have been identified:

- MMSE precoding is always the best solution, as also expected from the techniques design in D3.2 and from the scientific literature;
- the SS-MMSE approach is an interesting solution, since it avoids the need for accurate CSI vectors at the transmitter. The performance is acceptable, but in many scenarios it is quite distant from the MMSE performance;
- MB precoding is the worst in the vast majority of the scenarios, as expected since it is a beamforming technique that shall be combined with beam-hopping in order to provide a good performance.

Comparing the performance in the stand-alone and dual satellite scenarios, some very interesting system-level behaviours were found. In particular, the stand-alone scenario provides a significantly better performance in pure LOS and LOS propagation conditions. This is motivated by the peculiarity of the dual satellite scenario, extensively discussed in the document, which leads to a more difficult interference limitation procedure for the precoder, due to the implicit symmetry in the geometry and, in particular, due to the reduced angular distance between different users. In this context, other scenarios exploiting more than one satellite shall be taken into account in the next steps so as to exhaustively characterise this type of system. In particular, the hot-spot scenarios introduced in for the stand-alone case can be considered with multiple satellites as well; in addition, also a scenario in which each satellite in the swarm is covering its own service area, instead of a shared one, will be considered. In these scenarios, it is expected that the issues leading to a worsening in the performance will be limited.

In conclusion, while additional scenarios will be considered in order to better identify the solutions in which two or more satellites are beneficial, MMSE precoding provides a significant performance benefit compared to the other solutions. Thus, despite its complexity in terms of CSI estimation and provision at the transmitter side, this technique shall be further designed and evalutated for the long-term analyses. To this aim, in the next steps also the Location Based MMSE algorithm designed in D3.2 will be considered, which is expected to provide a performance still below that of MMSE, but significantly better than SS-MMSE or MB precoding.

4.2 Multi-Connectivity

This document provides brief description of the simulator used for the demonstration of the multi-connectivity techniques. The preliminary results are presented as proof-of-concept and to indicated progress of the simulator development. Later in the project extensive results with the enhanced simulator is presented in D3.5 and D3.6.

5 ANNEX A: LINK-LEVEL SIMULATOR

5.1 Software requirements

The simulation software has been implemented by using Matlab R2018b and the following versions up to R2020a. It relies on the 5G toolbox 1.0 (R2018b) for the simulation of the physical downlink shared channel (PDSCH) and the signal synchronization block (SSB) options, the 5G toolbox 1.1 (R2019a) for the physical uplink shared channel (PUSCH) option, and 2.0 (R2020a) for the physical random access channel (PRACH) option.

5.2 Main features and key performance indicators

The simulation software is fully compliant with the NR standard and has the following main features:

- **Simulation of the physical downlink/uplink shared channel (PDSCH/PUSCH)**

  The transmitted symbols are partitioned to payload (useful bits) and pilots (demodulation reference signals (DMRS), known symbols). The signal synchronization block burst (SSB burst) can be also transmitted, accordingly to the 5G NR protocol configurations, by reserving a dedicated number of resource elements in the time-frequency transmission grid. The simulation is performed on a slot-wise basis. Hybrid-ARQ has been modified to consider increased round-trip delay of the satellite link.

- **Physical random access channel (PRACH)**

  The 5G standard random access procedure relies on the uplink transmission of specific sequences following the specifications of 3GPP TR 38 series. There are several possible formats and transmission occasions within the NR frame structure, given the context. The detection of PRACH should be compliant with specific requirements and must allow the estimation of the timing delay and frequency offset to enable the frame synchronization. Performance is determined in terms of detection rate, false alarm rate, and cumulative distribution function of estimated timing and frequency.

- **Processing at transport and physical channel level**

  The processing at transmitter and receiver side can be divided in two levels. Encoder and decoder are software objects (DLSCH/ULSCH transport channel processing), which take care of data segmentation, CRC encoding, LDPC encoding and rate matching implementation. The functions nrPDSCH/Decode and nrPUSCH/Decode (physical channel processing) take care of scrambling, modulation and layer mapping.

- **Channel estimation**

  At the receiver side, the signal is assumed to be already synchronized, whereas channel estimation can be performed either ideally (i.e., not performed on the pilot symbols, as channel coefficients are taken from the channel generator function directly), or by exploiting the DMRS, which can be configured as envisaged by the standard; equalization is then performed on the true channel coefficients or on the estimated ones.

- **Satellite payload**

  The payload is supposed to be transparent, therefore the chain IMUX-amplifier-OMUX is implemented. Three kind of amplifier nonlinearity are available, namely linearized, conventional and SSPA. The signal is oversampled to be processed by the nonlinear characteristic, and then undersampled for the following processing.

- **Phase noise tracking**

The phase noise, generated according to loadable phase masks or by the Wiener model with proper variance, can be tracked by exploiting one or more subcarriers as pilot symbols, to implement the presence of the phase tracking reference signals (PTRS), in each OFDM symbol or in one every two. The estimation of the common phase error (CPE, a phase rotation common to all subcarrier within one OFDM symbol) is effective only for medium to high SNRs.

- **Signal synchronization block (SSB)**

  To test the synchronization capabilities in a satellite environment, the generation of SSB bursts has been implemented. In this case the simulation is run on a half-frame-wise basis, as the receiver explores a whole half-frame to search for possible synchronization blocks. If the signal can be successfully synchronized the downlink control information (DCI) block is decoded (it is encoded with polar codes).

The following KPIs can be evaluated given the scenario:

- Bit error rate (BER).
- Block error rate (BLER).
- Aggregate results on throughput.
- Synchronization analysis (physical cell-ID detection (PCID), false alarm rate, residual frequency and timing offset at 90% PCID SNIR).
- Different channel models for each orbit.
- Hybrid ARQ performance under high RTT.

REFERENCES

[1] 3GPP TR 38.821 V16.1.0, “Solutions for NR to support non-terrestrial networks (NTN) (Release 16),” May 2021
[2] 3GPP TS 22.261 V18.2.0, “Service requirements for the 5G system; Stage 1 (Release 18),” March 2021
[3] 3GPP TR 38.811 V15.4.0, “Study on New Radio (NR) to support non-terrestrial networks (Release 15),” September 2020
[4] P. Angeletti, R. De Gaudenzi, "A Pragmatic Approach to Massive MIMO for Broadband Communication Satellites," IEEE Access, vol. 8, 2020.
[5] A. Guidotti and A. Vanelli-Coralli, "Geographical Scheduling for Multicast Precoding in Multi-Beam Satellite Systems," 2018 9th Advanced Satellite Multimedia Systems Conference and the 15th Signal Processing for Space Communications Workshop (ASMS/SPSC), 2018, pp. 1-8, September 2018.
[6] Jani Puttonen, Lauri Sormunen, Henrik Martikainen, Sami Rantanen and Janne Kurjenniemi, “A System Simulator for 5G Non-Terrestrial Network Evaluations” The 22nd IEEE International Symposium on a World of Wireless, Mobile and Multimedia Networks (WoWMoM) conference, June 7–11, 2021.